MODELING TRITIUM RELEASE FROM TRISO-COATED NP-MHTGR TARGET PARTICLES

by

Sandra Lee Harms

Submitted to the Department of
Nuclear Engineering in Partial Fulfillment
of the Requirements for the Degrees of

Master of Science

and

Bachelor of Science

Massachusetts Institute of Technology
June 1992

Signature of Author _____
Department of Nuclear Engineering
April, 1992

Certified by _____
Dr. David D. Lanning - Thesis Advisor
Professor, Department of Nuclear Engineering

Certified by _____
Dr. David A. Petti - Thesis Reader
Senior Engineering Specialist, EG&G, Idaho, Inc.

Accepted by _____
Dr. Allan F. Henry
Chairman, Department Committee on Graduate Students

MODELING TRITIUM RELEASE FROM TRISO-COATED NP-MHTGR TARGET PARTICLES

by

Sandra Lee Harms

Submitted to the Department of Nuclear Engineering
in partial fulfillment of the requirements for the
Degrees of Master of Science and Bachelor of Science
in Nuclear Engineering

ABSTRACT

Gaseous diffusion through solids with trapping is studied to understand and model tritium release from TRISO-coated New Production-Modular High Temperature Gas Reactor target particles to support the Tritium Target Development Program. The tritium release is modeled in the first attempt to systematically examine and determine the parameters that affect tritium release at high temperatures. Scoping calculations performed with the Tritium Migration Analysis Program, TMAP, indicate that modeling all three layers of the particle, considering solubility in the pyrocarbon (PyC) and the silicon carbide (SiC), and taking into account depletion of tritium from the particle void volume are all required to accurately model tritium release from the particle. However, the trapping of tritium atoms in the layers does not significantly affect release because of the large quantity of tritium in the particle relative to the number of traps.

Sensitivity studies performed with the TMAP code revealed a simple electrical analogy for tritium transport through the particle. The inner PyC layer acts as a capacitor for tritium atoms because of its high solubility whereas the SiC layer provides a resistance to tritium release because of its low diffusivity. A simple analytic solution was developed to describe this behavior and encoded into TREL, a Tritium RELease code. Results from TREL compare very

well with the more detailed TMAP results with the added benefit that TREL requires significantly less computing time.

TREL release predictions have been compared with results from the Loose Particle Irradiation experiments to determine empirically the solubility of tritium in the SiC. The TREL predictions with the new empirical solubility compared well with data from two other tests. The detailed TMAP code and the faster running TREL have both proven to be extremely useful tools to model tritium release from target particles. This modeling effort has aided in developing a fundamental understanding of target behavior during normal and off normal conditions.

Thesis Supervisor: Dr. David Lanning

Title: Professor of Nuclear Engineering

CONTENTS

ABSTRACT 2
CONTENTS 4
ACKNOWLEDGEMENTS 6
NOMENCLATURE 7
1. INTRODUCTION 9
    1.1 Tritium Target Design 10
    1.2 Overview 10
2. BACKGROUND ON DIFFUSION AND TRAPPING THEORY 13
3. TMAP CODE AND INPUT MODEL 21
    3.1 TMAP Code Description 21
    3.2 Input Models 24
    3.3 TMAP Code Verification 29
        3.3.1 Constant Source Model/Slab Geometry 31
        3.3.2 Depleting Source Model/Slab Geometry 31
        3.3.3 Depleting Source Model/Spherical Geometry 33
        3.3.4 Constant Source Model of Semi-infinite Slab 35
        3.3.5 Partially Loaded Semi-infinite Slab 41
        3.3.6 Permeation Problem 41
        3.3.7 Composite Layer 45
4. RESULTS OF TMAP SCOPING CALCULATIONS 49
    4.1 Comparison of Depleting and Constant Source Calculations 49
    4.2 Comparison of the SiC and Trilayer Models 53
    4.3 Effects of Solubility in the Trilayer Model 56
    4.4 Burnup and Temperature Effects 56
    4.5 Effect of Prior Reactor Operation 67
    4.6 Summary 67
5. SENSITIVITY CALCULATIONS 69
    5.1 PyC Solubility and Diffusivity Results 70
    5.2 SiC Solubility and Diffusivity Results 76
    5.3 Pressure Results 79
    5.4 Trapping Studies 87
        5.4.1 Effect of Trap Concentration 91
        5.4.2 Effect of Trapping Rate 93
        5.4.3 Effect of Resolution Rate 95
    5.5 Sensitivity Study Conclusions 97

6. TREL 99
6.1 The Analytic Solution 99
6.2 The TREL Code 106
6.3 TREL vs. TMAP 109
7. COMPARISON OF MODEL PREDICTIONS WITH EXPERIMENTAL RESULTS 113
7.1 Solubility Determination using the LPI-1 Experimental Data 113
7.2 Data Comparisons to Model Predictions using the New Solubility Relation 120
8. SUMMARY AND CONCLUSIONS 133
8.1 The Final NP-MHTGR Target Particle Model 133
8.2 Further Work 135
9. REFERENCES 136
APPENDIX A SUPPORTING CALCULATIONS FOR INPUT MODELS 139
APPENDIX B SAMPLE TMAP INPUT DECKS 147
B.1 Input Deck for ATR-1 Particle Geometry 147
B.2 Input Deck for ATR-3 Particle Geometry 149
B.3 Input Deck for Dimensionless Geometry 152
APPENDIX C TREL CODE DESCRIPTION 155
C.1 TREL Code Listing 155
C.2 TREL Input 168
C.3 TREL Plot File 170
C.4 TREL Output File 171

ACKNOWLEDGEMENTS

The author would like to express her appreciation to the people who provided great support during this project. Dr. David Petti at EG&G, Idaho, Inc was especially helpful and insightful while supervising the project. Dr. David Lanning, the thesis advisor, also provided useful suggestions and constructive comments. And thanks to Mom and Dad who managed to find their way through the financial aid paperwork year after year and still give their love and support.

NOMENCLATURE

a	radius to outer surface of spherical layer
A	surface area (m^2)
b	radius to inner surface of spherical layer
C	mobile tritium concentration (m^{-3})
C_o	initial tritium concentration (m^{-3})
C^T	trapped tritium concentration (m^{-3})
CR	cumulative release (atoms)
D	diffusion coefficient (m^2/s)
D_c	diffusion coefficient constant (m^2/s)
E_D	diffusion activation energy (J/gmole)
E_T	trap site binding energy (J/gmole)
FR	fractional release
h	loaded portion of layer (m)
J	surface flux ($m^{-2}s^{-1}$)
k	Boltzmann's constant (J/K)
m	mass flow rate of T_2 (kg/s)
n_{mole}	number of gram moles
n	pressure exponent in solubility relation
N	number density of the host material ($atoms/m^3$)
N_{avg}	Avagodro's number (molecules/gmole)
N_{encl}	number of atoms in enclosure
N_{PyC}	number of atoms in PyC layer

$N_T(0)$	initial number of tritium gas (T_2) atoms
P	tritium partial pressure (Pa)
P_{eq}	equilibrium partial pressure (Pa)
P_o	initial partial pressure (Pa)
P(t)	pressure as a function of time (Pa)
Q_D	activation energy for diffusion (kJ/mole)
Q_S	heat of formation for solubility (kJ/mole)
r	trap release rate (s^{-1})
R	gas constant (J/gmole-K)
S	solubility (atoms/m^3Pa^n)
S_c	solubility constant (Pa^{-n})
t	time (s)
t_b	breakthrough time (s)
T	temperature (K)
V	void volume (m^3)
w	trapping rate (s^{-1})
x	location (m)
X_T^e	concentration of empty trapping sites (m^{-3})
X_T^0	initial concentration of traps (m^{-3})
δ	layer thickness (m)
λ	jump distance (m)
υ_o	release attempt frequency (s^{-1})

MODELING TRITIUM RELEASE FROM NP-MHTGR TARGET PARTICLES

1. INTRODUCTION

This report documents the use of the Tritium Migration Analysis Program, TMAP, Mod3[1] and the Tritium RELease program, TREL, to predict the release of tritium from target particles in the New Production Modular High-Temperature Gas-Cooled Reactor (NP-MHTGR). TMAP was developed at the Idaho National Engineering Laboratory (INEL) and originally modeled tritium behavior in fusion reactor systems. However, application of the code to NP-MHTGR target particles has proven to be very useful for studying tritium diffusion through the TRISO coating of the target particle. TREL, developed during this study, more specifically models tritium release from the TRISO-coated target particle.

This modeling effort is part of the Tritium Target Development Program.[2] The objective of this program is to provide the technical basis for a successful NP-MHTGR tritium target infrastructure, including fabrication, irradiation performance, safety, and tritium recovery. To meet this objective, numerous experiments are underway to understand the performance of the NP-MHTGR tritium targets during normal and off normal (accident) reactor operating conditions. Target compacts are being irradiated in the Advanced Test Reactor (ATR) at the INEL at prototypic burnup and temperature conditions to determine the amount of tritium leakage and to assess the limiting conditions for performance during normal operation. Irradiated compacts are also being used in out-of-pile postirradiation heating tests to measure tritium release under accident and tritium recovery conditions. A series of Loose Particle Irradiation (LPI) tests are being performed to increase the fundamental understanding of the TRISO-coated target particle design. Experiments are also currently being performed at Sandia National Laboratory-Livermore to measure the tritium transport parameters in SiC and PyC.[3] The tritium diffusion coefficient,

solubility, trap concentration, and trap energy will be determined for each material to aid in the development of tritium release modeling.

The tritium release modeling presented in this thesis is the first attempt to systematically examine and determine the parameters that affect tritium release at high temperatures. As pointed out in the Tritium Target Development Plan,[2] such modeling is necessary to aid in developing a fundamental understanding of target behavior during normal and off normal conditions.

1.1 Tritium Target Design

The target particles are tiny microspheres with a diameter of hundreds of microns. They are comprised of a lithium aluminate ($LiAl_3O_8$) kernel surrounded by a porous buffer carbon layer and a TRISO coating consisting of sequential layers of inner pyrolytic carbon (IPyC), silicon carbide (SiC), and outer pyrolytic carbon (OPyC). Two target particle designs have been used in the Tritium Target Development Program. The first particle design is the conceptual design from which the ATR-1 particles were manufactured The dimensions are given in Table A1 in Appendix A. The kernel diameter and the thickness of each of the layers were increased in the preliminary design. This design was used to fabricate the ATR-2/ATR-3 particles. The dimensions are given in Table A2. A full scale target compact consists of hundreds of thousands of these particles embedded in a porous graphite matrix. As shown in Figure 1, the target element assembly contains 20 target compacts.

1.2 Overview

The following modeling efforts are discussed in this report. Background on diffusion and trapping is provided in Section 2. The TMAP code capabilities, the input model, and code verification studies are presented in Section 3. Section 4 discusses the results of scoping calculations. Specifically, Section 4 presents (a) the results

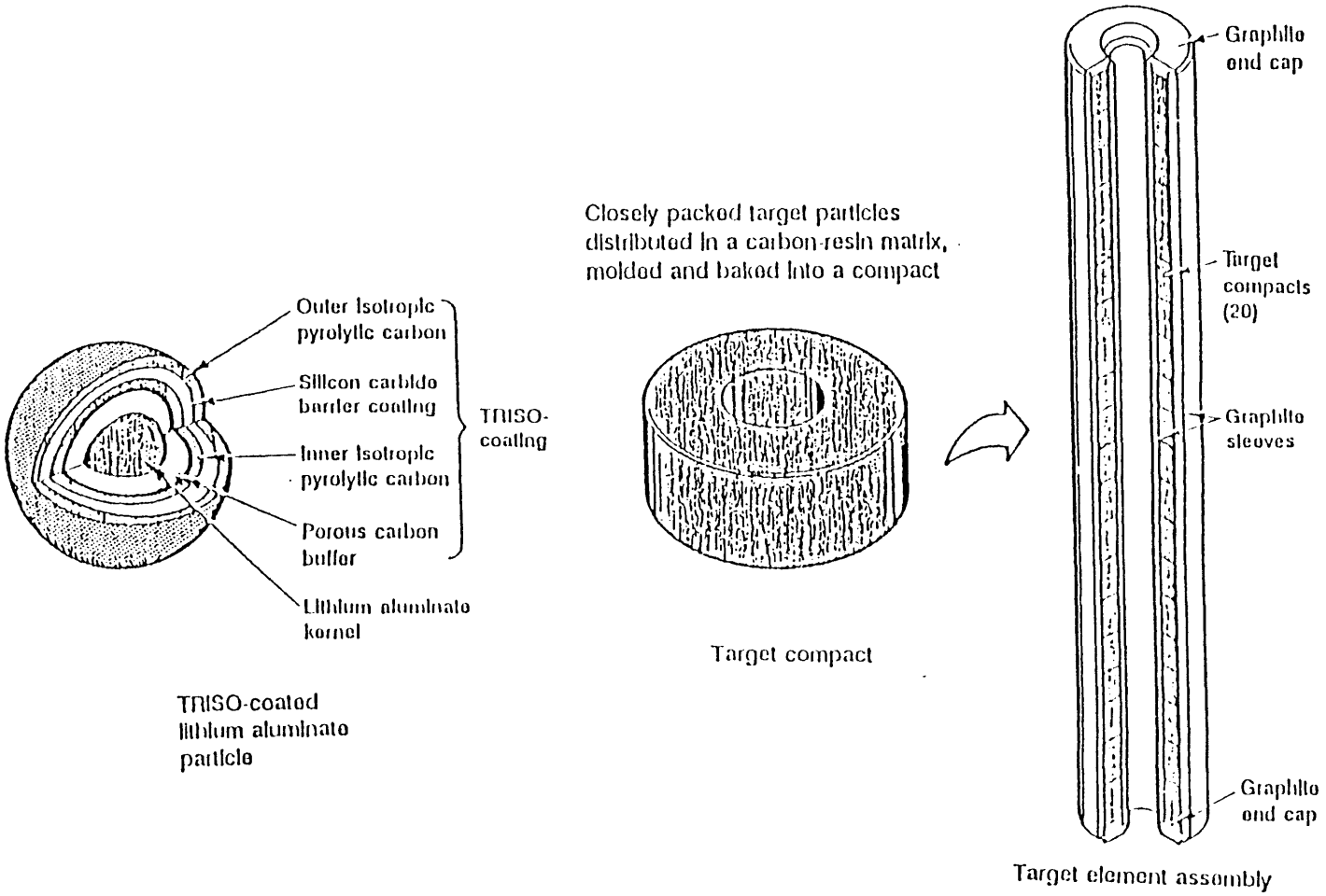

Figure 1. Target Element Components

of modeling the SiC layer alone versus all three layers of the coating, (b) the effect of using a constant versus a depleting tritium source in the calculations, (c) the effect of solubility in both the PyC and the SiC on tritium release, (d) a study of the effect of temperature and burnup on release as applicable to the safety experiments to be performed at Los Alamos National Laboratory (LANL), and (e) the amount of tritium that diffuses into the layers during normal operation and the need to model this behavior in postirradiation heating experiments. The results of sensitivity calculations to determine the effects of solubility, diffusivity, tritium pressure, and the trapping parameters on tritium release are presented in Section 5. Section 6 provides the theory supporting the development of an analytic solution for predicting tritium release from the target particles, explains the coding of the solution into the Tritium RELease code, TREL, and compares the code to TMAP. TMAP and TREL predictions are compared with experimental data in Section 7. The conclusions of the target particle modeling effort are presented in Section 8 and references are located in Section 9. Appendix A reports the details of the calculations and the input models, and Appendix B contains sample TMAP input decks. A listing of the TREL code along with sample input and output decks is given in Appendix C.

2. BACKGROUND ON DIFFUSION AND TRAPPING THEORY

The transport of a gas through a monocrystalline solid can be described using solid-state diffusion principles. The behavior is characterized using two parameters: diffusivity and solubility. The diffusivity, D, is a measure of the mobility of gas atoms transporting through the lattice. The solubility, S, is a measure of the amount of gas that can be dissolved in the solid. For many materials, the solubility is unknown or is high enough that it does not limit the transport. In these cases, simple diffusion theory, as found in classic texts such as Jost,[4] is used to describe the behavior of the gas in the solid.

The diffusion of a gas in a solid is believed to follow Fick's law of diffusion

$$\frac{\partial C}{\partial t} = D\nabla^2 C \tag{1}$$

where C is the concentration of the diffusing species (m^{-3}) and D is the diffusion coefficient (m^2/s). The surface flux, J ($m^{-2}s^{-1}$), as found from Fick's law is given by

$$J = -D\nabla C \tag{2}$$

Equation (1) can be solved for a variety of geometries and boundary conditions. For example, Olander[5] derives the fractional release, FR, of gas from a sphere of radius a (m) with an initial constant concentration in the sphere and zero concentration at the outer surface to be

$$FR = 6\left(\frac{Dt}{\pi a^2}\right)^{0.5} - 3\left(\frac{Dt}{a^2}\right). \tag{3}$$

Equation (1) can also be solved for the case of hydrogen diffusing

through a membrane or barrier using different boundary and initial conditions. For a membrane of thickness δ (m), boundary conditions of constant concentration C_o (m^{-3}) at the entrance side of the barrier and zero concentration at the exit side of the barrier, and an initial condition of no gas in the membrane, the solution to Equation (1), at sufficiently long times, is given by[4]

$$\frac{CR}{A} = \frac{DC_o t}{\delta} - \frac{C_o \delta}{6} \tag{4}$$

where CR is the cumulative release (atoms) and A is the surface area of the membrane (m^2). This constant concentration boundary condition, as illustrated above, is defined as the constant source condition. The value of the surface concentration can be defined to satisfy the boundary conditions of the problem of interest.

A plot of the actual solution for the constant source problem is compared with Equation (4) in Figure 2. As shown in the figure, a time lag exists from the time that the tritium begins to diffuse through the barrier until it reaches steady-state permeation as indicated by the constant slope of the release curve. This lag is termed the breakthrough time, or t_b (s), and is found by setting Equation (4) equal to 0, such that

$$t_b = \frac{\delta^2}{6D} \tag{5}$$

where δ is the thickness of the membrane (m) and D is the diffusion coefficient (m^2/s). Therefore, Equation (4) is only applicable after long times and, thus, predicts only the steady-state release accurately.

The constant source boundary condition is used in many applications. However, for the TRISO-coated target particles, a depleting source model is a better representation of the physical

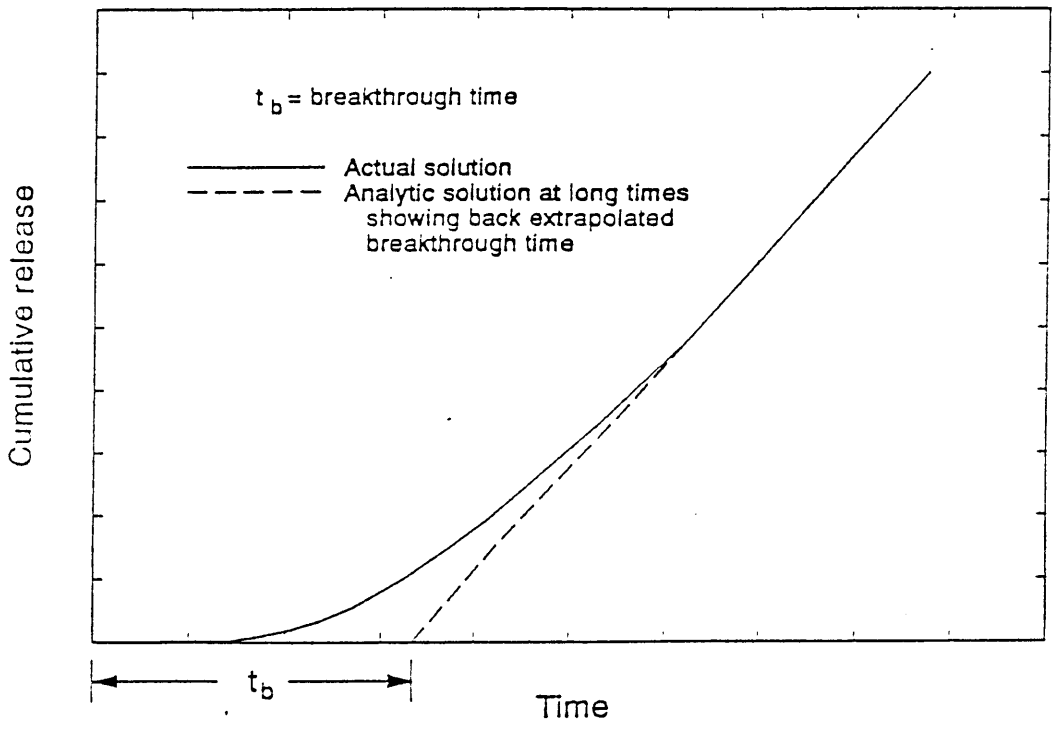

Figure 2. Comparison of release from a permeation experiment with Equation (3) indicating the classical breakthrough time.

situation because it models the limited tritium inventory in the particle. The depleting source consists of an initial concentration of gas in an enclosure of finite volume, or void volume, in contact with the surface of the material. The concentration in the enclosure depletes over time as the tritium diffuses into the material.

For a depleting source condition, the concentration at the void volume/membrane interface depends on the imposed boundary condition. Without solubility, this concentration, C (m^{-3}), is assumed to be equal to the average gas concentration in the enclosure which is found from the ideal gas law. Therefore,

$$C = \frac{n_{mole} N_{avg}}{V} = \frac{P}{kT} \tag{6}$$

where n_{mole} is the number of gmoles of the diffusing gas, N_{avg} is Avagodro's number (molecules/gmole), V is the volume of the enclosure (m^3), P is the partial pressure of the gas in the enclosure (Pa), k is Boltzmann's constant (J/K), and T is the temperature (K). In the event that the solubility of the gas in the material is important, as is the case for tritium, the concentration at the surface is related to the pressure in the enclosure by a solubility relation, such as

$$C = S_c N P^n \tag{7}$$

where S_c is the solubility constant (Pa^{-n}), N is the number density of the host material (m^{-3}), and n is an exponent less than or equal to 1. If n is equal to 1, then the concentration is said to follow Henry's law meaning the gas remains in molecular form during diffusion. If n is equal to 0.5, then Sievert's law of atomic transport applies indicating the gas dissociates and diffuses through the material in atomic form. The solubility constant, S_c, is the ratio of the number of atoms diffusing through the material to the number of host material atoms per Pa^n. It is specific to a certain material and is temperature and pressure dependent. (See Appendix A for additional details.)

The release rate of atoms from a membrane of thickness δ with a constant source and a solubility surface concentration boundary condition can be derived from the above equations. The cumulative release, CR, is given by Equation (4) with the substitution of C, the surface concentration given by Equation (7), for C_o to account for the solubility boundary condition. Thus, the flow rate of atoms released from the membrane, m (atoms/s), is obtained by differentiating CR with respect to time with the result given by

$$m = \frac{DSAP^n}{\delta} \tag{8}$$

where S denotes the solubility ($m^{-3}Pa^{-n}$) given by the product of the solubility constant S_c (Pa^{-n}) and N (m^{-3}), the number density of the host material. However, because Equation (4) only predicts steady-state diffusion, Equation (8) is also only applicable once steady-state release has begun. (This equation is also applicable for the quasi-steady case when P changes slowly with time due to depletion.)

This preceding discussion on transport works fairly well for isotropic monocrystalline materials. For polycrystalline materials however, the transport behavior of gases is more complex. The behavior has been described using the concepts of diffusivity and solubility; but the presence of grain boundaries, defects and/or impurities in the microstructure, and irradiation-induced defects complicates the picture. These defects in the solid matrix can cause trapping of the gas atoms during transport.

Trapping is a reasonably well-known phenomenon that is useful to describe the transport behavior of gases in a variety of materials, such as (a) tritium transport through graphite and other fusion reactor materials,[6,7] (b) hydrogen permeation through metals in aqueous solutions,[8] (c) hydrogen embrittlement in steels,[9] (d) fission gas release from irradiated nuclear fuels,[10] and (e) helium transport in irradiated metals.[11] Any type of flaw in the material, including natural and radiation-induced imperfections, bonds

strongly with gas atoms to cause trapping.[4] The traps act as a sink for gas atoms as they pass through the solid matrix. Irradiation produces many material defects, and thus the probability of trapping increases with radiation exposure. Because it takes a finite time to saturate the traps, gas is released more slowly from irradiated material than from material without traps. In other words, the breakthrough time increases with trap concentration. However, if the temperature is high enough, release of gas atoms from the traps, sometimes termed resolution, can occur.

Diffusion with trapping is modeled using the diffusion equation, Equation (1), with the addition of a sink term to describe the rate of trapping, as follows[1]

$$\frac{\partial C}{\partial t} = D\frac{\partial^2 C}{\partial x^2} - \frac{\partial C^T}{\partial t} \tag{9}$$

Trapping is governed by the equations[1]

$$\frac{\partial C^T}{\partial t} = w\frac{X_T^e}{N}C - rC^T \tag{10}$$

$$X_T^e = X_T^0 - C^T \tag{11}$$

$$w = \frac{D}{\lambda 2} \tag{12}$$

$$r = \upsilon_o \exp\left[-\frac{E_T - E_D}{RT}\right] \tag{13}$$

where

X_T^e = concentration of empty trapping sites (traps/m^3)

X_T^0 = initial concentration of traps (traps/m^3)

C = concentration of mobile gas atoms in the lattice (m^{-3})

C^T = concentration of trapped gas atoms (m^{-3})

N = number density of the host material (atoms/m^3)

w = trapping rate (s^{-1})

r = resolution rate (s^{-1})

D = diffusion coefficient (m^2/s)

λ = jump distance (m)

υ_o = release attempt frequency (s^{-1})

E_T = trap site binding energy (J/gmole)

E_D = diffusion activation energy (J/gmole)

R = gas constant (J/gmole-K)

T = temperature (K).[a]

Equation (10) indicates that the concentration of trapped atoms, C^T, varies over time as free atoms become trapped or are released from the traps. The rates of these processes are given by the trapping rate, w, and the release rate, r, in Equations (12) and (13) respectively. The concentration, C, is thus the concentration of untrapped, or mobile atoms diffusing through the material.

In the special case where the trapping and resolution rates are both high, the trapping and resolution processes are in a quasi-equilibrium. The effects of trapping can then be modeled with an apparent diffusion coefficient, D_{app} (m^2/s), given by

---

a. For simplicity, it is assumed in Equations (9) through (13) that only one gas is diffusing, only one type of trap exists, and only one gas atom can occupy a trap at any given time.

$$D_{app} = D\left(\frac{r}{r + w\frac{X_T^e}{N}}\right) \tag{14}$$

where all parameters are defined above.[5] With the substitution of D_{app}, diffusion with trapping can be modeled by Equation (1) and the release is given by Equation (3) for the stated boundary and initial conditions even though traps exist in the material.

3. TMAP CODE AND INPUT MODEL

3.1 TMAP Code Description

TMAP[b] was developed at the Idaho National Engineering Laboratory (INEL) and originally modeled tritium behavior in fusion reactor systems. However, application of the code to NP-MHTGR target particles has proven to be very useful for studying tritium diffusion through the TRISO coating of the target particle. The code, written in Fortran 77, is relatively small consisting of approximately 5000 lines in the preprocessor and about 2600 lines of main code. The preprocessor formats the input for the main program and checks for input errors. An output file and a plot file are generated by the code. The plot file contains user specified output in columnar format while the output file contains more detailed information. A schematic of the code execution scheme is shown in Figure 3. The code has been implemented on a MAC SE/30 under MPW Language Systems and on an IBM PS/2 with a Lahey compiler. Older versions of TMAP have been run on the MFE Cray.

The TMAP code solves the one-dimensional diffusion and trapping equations [Equations (9) through (13)] in a slab geometry for a range of heat and mass transport boundary conditions. Adiabatic and convective conditions can be declared as the thermal boundary condition, or a specified surface heat flux or temperature can be applied to the boundary. In addition to modeling diffusion with Fick's law, the Soret effect can also be invoked to model thermally driven diffusion. The diffusion modeling options include an impermeable barrier, a specified surface concentration, a rate dependent dissociation and recombination condition, and a Henry's or Sievert's law solubility condition. Adjacent materials can be linked to indicate contact in composite structures. The diffusion across the interface is then determined by modeling Sievert's or

---

b. TMAP Mod3 Cycles 3 and 4 were used in this work.

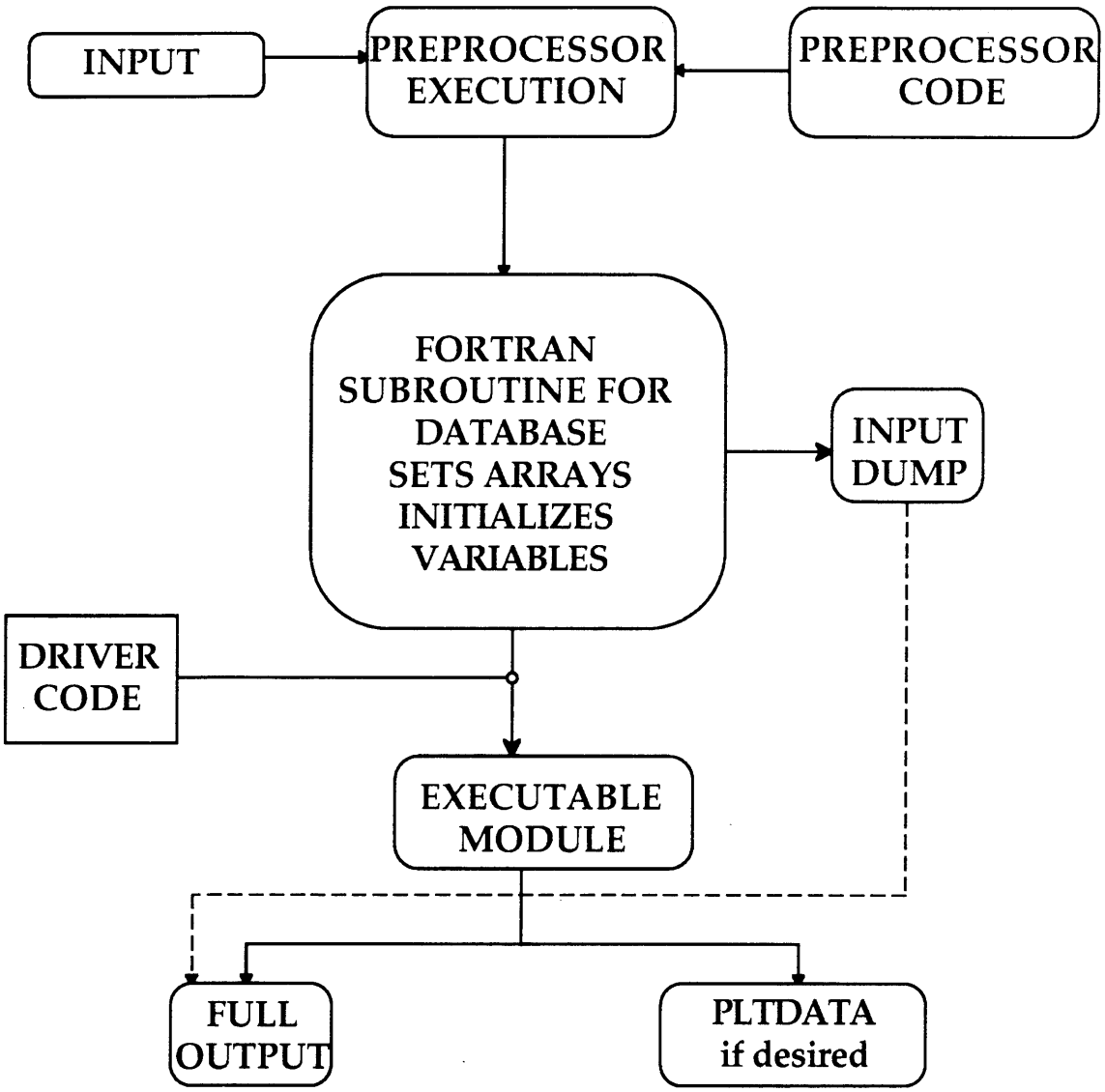

Figure 3. TMAP code execution scheme.

Henry's law which results in a discontinuous concentration gradient at the surface or by ignoring solubility effects to model a continuous concentration at the interface.

Transport volumes (e.g. the particle void volume and the tritium collection volume) are modeled in TMAP with enclosures. These enclosures can be joined to structures to model surface fluxes and transport paths in tritium processing systems. The volume and temperature of the enclosure are input along with the partial pressure of each specie present. The number of atoms in the volume is then calculated from the ideal gas law. Optional input parameters include the rate of outflow of atoms from one enclosure to another and any chemical reactions occurring in the enclosure. Use of the latter option models the formation of new species, such as tritiated water from the reaction of tritium and water. The code also models molecular tritium dissociation and the recombination of T to create T_2. These capabilities are used when Sievert's law of diffusion is imposed.

When trapping is considered, the concentration of traps in the material, the trapping rate, and the release rate must be specified. TMAP allows each trap to hold only one gas atom at any given time. A diffusing atom becomes trapped when it jumps into a specific unoccupied trapping site instead of an adjacent lattice site. Irreversible trapping is modeled by inputting a resolution rate of zero.

TMAP has a unique format for data input. The diffusivity, solubility, and any other user-specified parameter can be input as time, temperature, and/or specie concentration dependent equations. Tables can also be used to define parameters as a function of time or temperature. This format gives the user the added flexibility of varying these parameters but also requires a portion of the code to be recompiled and linked at the beginning of each run.

The TMAP code does have some limitations. Spherical

geometries cannot be modeled explicitly as the code is limited to a one-dimensional slab geometry. (Spherical geometries can be modeled in dimensionless form for specialized boundary conditions. However, the depleting source condition and trapping cannot be modeled, and thus, the dimensionless spherical model was not considered.) Although the temperature of the structures can be changed with time either on input or as the solution to the heat conduction equation dictates, the temperature in the enclosure cannot be changed. As a result, the code cannot be used for transient cases where the amount of tritium in the enclosure is temperature dependent. Also, when using solubility relations, only Sievert's or Henry's laws can be used, when in reality, the value of the pressure exponent may not be exactly equal to 0.5 or 1.0. Additional information about the code is found in the TMAP manual.[1]

3.2 Input Models

Two different input models were developed to understand tritium transport through the TRISO-coated, NP-MHTGR target particle. (See Section 1.1 for a description of the particle.) In the first model, the porosity in the buffer and the lithium aluminate kernel is modeled as a void volume, or enclosure, filled with tritium gas that diffuses through the SiC layer; the IPyC and OPyC layers are omitted from the analysis. This representation is termed the SiC model. In the second model, the porosity in the buffer and the lithium aluminate kernel is again represented by an enclosure; however, transport through all three of the layers is considered. This model, as shown schematically in Figure 4, is called the trilayer model. In both cases, all tritium gas generated by the irradiation of lithium is assumed to be released and to reside in the buffer void volume. Because the TMAP code cannot easily model a sphere, the PyC and SiC layers are depicted as slabs. However, the use of the slab model is validated in Section 3.3.2 and 3.3.3 where the analytic solution for the slab is compared with the spherical solution. The tritium release from the particle accumulates in an enclosure on the exit side or outer surface of the TRISO coating. The compact matrix material is

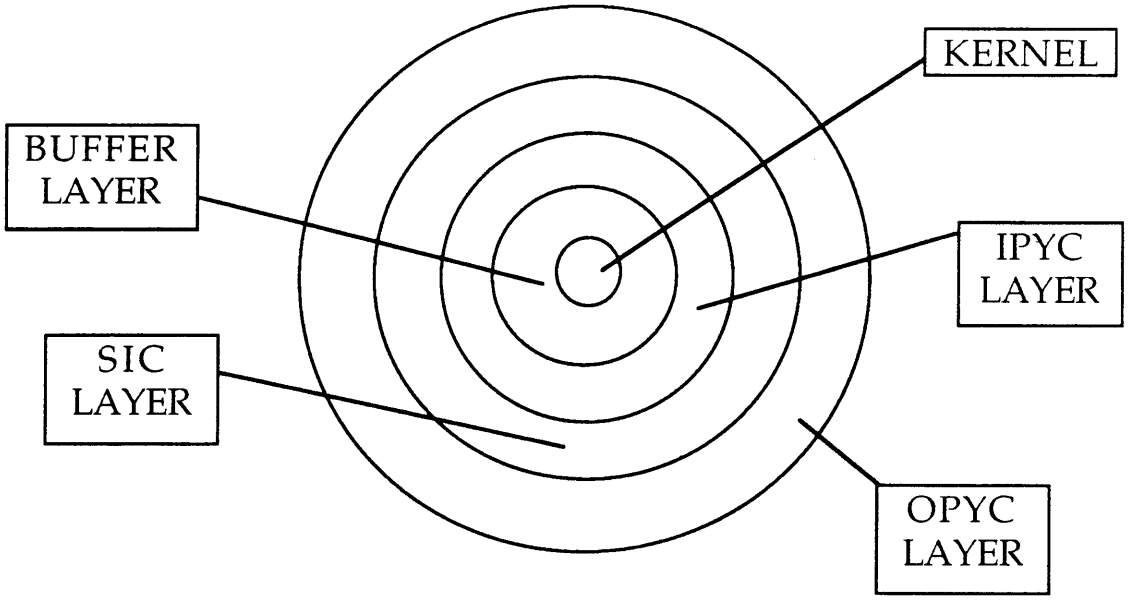

TRITIUM TARGET PARTICLE
(NOT TO SCALE)

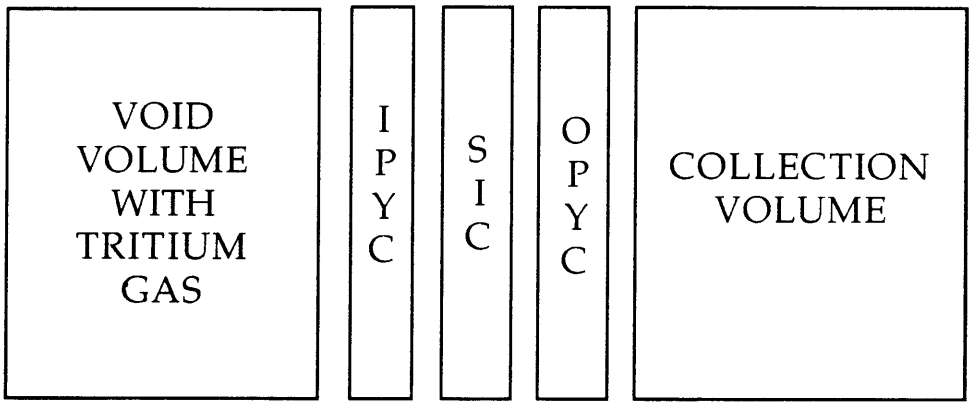

TMAP TRILAYER MODEL OF TARGET PARTICLE

Figure 4. Schematic of target particle and TMAP model.

not considered in the model because its large internal porosity is assumed to result in limited tritium retention.

Two types of boundary conditions were applied to the tritium source. The constant source condition consists of a constant tritium concentration applied to the surface of the first layer. This concentration does not change with time. With the depleting source condition, on the other hand, the entire concentration of tritium available for diffusion resides in an enclosure connected to the surface of the first layer at time zero. Then, the number of atoms in the enclosure depletes over time as the tritium diffuses through the particle. The concentration at the exit side of the particle was set to zero in both cases.

Early calculations assumed the concentration at the surface of the layer to be equal to the average concentration in the enclosure. Later, solubility relations for the PyC and the SiC, as measured by Causey[6,12,13] were added to the model. Causey's work indicates that Sievert's law [see Equation (7)] is applicable to describe the relationship between the concentration of tritium at the surface and the partial pressure of tritium gas, or T_2, in the void volume. A similar solubility condition was also applied at the PyC/SiC interfaces. Thus, the surface concentrations at each interface are related by the ratio of solubility constants. Causey's research[6,12,13] also supplied the empirical data on tritium diffusivity in PyC and SiC. (Calculations in Sections 4 and 5 used the PyC relations given in Reference 12 while Sections 6 and 7, including the TREL code, used more recent data from Reference 6.) The solubility and diffusivity relations[6,13] are plotted in Figure 5 as a function of temperature for reference.

Because of the particle's small size and good heat transfer characteristics, the entire particle is always assumed to be at the same temperature; thus Soret's effect for thermal diffusion is not modeled. During temperature ramp experiments, the layers were modeled with a high thermal conductivity and a low specific heat to

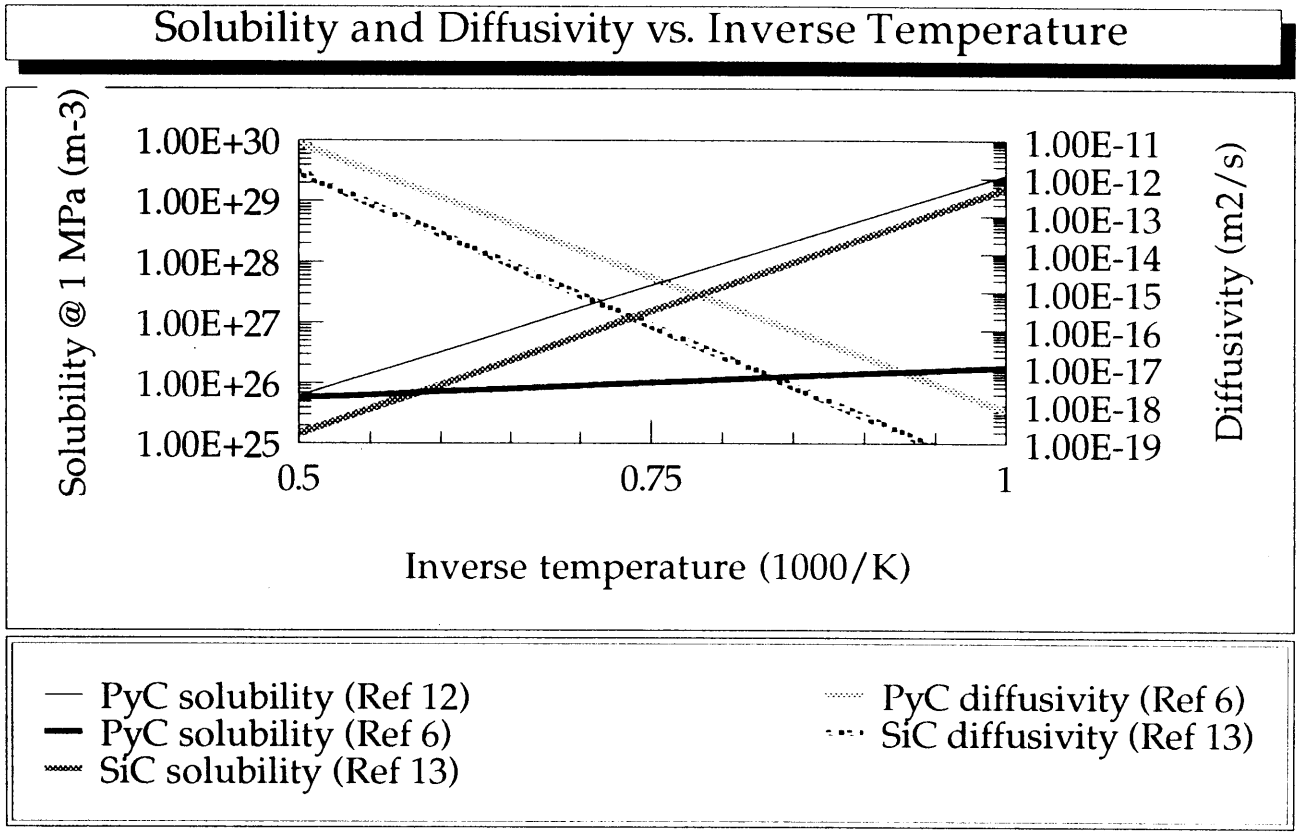

Figure 5. Comparison of SiC and PyC solubilities and diffusivities.

achieve this uniformity. Thermal expansion effects which could result in gaps between the layers and affect the concentration equilibrium at the coating surfaces, were assumed to be negligible in all calculations because the layers are bonded together during manufacturing.

The initial concentration of tritium gas is a function of the internal tritium partial pressure in the particle, which in turn is a function of the particle void volume, burnup,[c] and temperature. Tritium partial pressures as a function of burnup and temperature for ATR-3 particles are shown in Table 1. Details of the calculation are given in Appendix A.

Table 1. Tritium partial pressure (MPa) as a function of temperature and burnup for ATR-3 particles

	Temperature(°C)						
Burnup (%)	1200	1300	1400	1500	1600	1700	1800
45	10.0	10.7	11.4	12.0	12.8	13.5	14.1
33	7.36	7.86	8.36	8.86	9.36	9.86	10.4
18	4.02	4.29	4.56	4.83	5.11	5.38	5.65

Different particle dimensions were used during the course of the work to reflect the different target particle designs used in the

c. Burnup is given in % which is understood to represent atom percent of ^{6}Li.

Tritium Target Program.[2] Dimensions of the particles used in the ATR-1 test were used in the calculations discussed in Sections 4.1 through 4.4 while dimensions of particles from the ATR-3 irradiations, which represent the latest NP-MHTGR reference target particle design, were used in calculations in Section 4.5.[d] Appendix A provides detailed descriptions of each of the geometries. It is important to note that the changes in geometry do not affect the results presented in these sections because only models with the same dimensions are compared.

3.3 TMAP Code Verification

A variety of boundary conditions were applied to the basic diffusion equation, Equation (1), and the analytic solutions were compared with the results from the TMAP code. The following problems were examined using the SiC layer model at 2100°C: tritium release for a depleting source boundary condition, diffusion in a semi-infinite slab with a constant source, diffusion in a partially loaded semi-infinite layer, and permeation through a layer affected by trapping and resolution. Diffusion through a composite structure containing a PyC and a SiC layer was also studied. Schematics of the input models are shown in Figure 6. The TMAP solution often differed greatly from the analytic solution in the first 6.92 seconds (breakthrough time at 2100°C) because the initial filling of the layer is a very difficult numerical problem for TMAP. However, these differences are not significant because they dampen out quickly; the code exhibited agreement with the analytic solutions to within 1%

---

d. The ATR-1 model was scoping in nature and different surface areas were used at each interface to mockup the spherical geometry. Since TMAP only models slab geometry, these results are somewhat inaccurate. However, the conclusions derived from these results are still valid when compared to one another. The ATR-3 model used a constant surface area at all interfaces for consistency and accuracy.

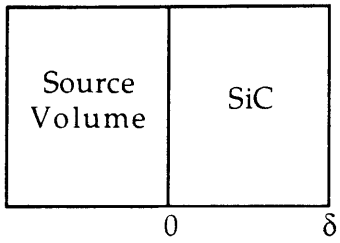

Depleting Source Model
w/ Slab Geometry

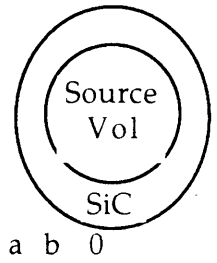

Depleting Source Model
w/ Spherical Geometry

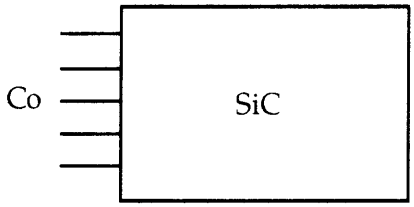

Constant Surface
Concentration on
Semi-infinite Slab

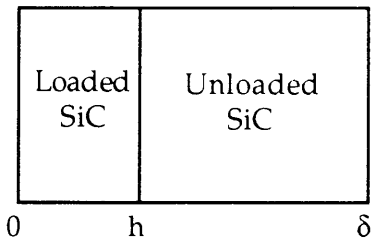

Partially Loaded
Semi-infinite Slab

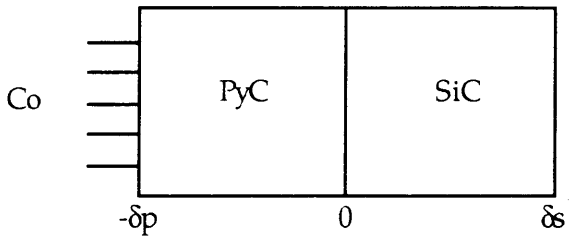

Constant Surface Concentration
on Composite Slab

Figure 6. Schematics of Physical Situations Modeled in Verification Studies

breakthrough time is reached as discussed in the following sections. These simple test cases provide the initial verification of the TMAP code for modeling NP-MHTGR target particles.

3.3.1 Constant Source Model/Slab Geometry

The results for a constant source of tritium applied at the inner SiC boundary at 1200°C are compared with the analytic solution, Equation (4), in Figure 7. An initial variance occurs because Equation (4) holds only when steady-state conditions are established. Otherwise, differences between the two solutions are within 1%.

3.3.2 Depleting Source Model/Slab Geometry

The depleting source model consists of an enclosure containing a finite concentration of atoms which are allowed to diffuse into the SiC layer over time as shown in Figure 6. Evans and Morgan[14] give the fractional release, FR, from a depleting source model in slab geometry as

$$FR = 1 - \sum_{1}^{n} \frac{2L\sec\alpha_n \exp\left(-\alpha_n^2 \frac{Dt}{\delta^2}\right)}{L(L+1) + \alpha_n^2} \qquad (15)$$

where

$$L = \frac{\delta A}{V\phi}$$

$$\phi = \frac{\text{source concentration}}{\text{layer concentration}} = 1 \text{ (no solubility)}$$

A = surface area (m^2)

V = source volume (m^3)

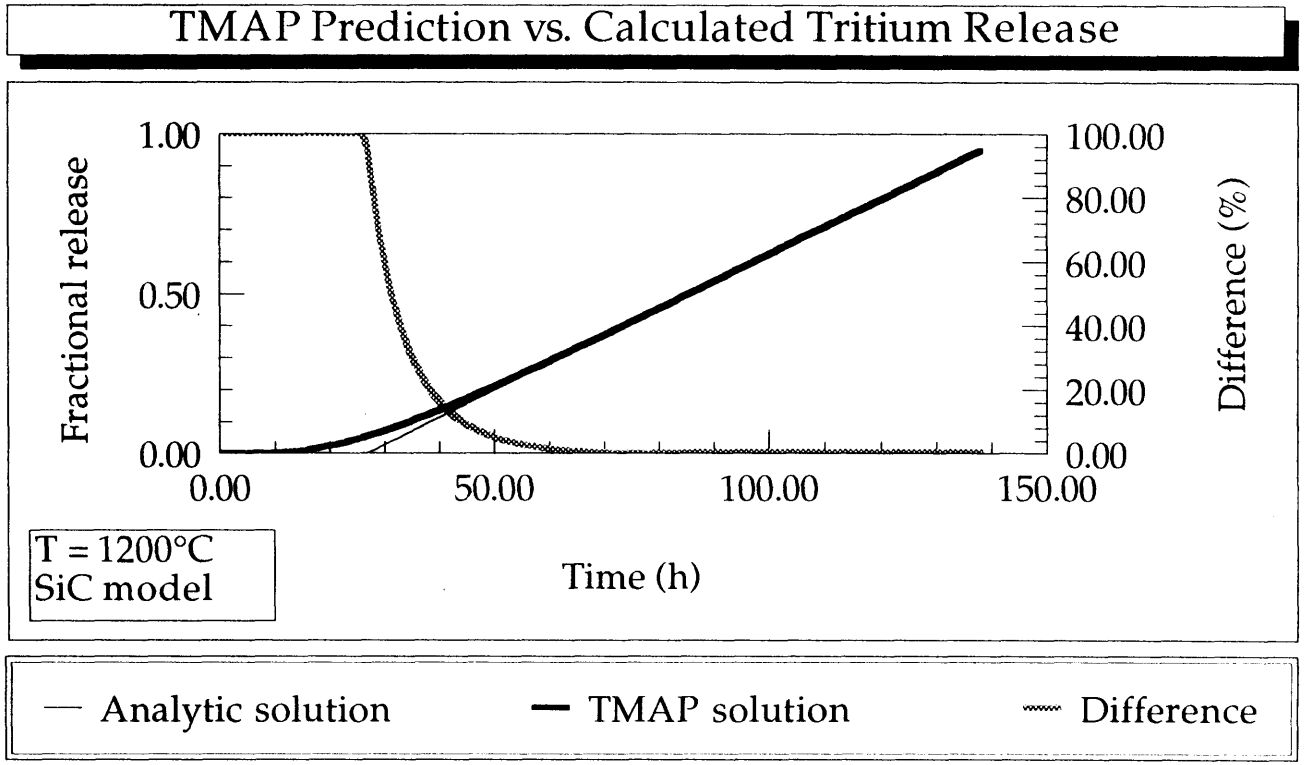

Figure 7. Comparison of TMAP tritium release prediction vs. analytic solution [Equation (4)] at 1200°C from the SiC model.

δ = layer thickness (m)

D = diffusion coefficient (m^2/s)

and α_n are the roots of

$$L = \alpha_n \tan\alpha_n \tag{16}$$

The TMAP release is compares very well with this solution as shown in Figure 8. A 10% difference is seen after breakthrough but the difference decreases to approximately 2% at long times.

3.3.3 Depleting Source Model/Spherical Geometry

The solution of the depleting source problem in spherical coordinates is given by Morgan and Malinauskas[15]

$$FR = 1 - \frac{4Ka}{b}\sum_{1}^{n} \frac{\exp\left(-\alpha_n^2 \frac{Dt}{\delta^2}\right)\sin\alpha_n}{\left[2K\alpha_n + \frac{4b\alpha_n}{\delta}\sin^2\alpha_n - K\sin(2\alpha_n)\right]} \tag{17}$$

where

$$K = \frac{Ab}{V\phi}$$

a = outer radius of layer (m)

b = inner radius of layer (m)

and α_n are the roots of

$$\cot\alpha_n = \frac{b\alpha_n}{K\delta} - \frac{\delta}{b\alpha_n} \tag{18}$$

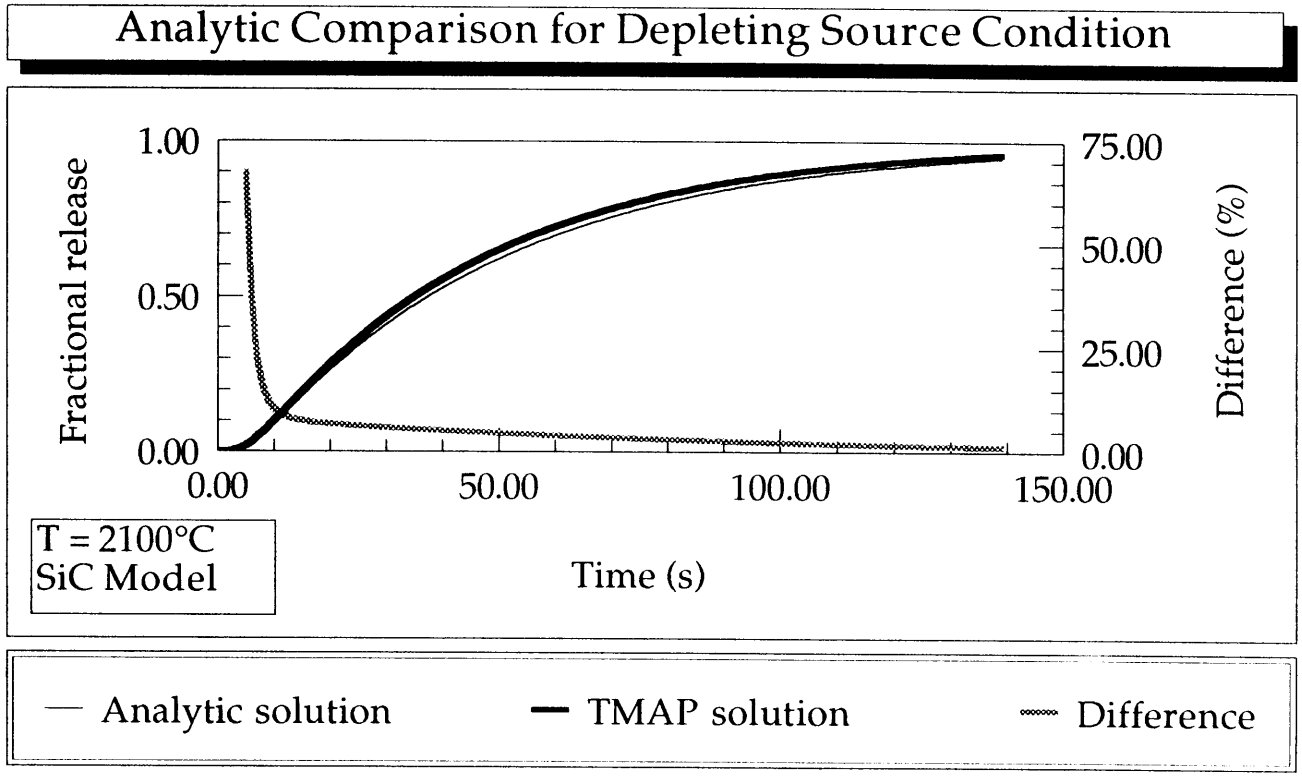

Figure 8. Comparison of the TMAP fractional release for a depleting source condition and slab geometry with the analytic solution given by Equations (15) and (16).

in addition to the variables defined in Section 3.3.2. As shown in Figure 9, the spherical solution agrees with the TMAP slab model prediction to within 1% which indicates that the slab representation adequately models the spherical geometry of the actual target particle. The difference is small because the spherical solution approaches that of the slab for a large radius to thickness ratio as is the case for the SiC layer. The spherical and slab analytic solutions are compared directly in Figure 10. The results from the two geometries differ by less than 10% with the variance decreasing with time. The TMAP prediction falls between the spherical and slab solutions and does not differ significantly from either analytic result.

3.3.4 Constant Source Model of Semi-infinite Slab

The concentration, C (m^{-3}), in a semi-infinite slab with a constant surface boundary condition is given by[16]

$$C = C_o \text{erfc}\left(\frac{x}{2\sqrt{Dt}}\right) \tag{19}$$

where C_o (m^{-3}) is the concentration applied to the surface and x (m) is the location in the slab. The diffusion coefficient and initial concentration were set to one in the semi-infinite model for simplicity. Figure 11 shows that the TMAP calculation is within 1% of the analytic solution for the concentration as a function of time at x = 0.2 m. The concentration versus position in the slab after 25 s is compared in Figure 12. The code results are in excellent agreement, within 0.5%, with the analytic solution. The diffusive flux, J ($m^{-2}s^{-1}$), into the semi-infinite layer is found from Equation (2) using the concentration given in Equation (19) yielding

$$J = C_o\sqrt{\frac{D}{\pi t}}\exp\left(\frac{x}{2\sqrt{Dt}}\right) \tag{20}$$

The TMAP flux prediction is compared with this solution in Figure 13. A large initial variance occurs but the difference decreases to less than

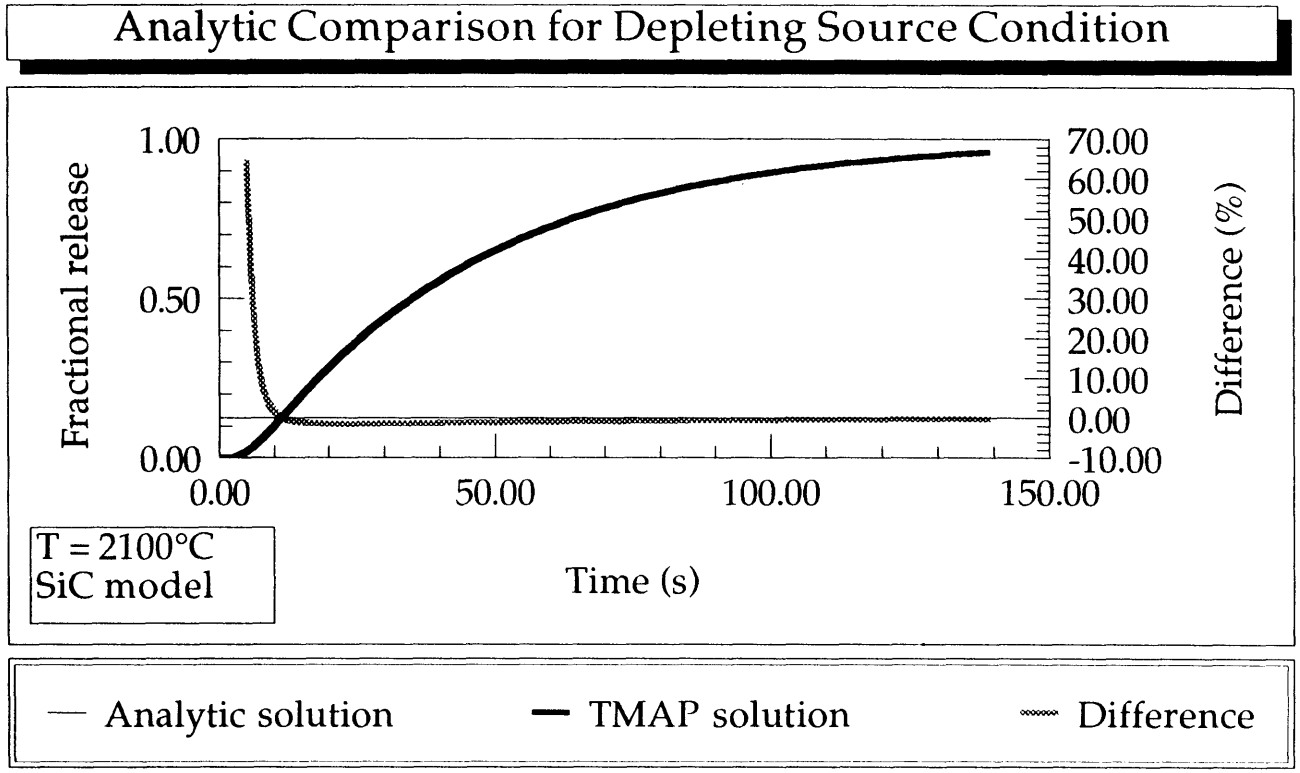

Figure 9. Comparison of the TMAP fractional release for a depleting source condition and spherical geometry with the analytic solution given by Equations (17) and (18).

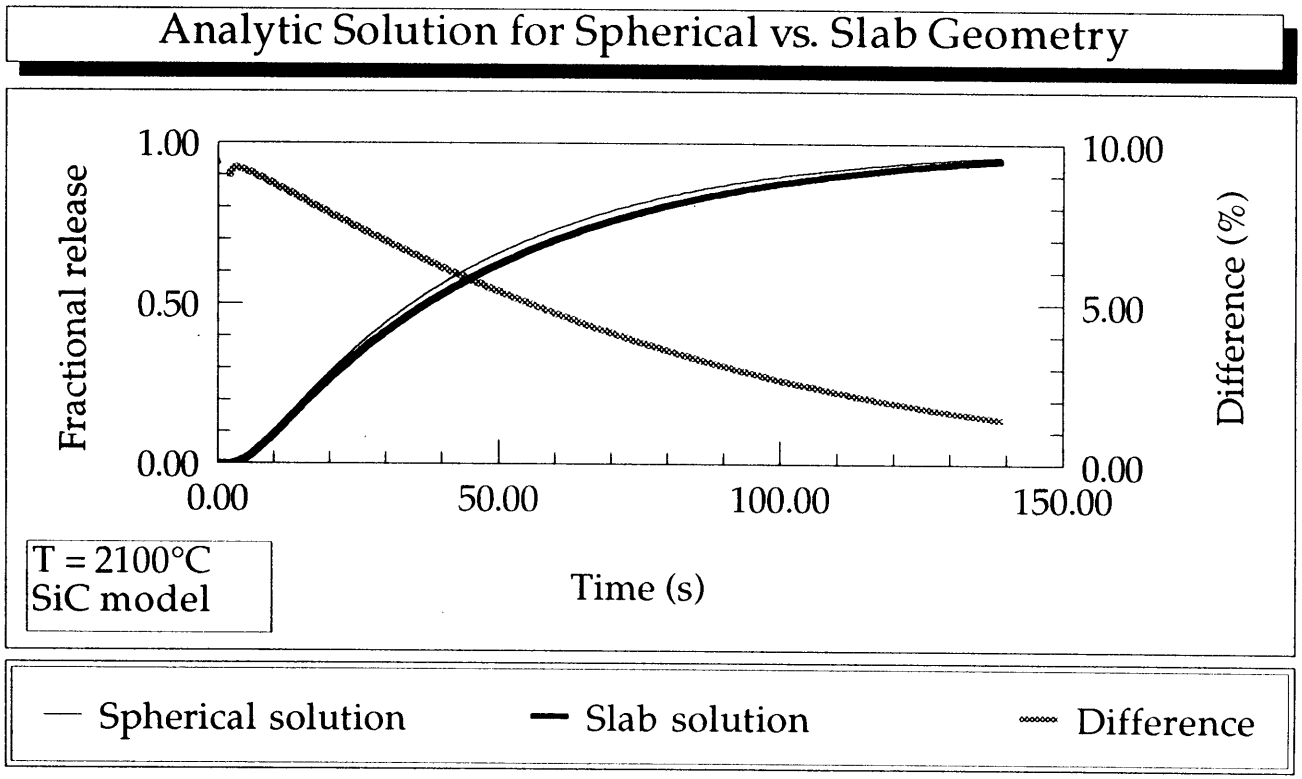

Figure 10. Comparison of the analytic solutions for spherical vs. slab geometry with the depleting source condition.

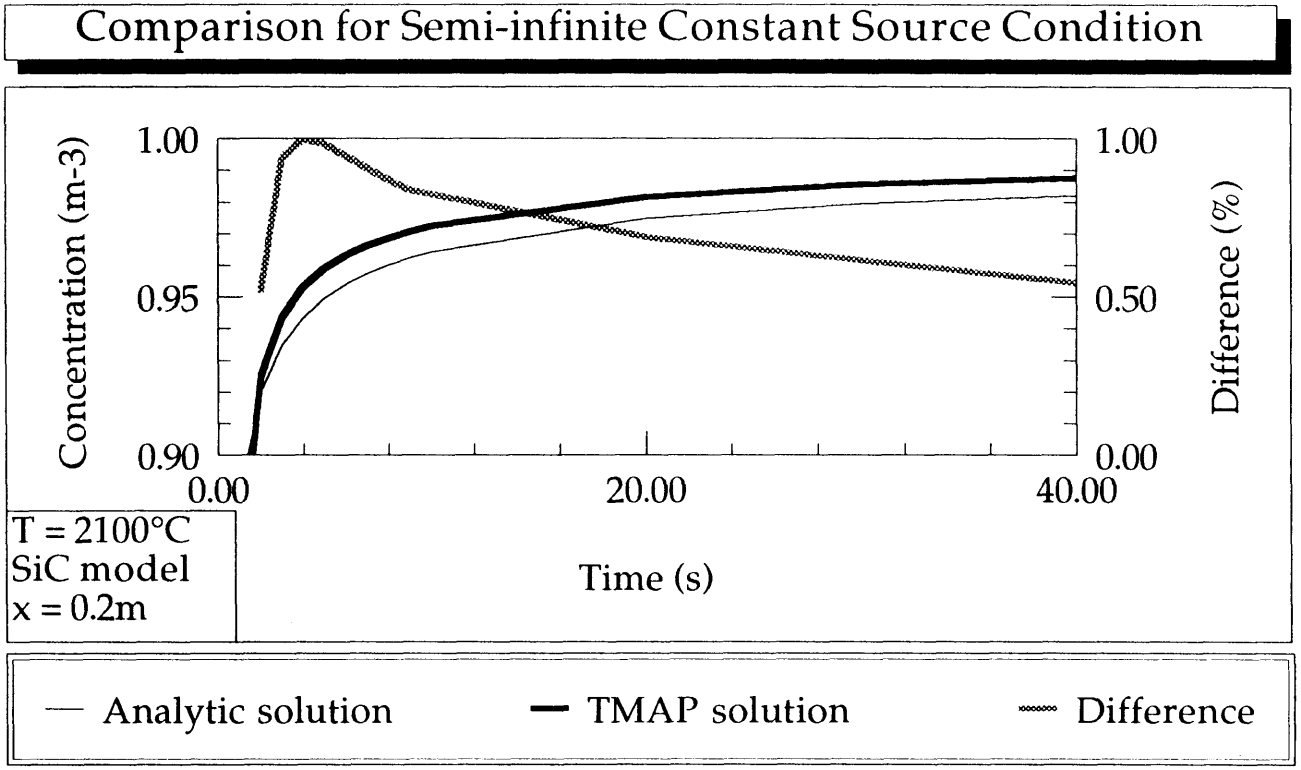

Figure 11. Comparison of the TMAP concentration as a function of time for the constant source condition applied to a semi-infinite layer with the analytic solution given by Equation (19).

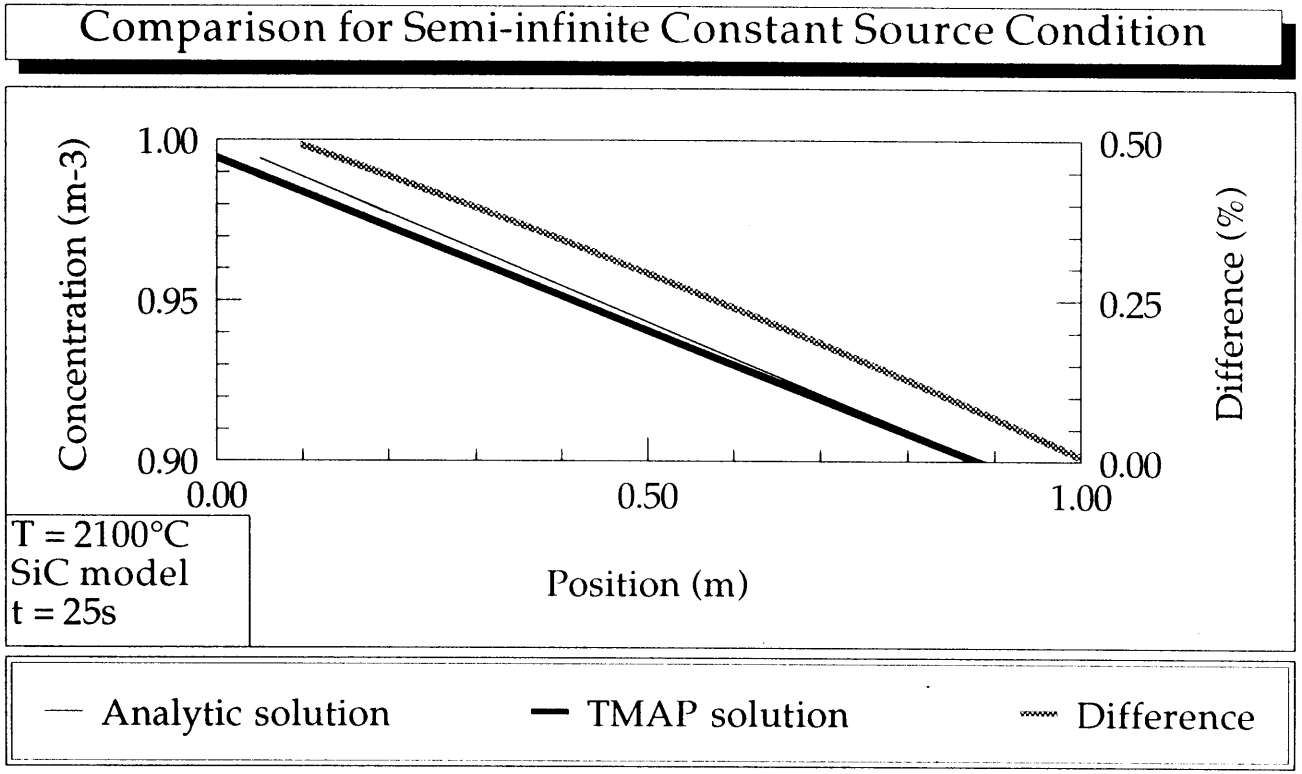

Figure 12. Comparison of the TMAP concentration as a function of position for the constant source condition applied to a semi-infinite layer with the analytic solution given by Equation (19).

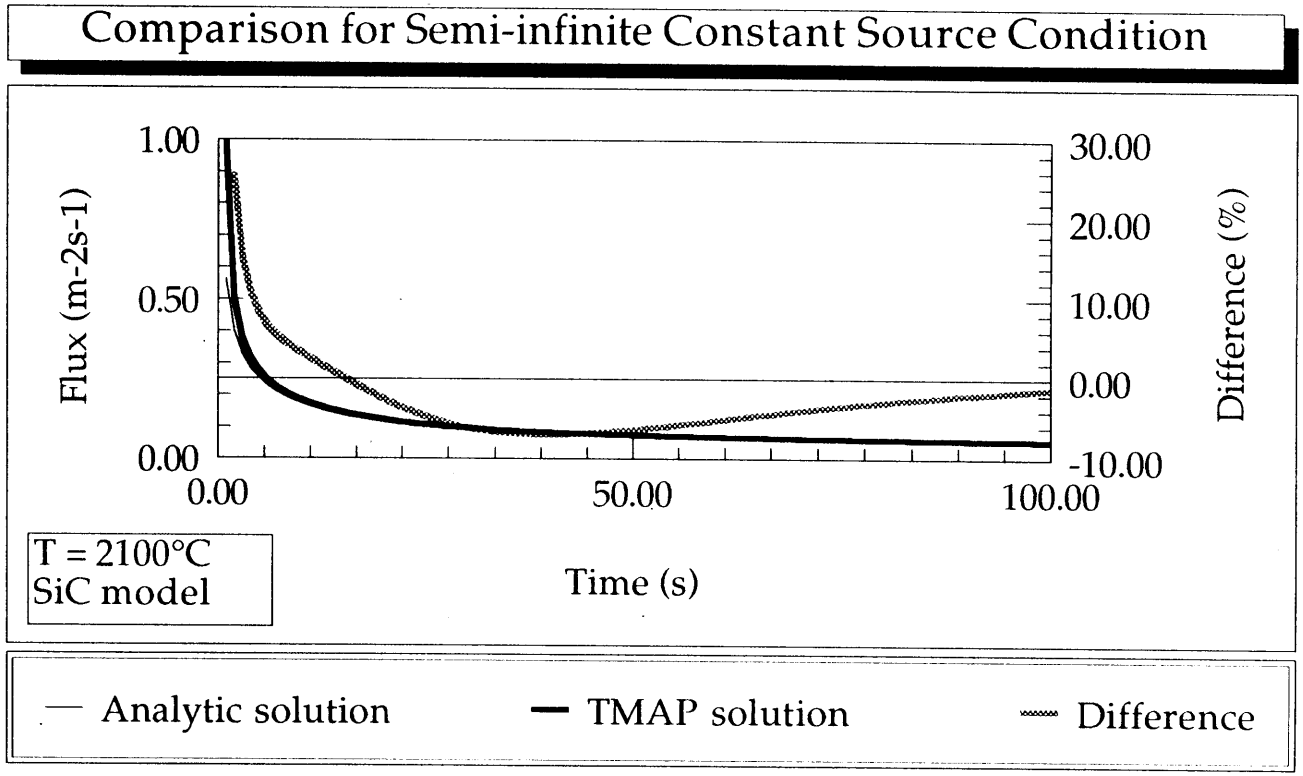

Figure 13. Comparison of the TMAP flux into the layer for the semi-infinite constant source condition with the analytic solution given by Equation (20).

7% after 6 seconds.

3.3.5 Partially Loaded Semi-infinite Slab

The solution for a semi-infinite, partially loaded SiC layer was also compared. The first 10 m of a 2275-m slab (i.e. semi-infinite) were initially loaded to a concentration of 1 atom/m^3. (See Figure 6) The analytic solution to this problem is given by Jost[3] to be

$$C = \frac{C_o}{2}\left[\text{erf}\left(\frac{h-x}{2\sqrt{Dt}}\right) + \text{erf}\left(\frac{h+x}{2\sqrt{Dt}}\right)\right] \tag{21}$$

where h (m) is the thickness of the loaded portion of the layer. The results for the concentration as a function of time at x = 12 m are plotted in Figure 14. The concentration at the surface, x = 0, is given by

$$C = C_o\text{erf}\left(\frac{h}{2\sqrt{Dt}}\right) \tag{22}$$

and at x = h as

$$C = \frac{C_o}{2}\text{erf}\left(\frac{h}{\sqrt{Dt}}\right) \tag{23}$$

The TMAP-calculated concentrations overlay the respective analytic solutions at x = 0 and x = h as shown in Figures 15 and 16, respectively. At x = 0, the two solutions vary by less than 0.2% which is reduced to less than 0.05% after 20 seconds. At x = h, the variance never exceeds 0.05%.

3.3.6 Permeation Problem

For the classic problem of permeation through a membrane

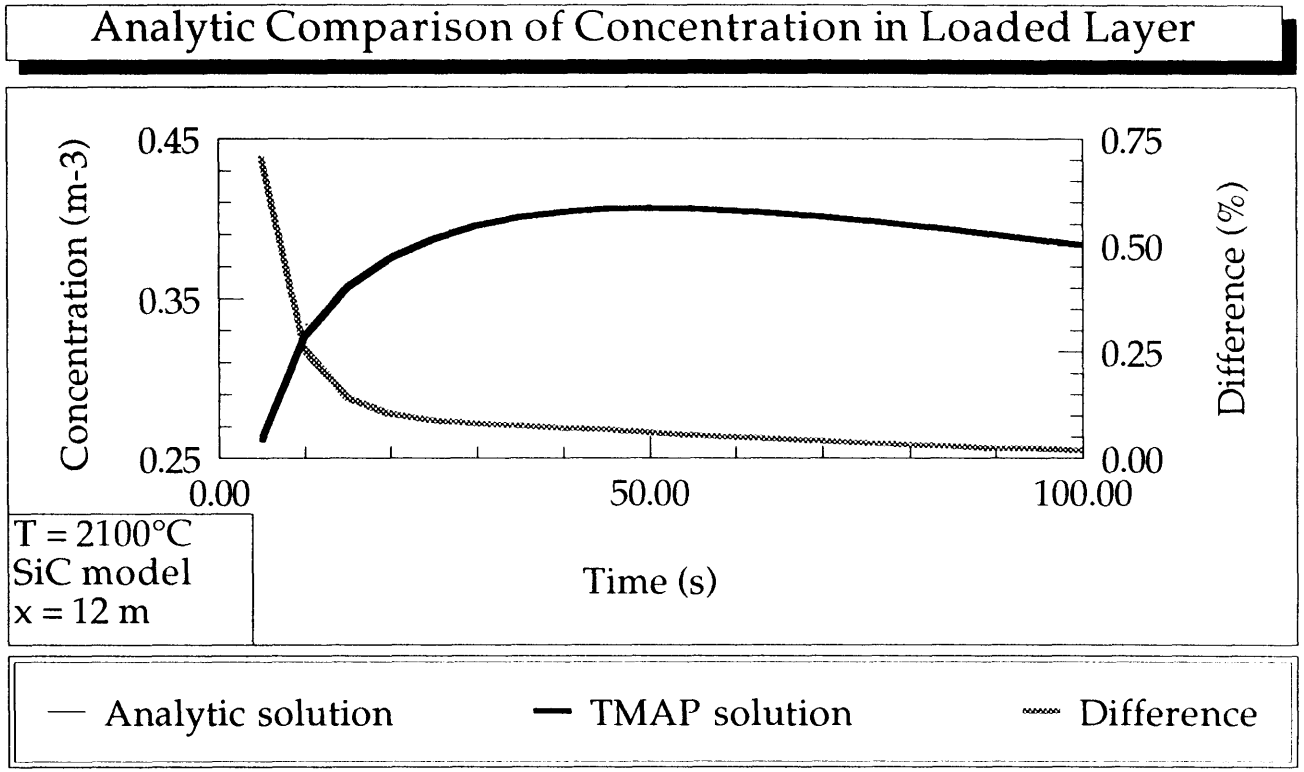

Figure 14. Comparison of the TMAP concentration for a partially loaded semi-infinite layer with the analytic solution given by Equation (21).

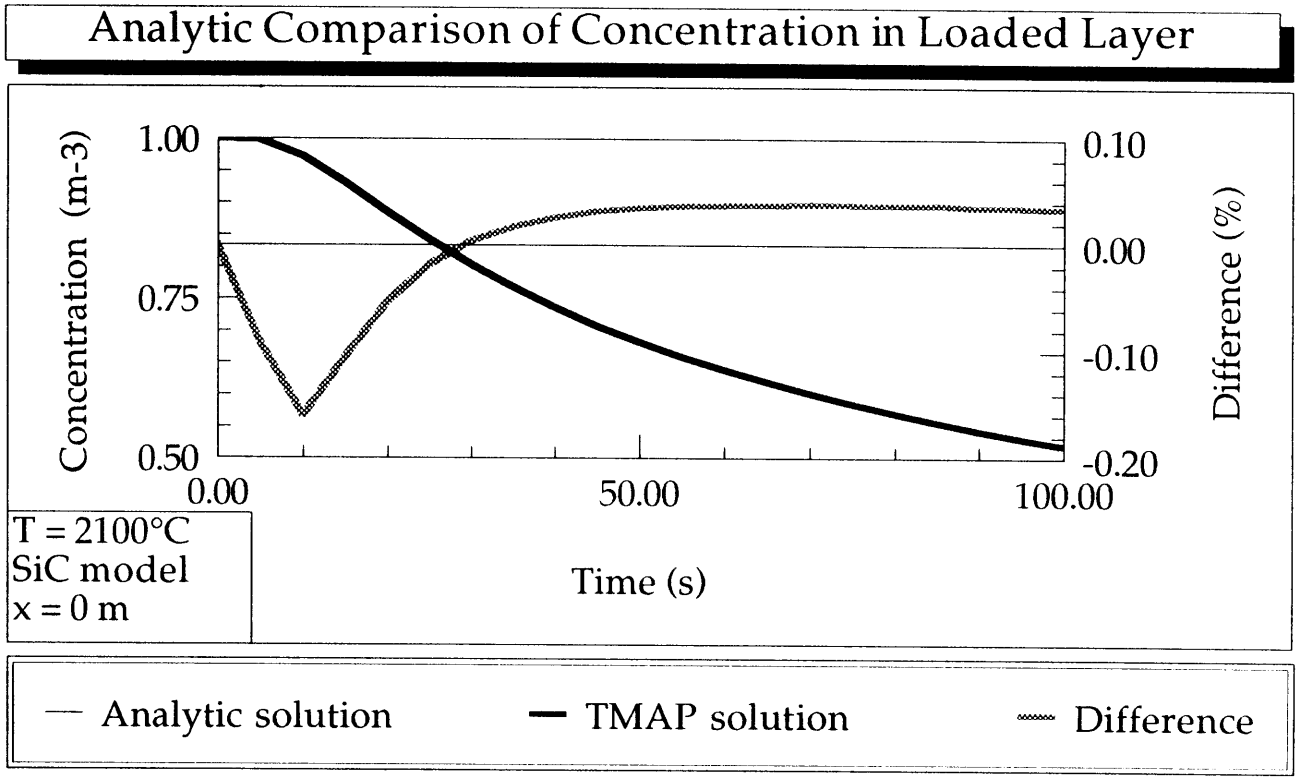

Figure 15. Comparison of TMAP concentration for a partially loaded semi-infinite layer with the analytic solution given by Equation (22).

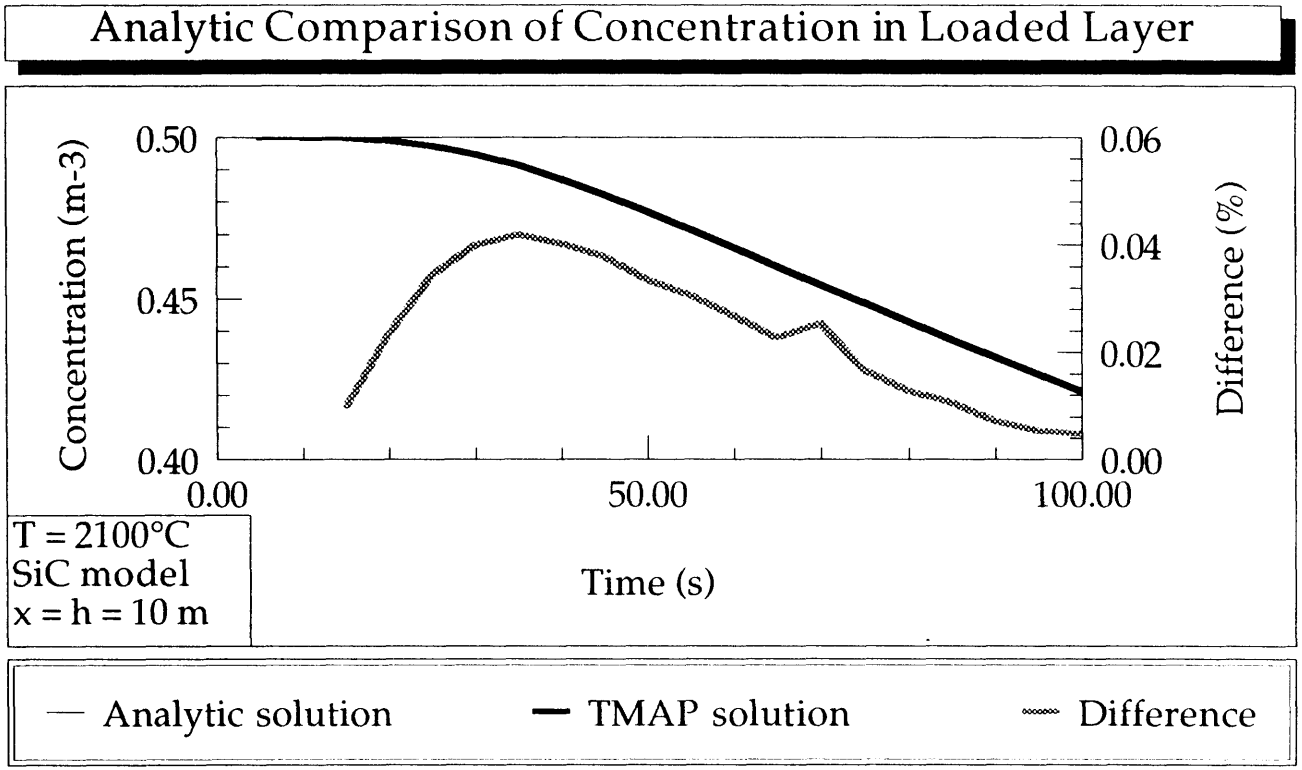

Figure 16. Comparison of the TMAP concentration for a partially loaded semi-infinite layer at x = h with the analytic solution given by Equation (23).

under the condition of a constant source, the breakthrough time, t_b (s), is given by Equation (5). When trapping occurs with high resolution and trapping rates, the process can be modeled with an apparent diffusion coefficient, D_{app}, given by Equation (14). With the use of D_{app}, the breakthrough time for diffusion with trapping is given by Equation (5).[5] From the TMAP solution, the breakthrough time is determined from a back extrapolation of the steady state release portion of the curve to zero as illustrated in Figure 2. Figure 17 compares the breakthrough time found from the TMAP results with the analytic solution for a trapping rate of 1.52×10^9 s^{-1} and a resolution rate of 1.52×10^8 s^{-1}. The back extrapolated result is within 0.5% of the analytic solution.

3.3.7 Composite Layer

A composite layer of PyC ($-\delta_p < x < 0$) and SiC ($0 < x < \delta_s$) as shown in Figure 6 was also studied. With a constant concentration applied to the exposed surface of the PyC, the concentration in the second layer (SiC) of the composite is given by Carslaw and Jaeger[17]

$$C = C_o \frac{D_{PyC}(\delta_s - x)}{\delta_s D_{PyC} + \delta_p D_{SiC}} - 2C_o \sum_{1}^{n} \frac{\sin(\delta_p \beta_n) \sin(G\delta_s \beta_n) \sin[G(\delta_s - x)\beta_n]}{\beta_n [\delta_p \sin^2(G\delta_s \beta_n) + \delta_s \sin^2(\delta_p \beta_n)]} \exp(-D_{PyC} \beta_n^2 t) \quad (24)$$

where

$$G = \sqrt{\frac{D_{PyC}}{D_{SiC}}}$$

$$\sigma = \frac{1}{G}$$

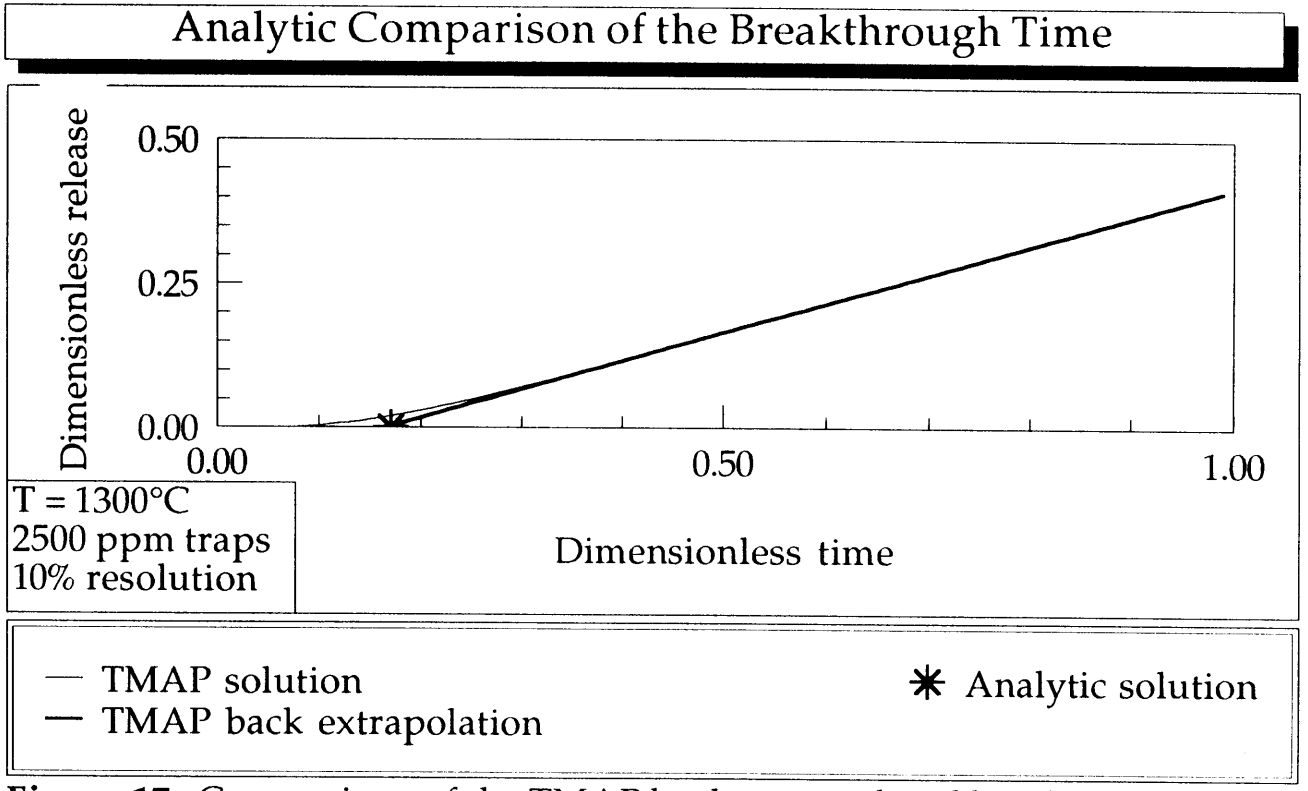

Figure 17. Comparison of the TMAP back extrapolated breakthrough time in the presence of trapping with the analytic solution given in Equations (5) and (14). The trapping rate is 1.52e9 s-1 and the resolution rate is 1.52e8 s-1.

and β_n are the roots of

$$\cot\beta\delta_p + \sigma\cot G\beta\delta_s = 0 \qquad (25)$$

The TMAP-calculated concentration at $x = 8\times10^{-6}$ m (for the case of $\delta_s = 33\times 10^{-6}$ m and $\delta_p = 63\times10^{-6}$ m) is compared to the analytic solution in Figure 18. The results are in excellent agreement and vary less than 1% after the first 20 seconds.

The results of the forementioned validation studies strongly support the use of TMAP in modeling target particles. Except during the initial seconds when the layer is filling with tritium, the TMAP solutions are in excellent agreement with analytic solutions pertinent to the target particle model. The initial discrepancy is not considered important because it does not propagate through the calculation but dampens out after breakthrough is reached. Therefore, TMAP can be used to model the NP-MHTGR target particles with confidence in its accuracy.

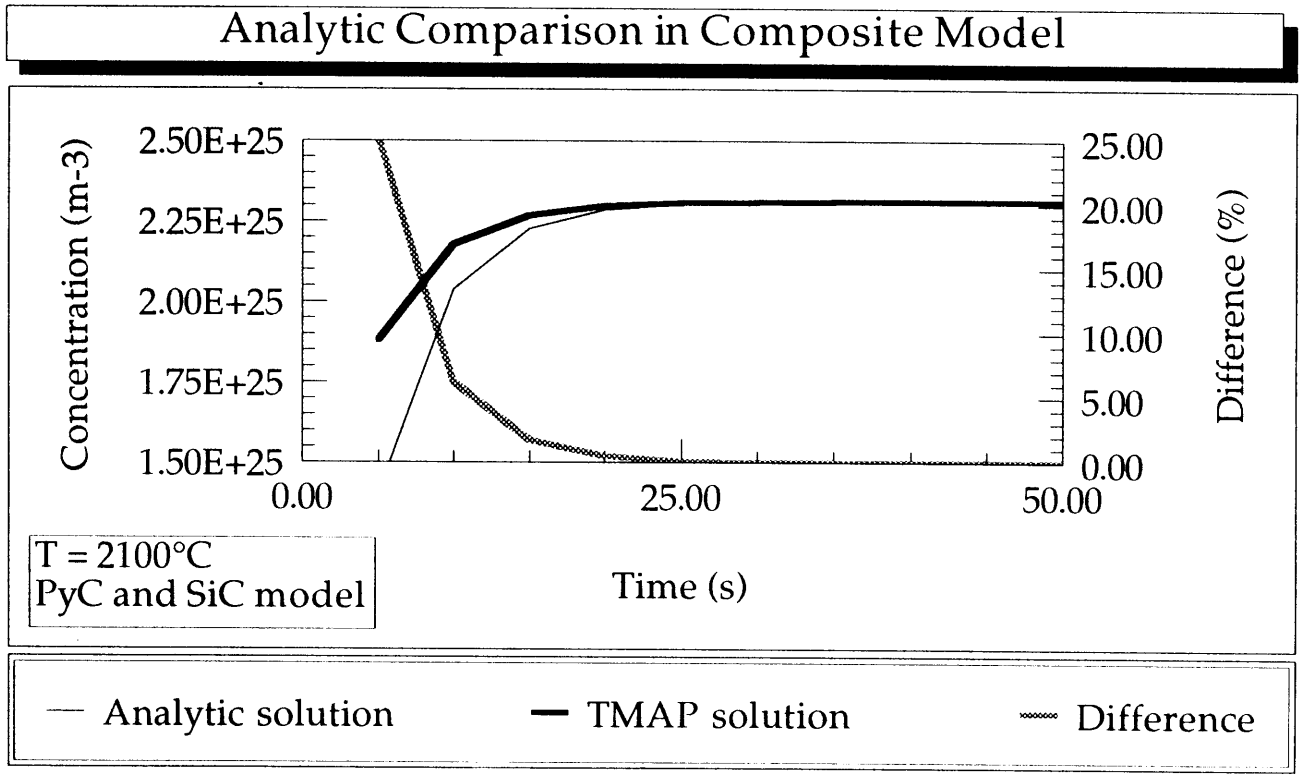

Figure 18. Comparison of the TMAP concentration for the composite model with a constant source condition with the analytic solution given by Equations (24) and (25).

4. RESULTS OF TMAP SCOPING CALCULATIONS

Results of TMAP scoping calculations for NP-MHTGR target particles are presented in this section. Effects of various parameters are examined systematically and sequentially in each of the following sections in an attempt to understand which phenomena need to be considered in a target particle tritium release model. Important effects are incorporated into the model and used in subsequent sections. Comparisons of the constant and depleting tritium sources are made in Section 4.1. In Section 4.2, the results from the SiC model are compared with results from the trilayer model. The effects of solubility in both PyC and SiC on tritium release are given in Section 4.3 and the effects of temperature and burnup are presented in Section 4.4. Section 4.5 studies the effect of tritium diffusion during normal reactor operation on tritium release during subsequent heating of the particles.

4.1 Comparison of Depleting and Constant Source Calculations

The TMAP code was used with the SiC model to understand the effects of both a constant and a depleting tritium source on the tritium release. Figures 19 and 20 compare the fraction of tritium released from the SiC model under these conditions at 1200 and 2100°C, respectively. Figure 21 compares the two cases for the trilayer model at 1300°C. The results indicate that the fractional release rate of tritium is lower when the tritium is allowed to deplete from the void volume. Because the diffusive flux off the surface, J, is driven by the concentration gradient according to Fick's law [See Equation (2)], this behavior is expected. As the tritium source depletes, the concentration at the inner surface and thus the concentration gradient decrease, which reduces the rate of release. Therefore, these results indicate that all tritium release calculations should include depleting source effects.

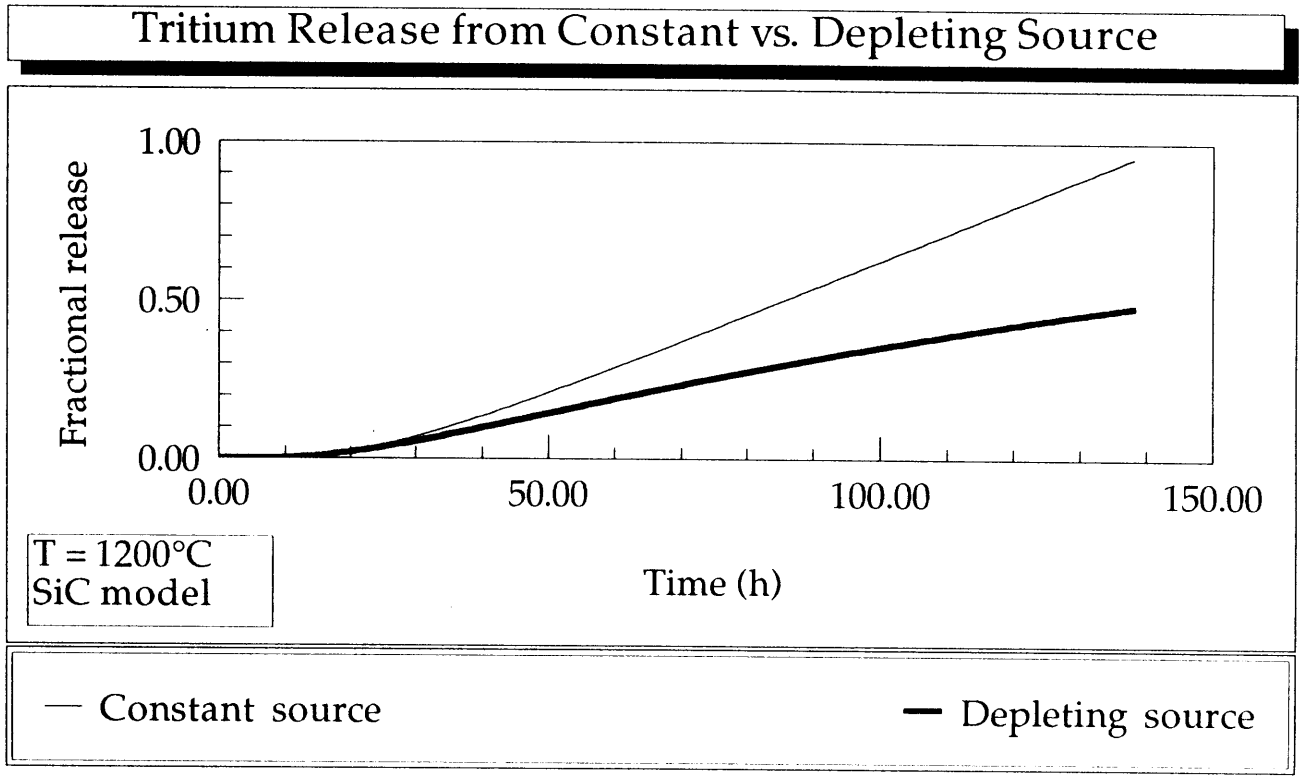

Figure 19. Comparison of tritium release fom the SiC model with a constant vs. depleting source at 1200°C.

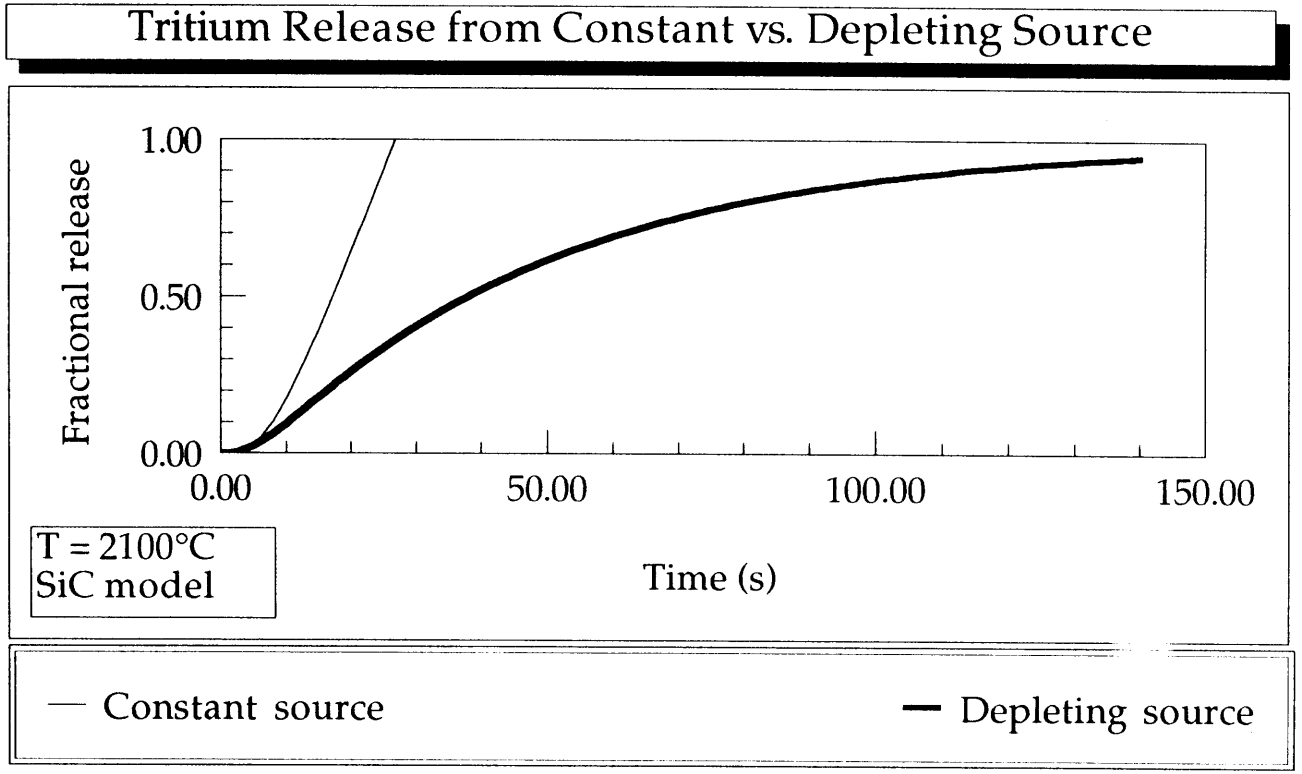

Figure 20. Comparison of tritium release from the SiC model with a constant vs. depleting source at 2100°C.

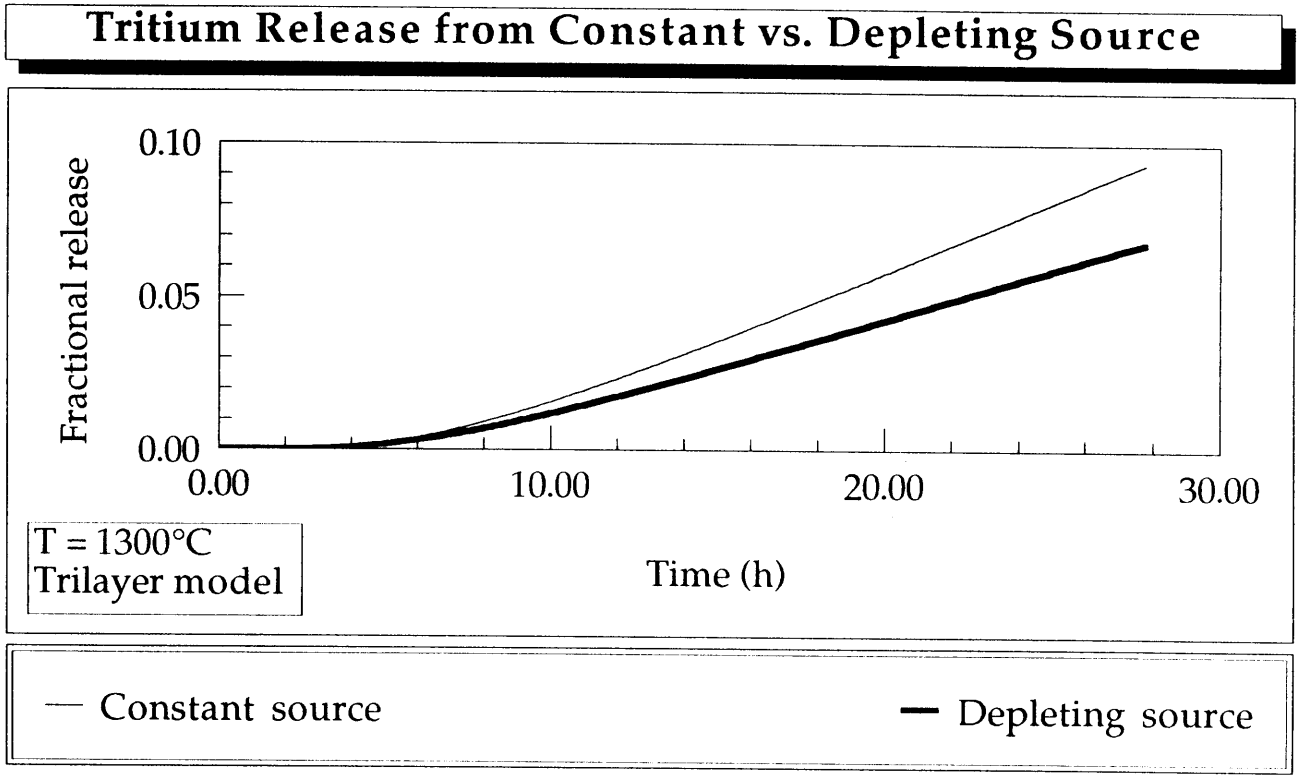

Figure 21. Comparison of tritium release from the trilayer model with a constant vs. depleting source at 1300°C.

4.2 Comparison of the SiC and Trilayer Models

Originally, the SiC layer was thought to be the principal tritium retention layer in the particle. Thus, the entire TRISO-coated particle was modeled to test the theory. Figures 22 and 23 compare the tritium release fractions from the SiC model and the trilayer model at 1200 and 2100°C. At 1200°C, the release fraction at 140 hours from the trilayer model is a factor of 1.6 less than from the SiC model. At 2100°C, similar reductions are seen at moderate release levels. However, breakthrough time does not change between the SiC model and the trilayer model and the calculations reconverge as the release fraction approaches 1.0. Conceptually, the three layers of the trilayer model act as three resistors in series. A lower diffusion coefficient creates a greater resistance to atomic movement through the material; the diffusion coefficient of tritium in SiC is lower than that in PyC and, thus, creates the greatest resistance. Therefore, the SiC is the dominant barrier to tritium diffusion in the particle, resulting in equivalent breakthrough times for the two models.

The difference in the rate of tritium release from the two models can be explained by examining Equation (8)[e] which states the release rate is proportional to the concentration at the inner surface of the layer as given by the appropriate pressure relation. In the SiC model, the concentration at the SiC surface is the concentration in the void volume. In the trilayer model, the concentration at the SiC surface is less than that in the void volume because the IPyC layer acts as a sink for the tritium atoms. This decrease in concentration at the inner surface of the SiC reduces the tritium pressure at this interface and thus the overall release rate. These results indicate that even though the SiC is the dominant barrier to tritium diffusion, it is important to model the PyC in all release calculations because of

e. Although this equation is for a single membrane, it can be used here to qualitatively understand the trilayer model.

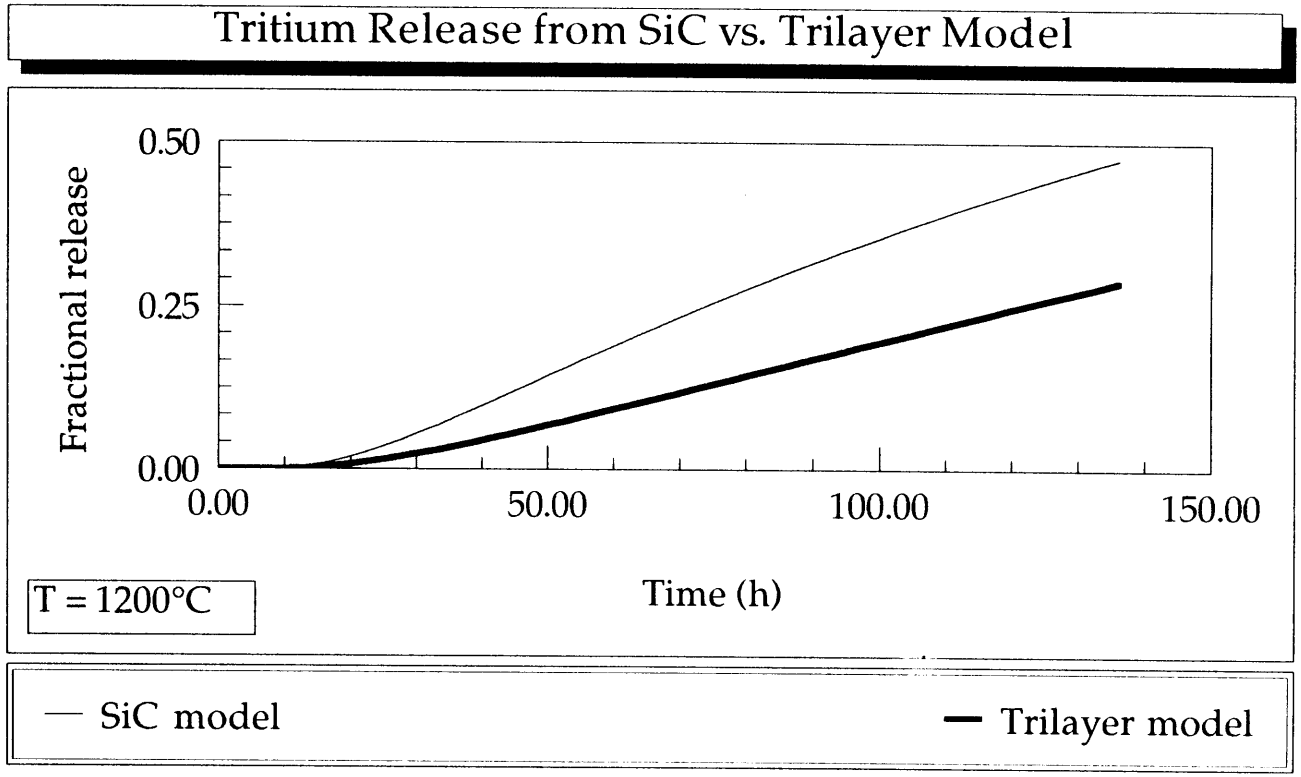

Figure 22. Comparison of tritium release from the SiC vs. trilayer model at 1200°C.

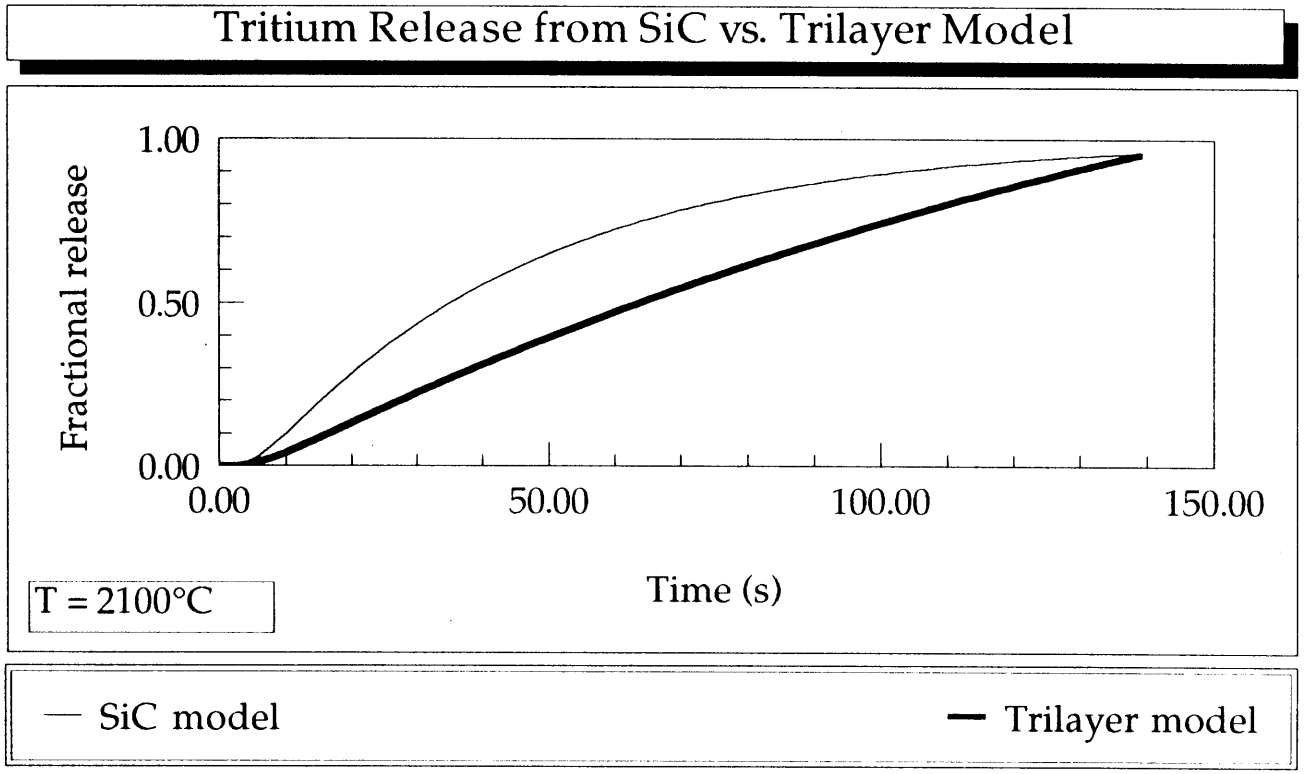

Figure 23. Comparison of tritium release from the SiC vs. trilayer model at 2100°C.

its capacity to hold tritium atoms. The role of the PyC layers in the diffusion process is examined in greater detail in Section 5.1.

4.3 Effects of Solubility in the Trilayer Model

In addition to modeling the PyC layer explicitly, calculations have been performed to study the effects of tritium solubility in SiC and PyC. In the previous calculations "without solubility", a continuous concentration at the PyC/SiC interfaces was modeled by inputting a solubility constant of 1.0 between the linked layers. As discussed in Section 2, Equation (6) was used to determine the initial surface concentration in the case "without solubility" whereas Sievert's law correlations were used to model solubility explicitly. The Sievert's law correlation results in a discontinuity in concentration at the PyC/SiC interfaces, and, for the values of the solubilities in the materials studied here, the initial surface concentration is reduced when solubility is considered.

The results with and without solubility are compared using the trilayer model at 1200 and 2100°C in Figures 24 and 25, respectively. As illustrated, the tritium release fraction at the end of the calculations was reduced by a factor of 2 to 4 when tritium solubility in the TRISO coating materials was considered. The solubility surface boundary condition imposed in the model limits the amount of tritium that can be dissolved in the solid, which, in turn, affects the concentration of tritium in each layer. This reduction in tritium concentration reduces the rate of release.

4.4 Burnup and Temperature Effects

Pretest tritium release calculations were performed by D. A. Petti to help plan the postirradiation high temperature heating experiments to be performed at LANL.[2] The main objective of these tests is to understand the effects of burnup and temperature on tritium release from ATR-3 type irradiated compacts at high temperatures representative of NP-MHTGR accident conditions.

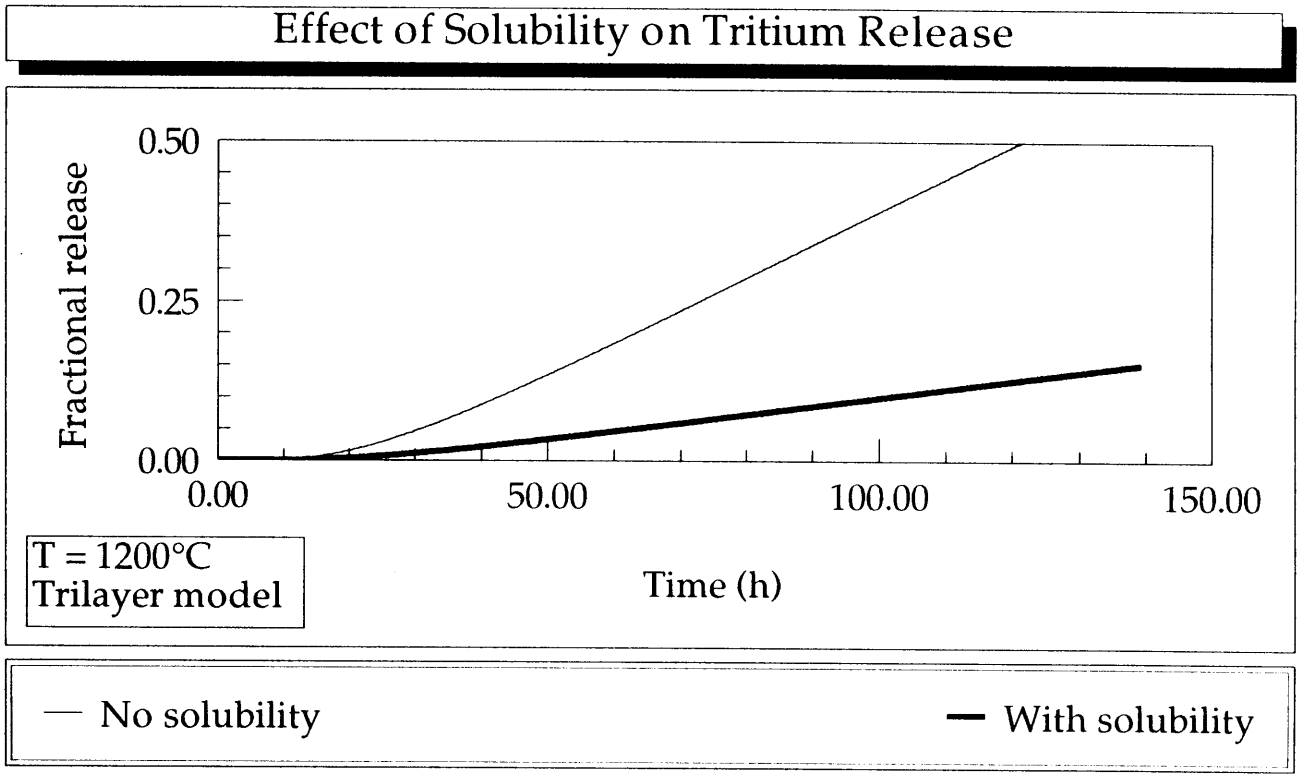

Figure 24. Effect of solubility on tritium release from the trilayer model at 1200°C.

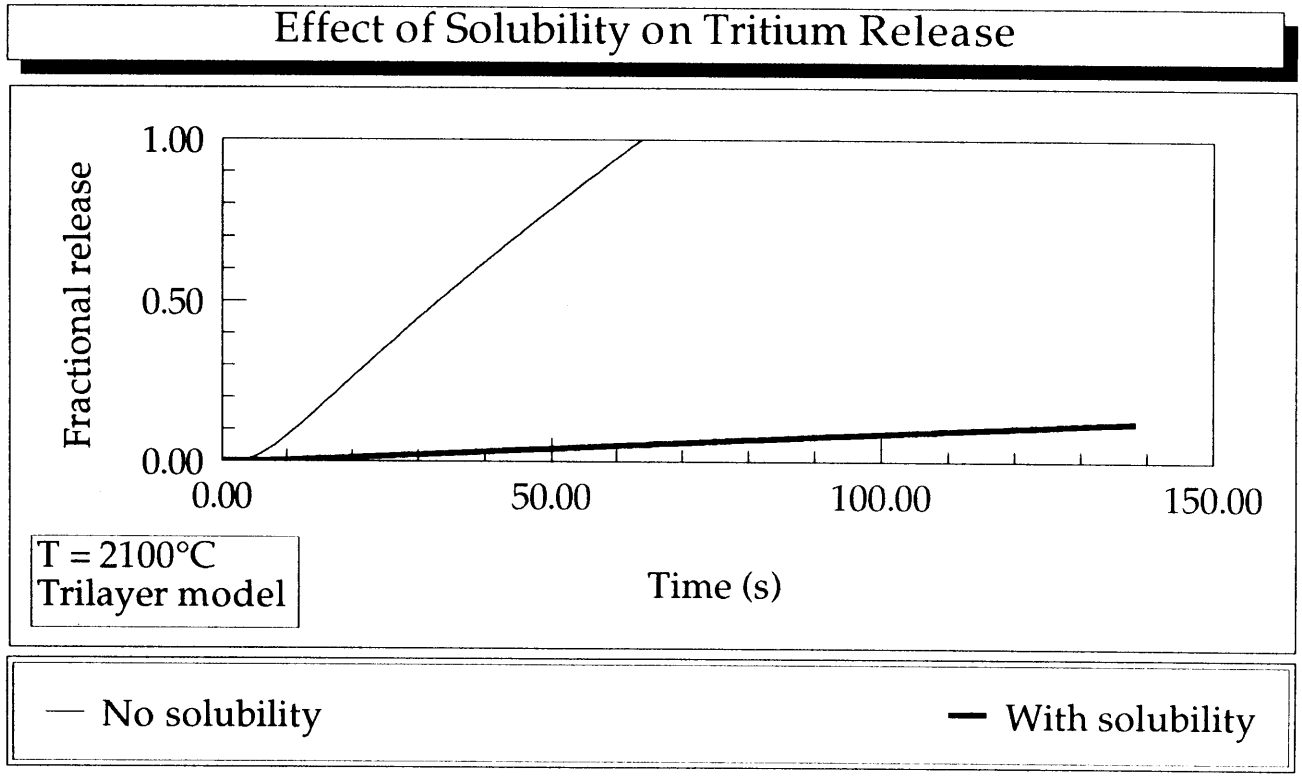

Figure 25. Effect of solubility on tritium release from the constant source trilayer model at 2100°C.

Because of time limitations, TMAP calculations could not be performed for all the burnup and temperature combinations that will be examined in the safety experiments. Table 2 compares the combinations that will be tested in the experiment with those modeled using TMAP. Details of the input model used in these calculations are found in Appendix A.

Particle burnup affects both the concentration of tritium in the void volume and the concentration gradient through the particle. The effect of burnup on the fractional release of tritium at 1800°C is illustrated in Figure 26. Higher burnup particles have a larger initial tritium inventory resulting in greater tritium permeation rates

Table 2. Temperature and burnup combinations for the LANL safety experiments and TMAP calculations.

	Temperature(°C)						
Burnup (%)	1200	1300	1400	1500	1600	1700	1800
45	L	L,T	L	L,T	L,T	L,T	L,T
33		L		L		L	T
18	T	L		L		L,T	T

L - LANL safety experiments
T - TMAP code

because of the larger concentration gradient across the particle. Based on Sievert's law, the concentration gradient should scale with the square root of burnup. However, because the tritium inventory increases linearly with burnup, the high burnup particle requires a longer time to release all of its tritium. The release curves at 45, 33, and 18% burnup clearly show that the time to release all of the

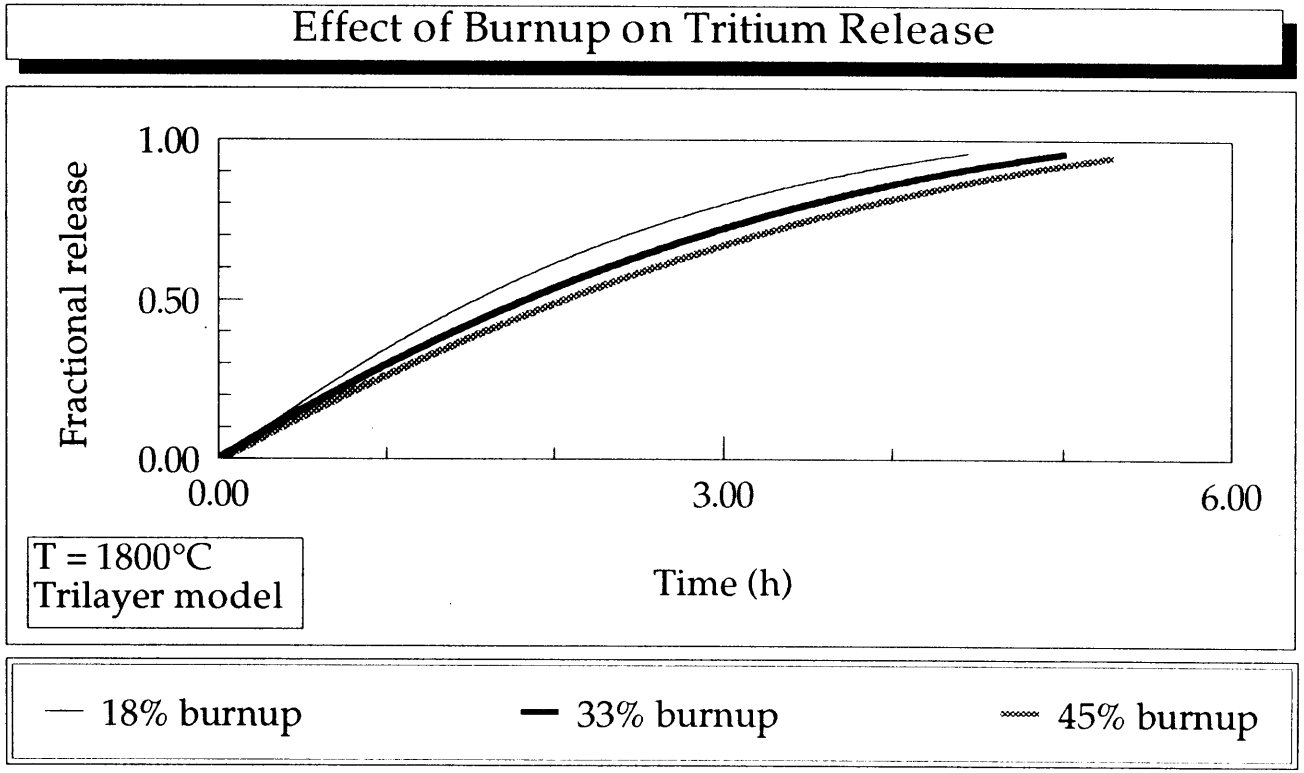

Figure 26. Effect of burnup on tritium release from the trilayer model at 1800°C.

tritium from the particle increases with burnup. Thus, at a given time and temperature, the increased tritium inventory has a stronger effect on release than the larger concentration gradient, causing the fractional release to decrease with burnup. Similar results are shown at 1700°C in Figure 27.

The effect of temperature on the fractional release of tritium at 45% burnup is shown in Figure 28. These results indicate that tritium release is a strong function of temperature. Figure 29 is a plot of the permeation rate of tritium (product of the diffusivity and solubility) through SiC. As indicated in the figure, the tritium permeation (or release) rate can drop by one to two orders of magnitude between 1800 and 1200°C, depending on the tritium partial pressure (burnup) in the particle.

Figure 30 is a plot of the fractional release of tritium at 1800°C and 45% burnup. Although not shown on the figure, detailed examination of the release indicates that it follows an S-shaped curve, showing the classical breakthrough time at about 85 seconds, in agreement with the SiC diffusivity used in the model. However, at longer times, the release is no longer linear with time because of depletion of the tritium from the void volume. The calculated results indicate that 95% of the tritium would be released in 5.3 hours. Extrapolation of the curve indicates that total release would occur after approximately 6 hours. Figure 31 is a plot of the fractional release of tritium at 1200°C and 18% burnup. The plot indicates that it will take ~2200 hours to release all of the tritium from the target particle under these conditions. Thus, temperature appears to have a strong influence on the time required to release all of the tritium from the target particle with the burnup also affecting the results to a lesser extent.

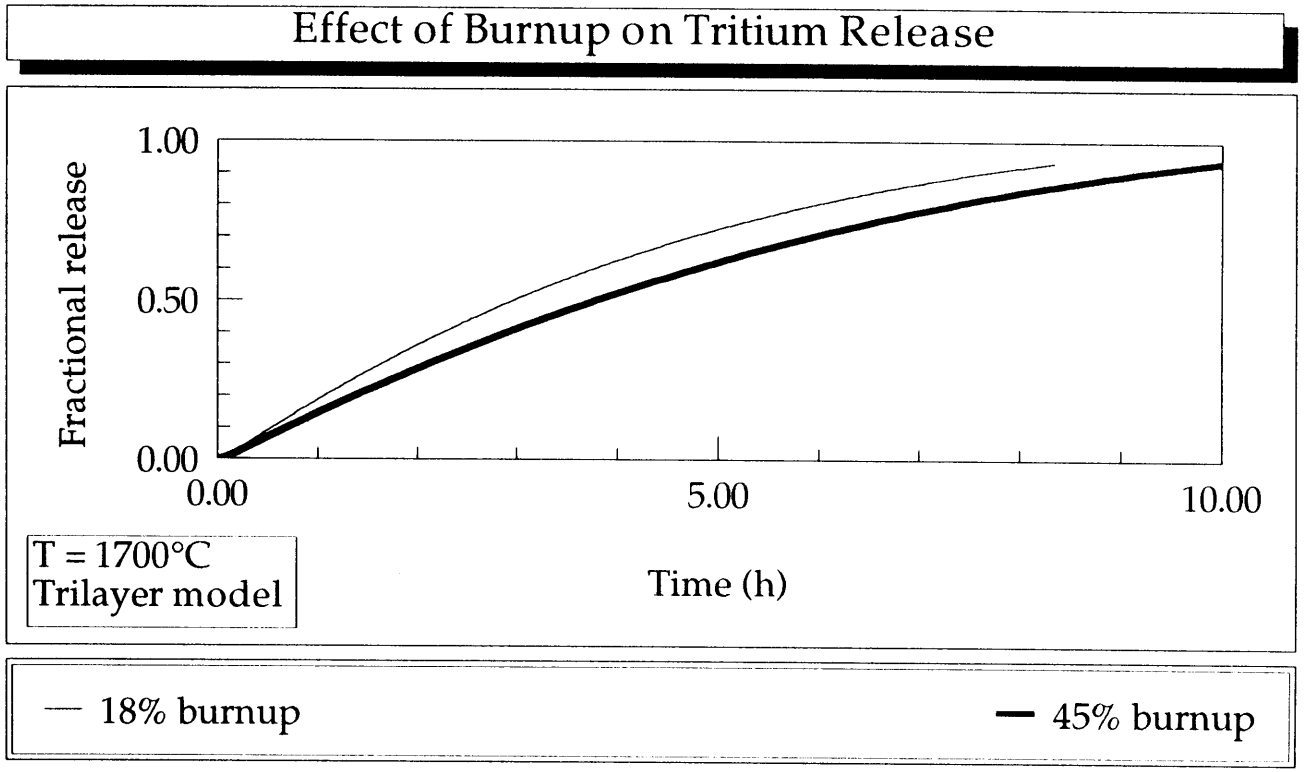

Figure 27. Effect of burnup on tritium release from the trilayer model at 1700°C.

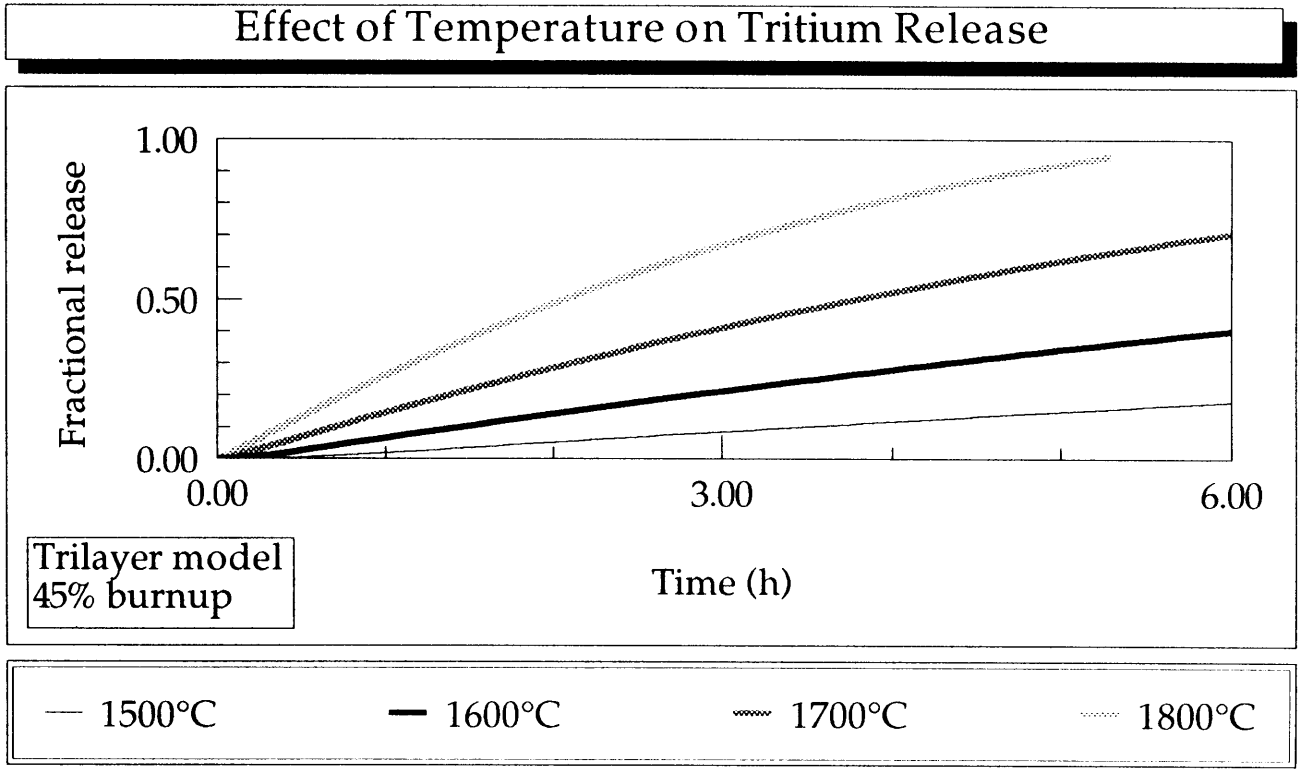

Figure 28. Effect of temperature on tritium release from the trilayer model at 45% burnup.

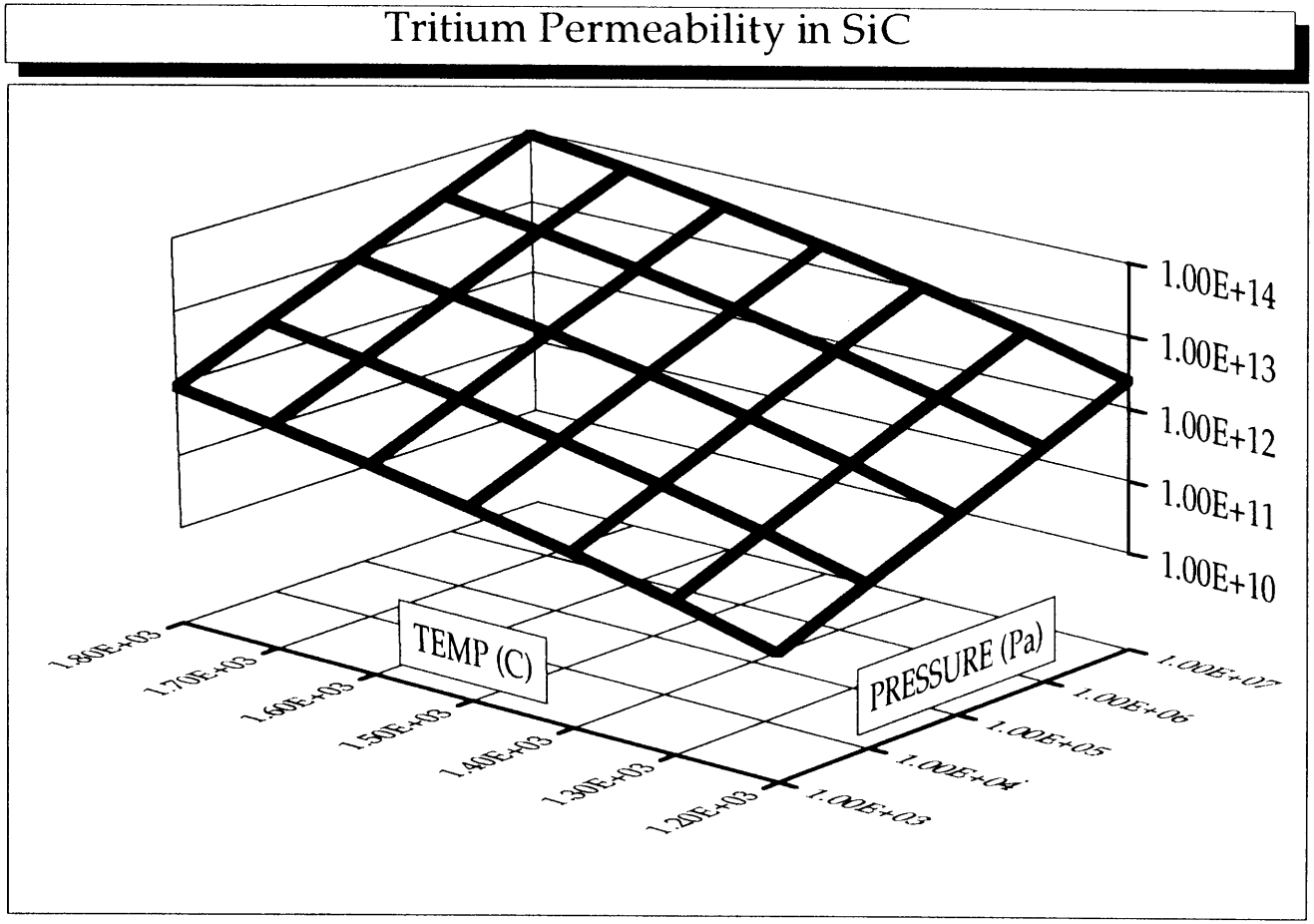

Figure 29. Effect of temperature and pressure on tritium permeability in SiC.

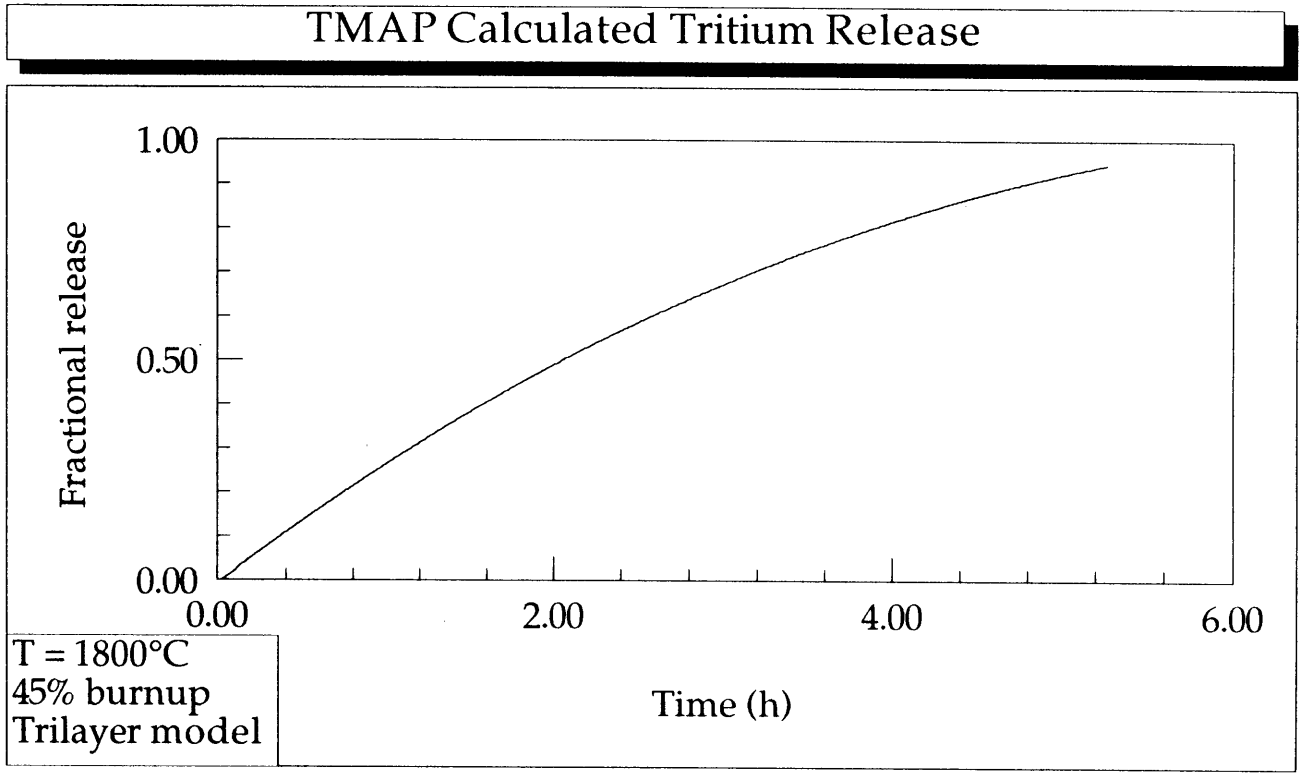

Figure 30. Fractional tritium release from the trilayer model at 1800°C and 45% burnup.

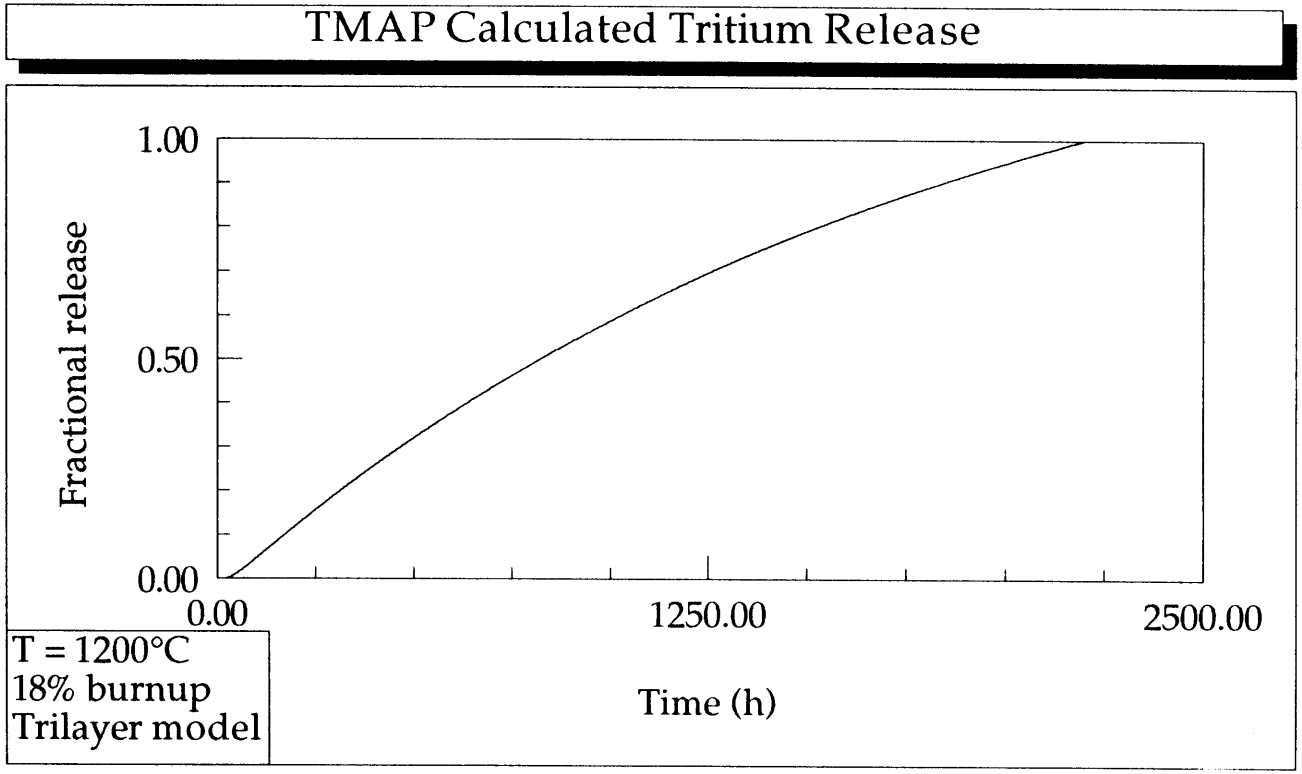

Figure 31. Fractional tritium release from the trilayer model at 1200°C and 18% burnup.

4.5 Effect of Prior Reactor Operation

The target particle was modeled in TMAP under reactor operating conditions to determine the extent of tritium diffusion into the layers during operation and its effect on tritium release during subsequent postirradiation heating. The peak reactor operating temperature of 780°C and the six month irradiation period[2] were used in the calculation. A constant tritium partial pressure corresponding to 45% burnup at this temperature was used to ensure conservatism. Because significant depletion does not occur over this time (in fact, breakthrough is not reached), a constant source condition was used to reduce the computational time. Then, the calculated tritium distribution in the particle coatings at the end of the TMAP calculation and the reduced tritium partial pressure accounting for the tritium that had diffused out of the void volume were input into a new TMAP calculation simulating a postirradiation heatup test at 1600°C. This output is compared to results for a particle in which prior reactor operation was neglected in Figure 32. A difference of 15% occurs initially at very low release fractions because some of the tritium (54%) is already in the particle (mainly in the IPyC) when normal reactor operation is modeled. However, the difference decreases to less than 1% within 5 hours indicating that tritium diffusion during normal operation does not have to be modeled for the conditions expected in the NP-MHTGR.

4.6 Summary

The results of these scoping calculations indicate that the NP-MHTGR target particle model should (1) include a depleting tritium source, (2) consider all layers of the TRISO coating (i.e. trilayer model), and (3) use solubility boundary conditions at the void volume/IPyC, IPyC/SiC, and SiC/OPyC interfaces. When predicting tritium release from postirradiation experiments, prior reactor operation is not important if the reactor operating conditions are less than 780°C for a six month irradiation period.

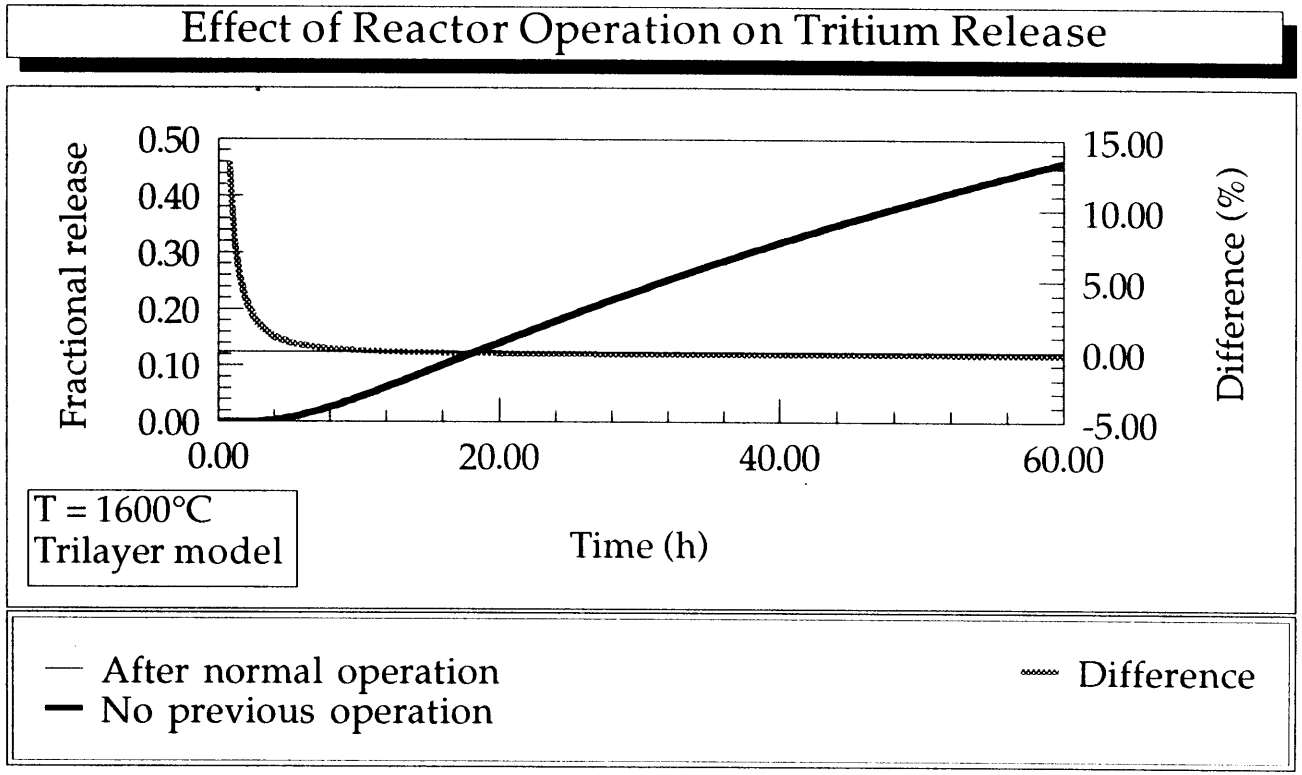

Figure 32. Effect of reactor operation at 780°C for 6 months on tritium release.

5. SENSITIVITY CALCULATIONS

Sensitivity calculations were run with TMAP to determine separately the effects of solubility, diffusivity, tritium partial pressure, and the trapping parameters on tritium release to aid in understanding and analyzing experimental data. Like previous TMAP calculations, the target particle was modeled using the trilayer model with the ATR-3 geometry[2] and the nominal values for the diffusion coefficient and the solubility in PyC and SiC taken from Causey.[12,13] Changes in the parameters in the outer PyC (OPyC) layer had negligible effect on release and thus were not modeled; therefore, PyC refers to the inner PyC (IPyC) layer in this discussion. Of all the LANL test conditions, 1800°C and 45 atom% burnup were selected for the study of diffusion coefficient, solubility, and tritium partial pressure[e] because previous calculations indicated a relatively short time is required to release significant amounts of tritium, thus saving computer time, while remaining within the proposed accident temperature range. Trapping studies were conducted dimensionlessly at 1300°C with the SiC model. Only one parameter in one of the layers was changed in each sensitivity calculation. A matrix of the sensitivity calculations performed is shown in Table 3.

Section 5.1 presents the results of the PyC diffusivity and solubility sensitivity studies while Section 5.2 discusses the results of these studies for SiC. Section 5.3.1 contains the pressure sensitivity calculations. Parametric studies of the effect of the trapping rate, the release rate, and the number of traps are presented in Section 5.4. Conclusions from this sensitivity study are drawn in Section 5.5.

---

e. The results of these sensitivity calculations are strictly valid at the conditions listed. The results will vary somewhat at different temperatures and burnups due to the strong Arrhenious temperature dependence in the solubility and diffusivity correlations and the effect of pressure on release.

Table 3. Matrix of sensitivity calculations performed with TMAP

	Factor								
Parameter	*10	*5	*4	*2	*1	÷2	÷4	÷5	÷10
Diffusivity									
PyC	X				X				X
SiC	X	X	X	X	X	X	X	X	X
Solubility									
PyC	X	X			X			X	X
SiC	X	X	X	X	X	X	X	X	X
Pressure			X		X		X		

5.1 PyC Solubility and Diffusivity Results

The results of the PyC diffusion coefficient sensitivity calculations are shown in Figure 33. A factor of 10 change in the diffusivity results in small changes in the fraction of tritium released. This result is expected and can be explained by examining Equation (5), the equation for the breakthrough time, t_b (s). To apply this equation to the trilayer system, an effective term must be used such that

$$t_b = \frac{1}{6}\left(\frac{\delta^2}{D}\right)_{eff} \tag{26}$$

where

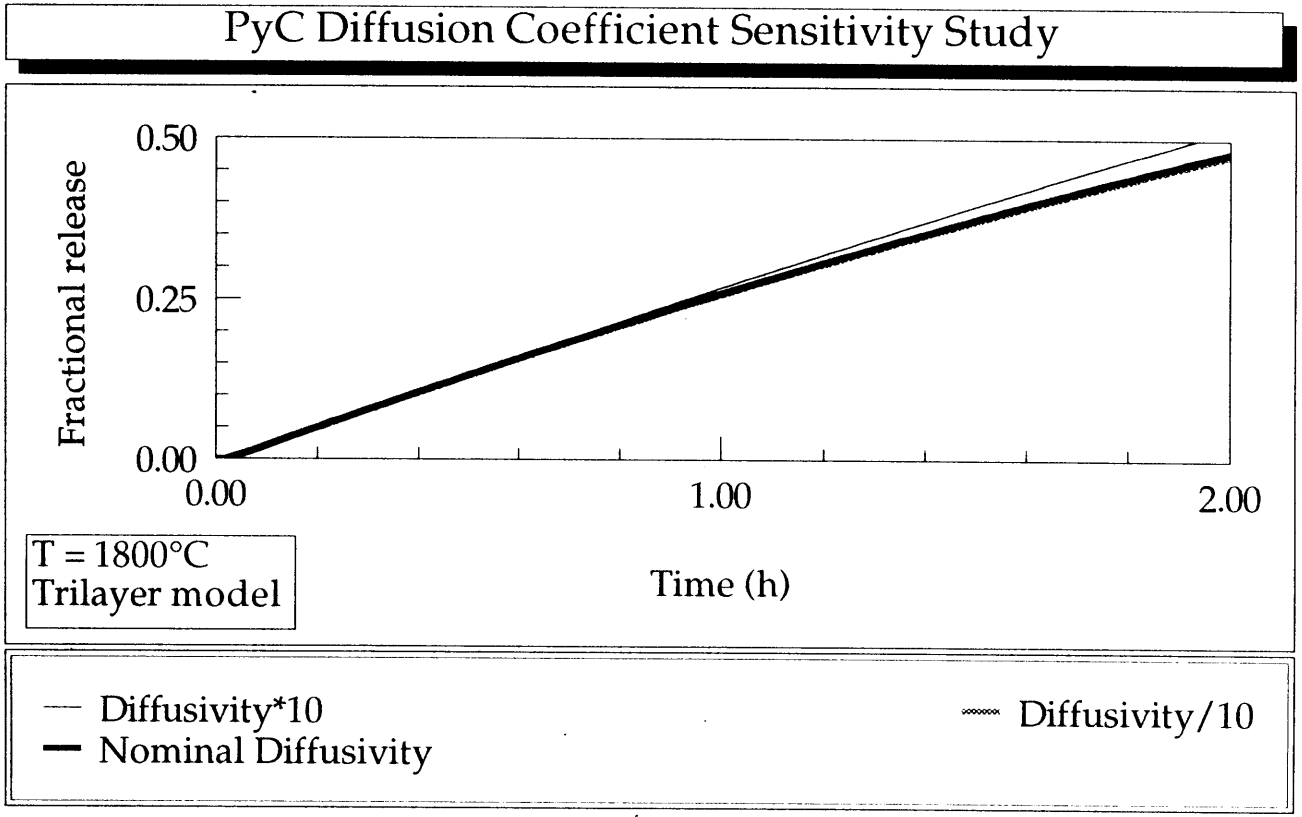

Figure 33. Effect of the PyC diffusion coefficient on tritium release.

$$\left(\frac{\delta^2}{D}\right)_{eff} = \left(\frac{\delta^2}{D}\right)_{IPyC} + \left(\frac{\delta^2}{D}\right)_{SiC} + \left(\frac{\delta^2}{D}\right)_{OPyC} \quad (27)$$

and δ and D are the respective thickness (m) and diffusion coefficient (m^2/s) for each layer. For a composite layer, the diffusional resistances add "in series." The diffusion coefficient of tritium in SiC is much lower than that in PyC, and thus, the SiC layer dominates the breakthrough time as discussed previously in Section 4.2. The addition of the PyC terms changes t_b by only 0.03%. Thus, D_{PyC} does not have to be known to a high degree of accuracy and the value given by Causey can be used unless it is found to be grossly in error (i.e. a factor of 100).

The solubility sensitivity results are plotted in Figure 34. A change in the PyC solubility value affects the amount of tritium in the layer that, in turn, affects the concentration at the PyC/SiC interface. In the TRISO coating, the PyC acts as a capacitor. The layer "fills" with tritium atoms in a few seconds with more atoms being "held" in the layer as the solubility increases. After this initial charging, the diffusion process occurs. As tritium depletes from the void volume, the number of tritium atoms in the PyC decreases as the solubility decreases according to Sievert's law and the PyC capacitor slowly drains. Therefore, at high solubilities, the tritium concentration and the pressure at the SiC inner surface are lowered causing the release rate to decrease, and thus, the time to release all of the tritium to increase.

The figure also indicates that an increase in the solubility produces a greater change in the release than a decrease by the same factor. Fewer atoms are held in the PyC layer at low solubilities as illustrated in Figures 35 and 36. Figure 35 compares the atom flux into the layer with the atom flux out of the layer for each solubility value while Figure 36 compares the mobile tritium inventory for the two cases. At the reduced solubility, the mobile inventory in the PyC is quite low signifying a large concentration of tritium still resides in

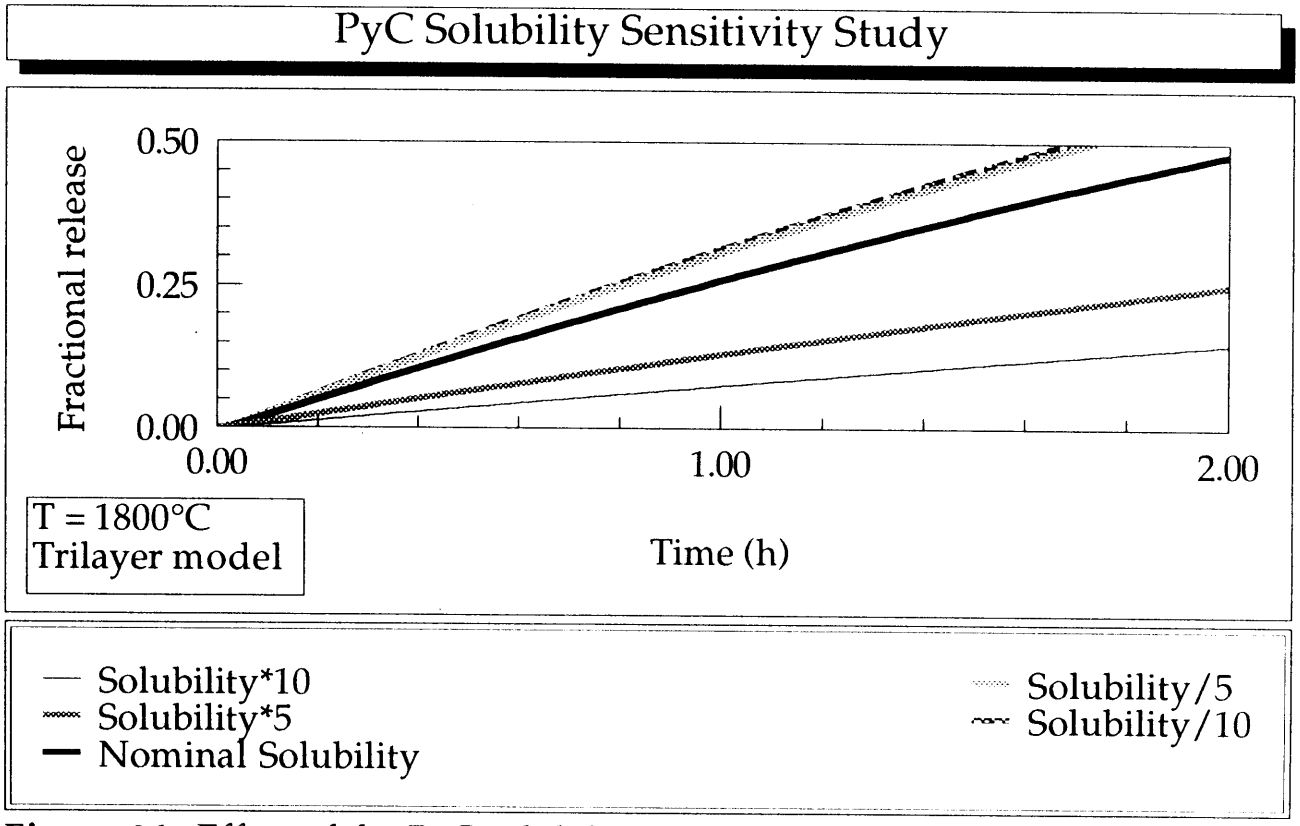

Figure 34. Effect of the PyC solubility on tritium release.

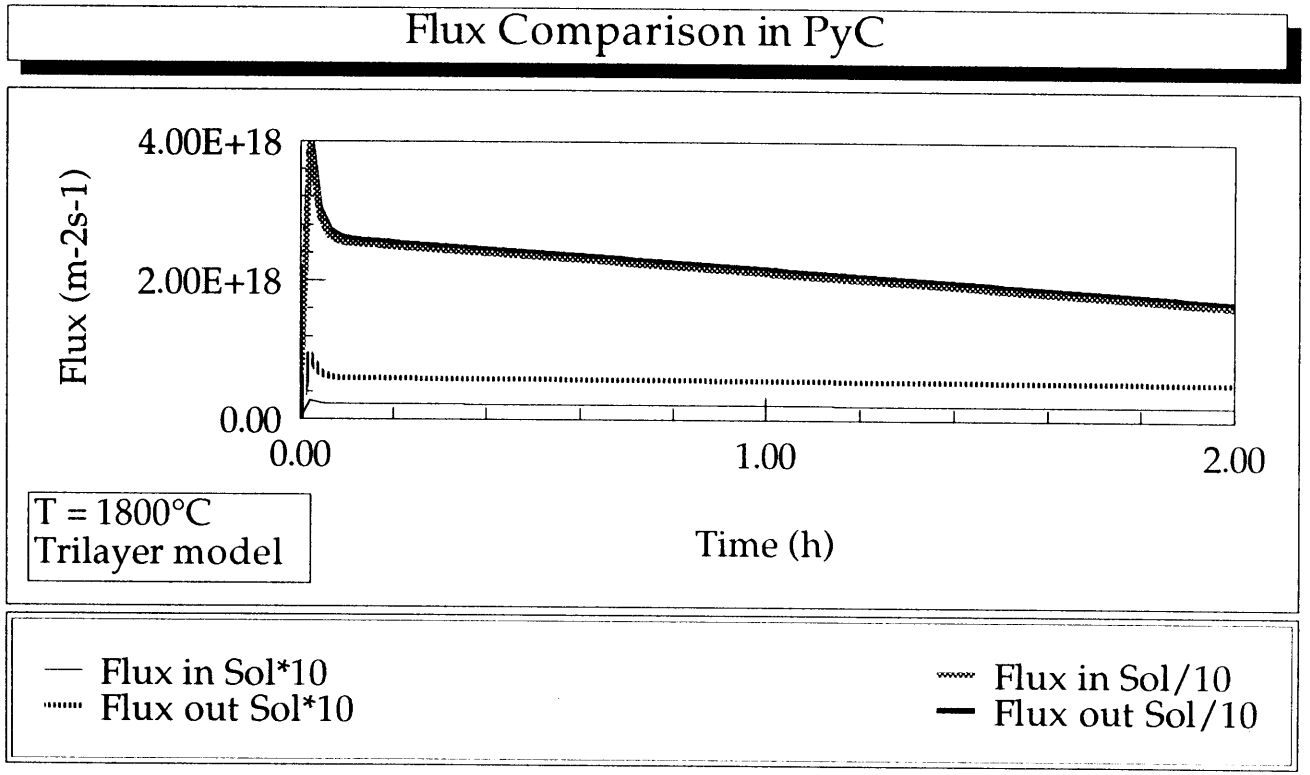

Figure 35. Effect of the PyC solubility on the surface flux of tritium into and out of the PyC layer.

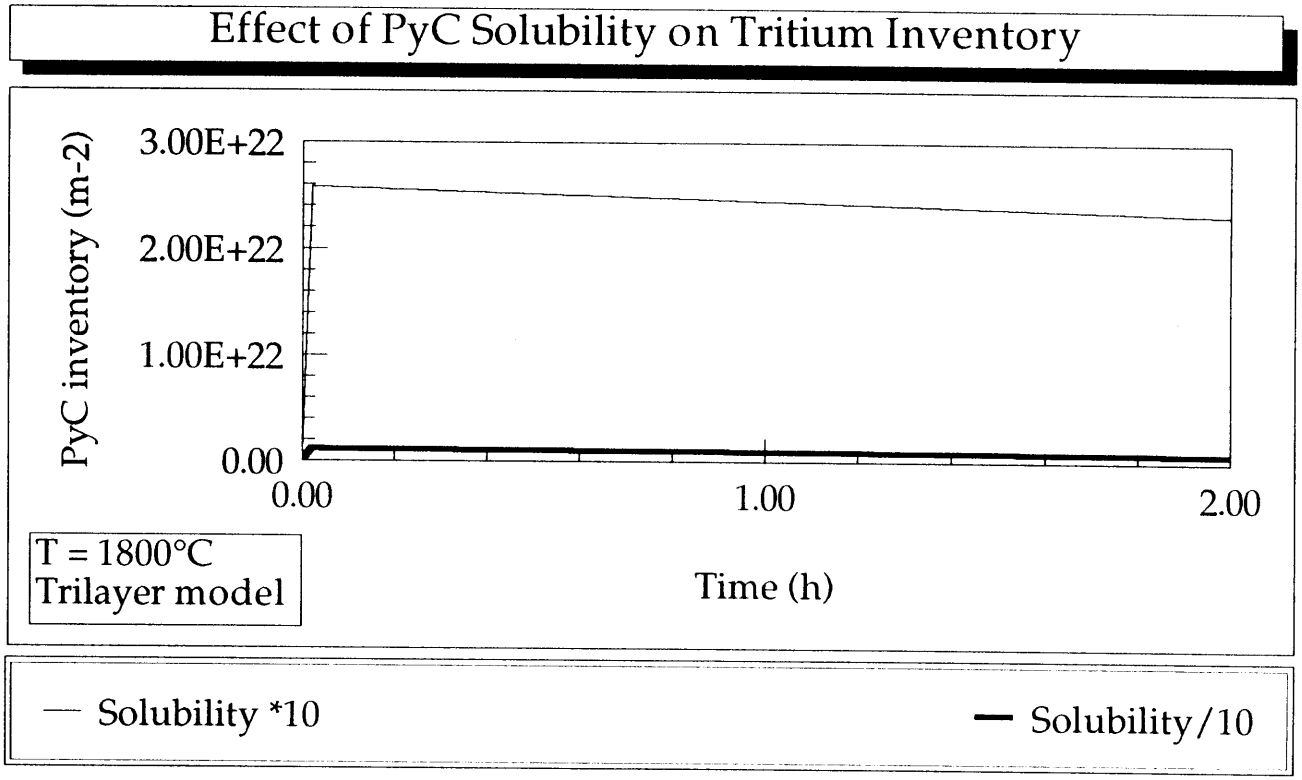

Figure 36. Effect of the PyC solubility on the mobile inventory of tritium in the PyC layer.

the void volume. The surface fluxes equilibrate fairly quickly indicating the layer is at equilibrium and its capacitance is unimportant in the problem after a few seconds. In the case of increased solubility, the strong capacitance effect of the PyC is evident. A rapid uptake of tritium into the PyC results in a lowered tritium pressure in the void volume and a mobile inventory that is 25 times larger than in the decreased solubility case. Therefore, the tritium in the void volume has depleted significantly as is also indicated by the reduced surface fluxes. As the solubility increases, less tritium remains in the void volume after the initial filling of the PyC layer resulting in a smaller release rate. Thus, the tritium release decreases as the solubility or capacitance effect of the PyC layer increases.

5.2 SiC Solubility and Diffusivity Results

Figures 37 and 38 show the results of varying the SiC diffusivity and solubility, respectively. The plots directly overlay indicating a change in the diffusivity or the solubility by the same factor produces the same overall release as shown numerically in Table 4. This result can be interpreted by inspecting the analytic solution for the mass flow rate of T_2 molecules, m, released at steady state in a permeation experiment,

$$m = \frac{ADSP^{0.5}}{2\delta} \tag{28}$$

where A is the surface area (m^2), S is the solubility ($atoms/m^3Pa^{0.5}$), P is the pressure (Pa), and the factor of 2 converts atoms of T to molecules of T_2. Because this equation exhibits an identical dependence on the diffusivity and the solubility, the release rate is expected to vary by the same factor regardless of which parameter is changed. To further test this theory, the TMAP code was run with both the solubility and diffusivity in the SiC layer increased by a factor of 2 and compared with the results of the cases where the solubility and diffusivity were increased separately by a factor of 4.

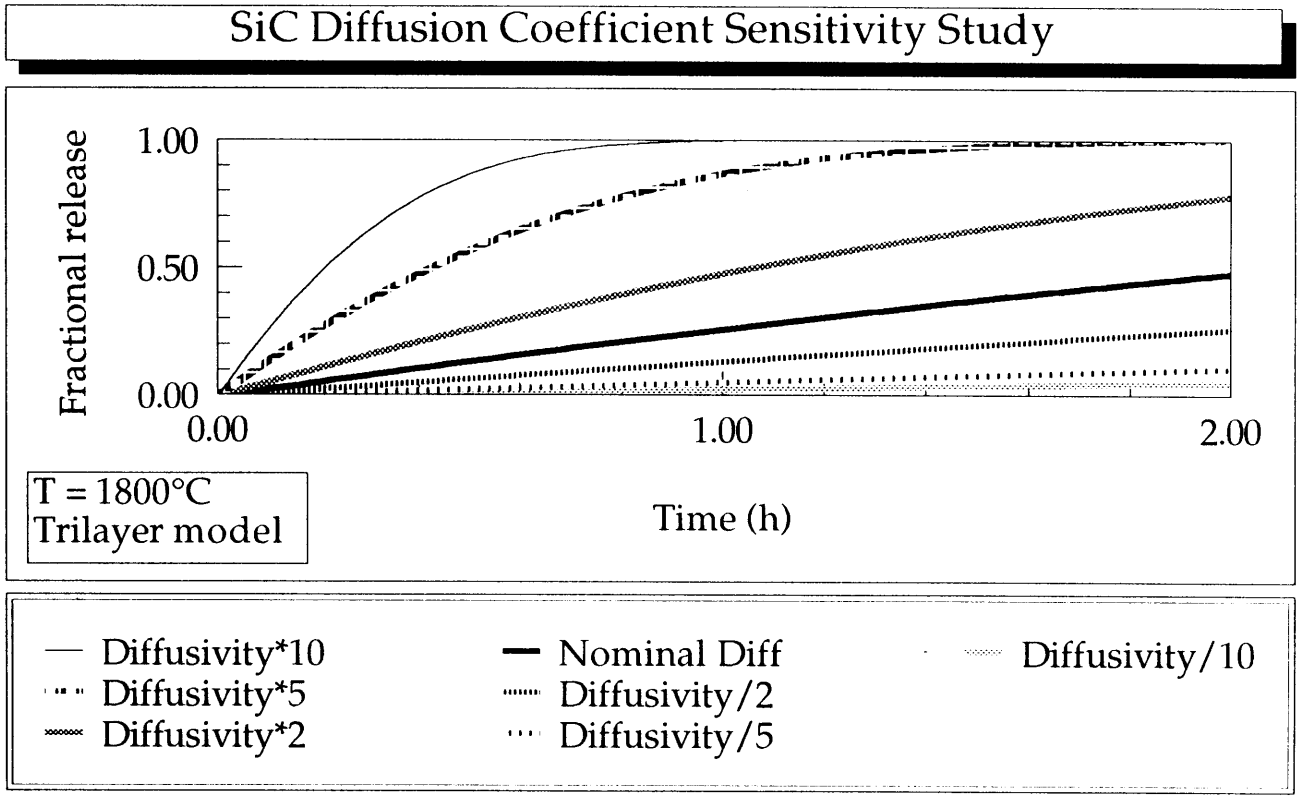

Figure 37. Effect of the SiC diffusion coefficient on tritium release.

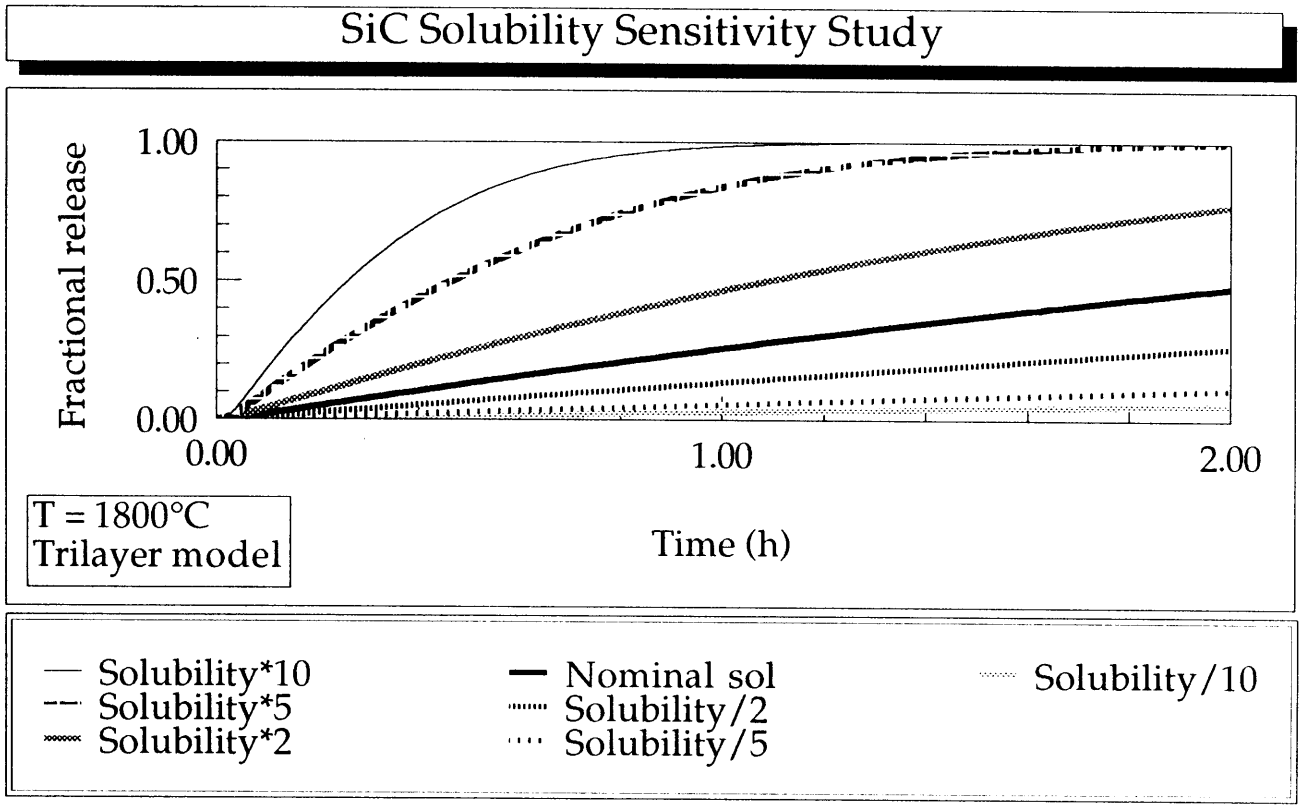

Figure 38. Effect of the SiC solubility on tritium release.

Table 4. Fractional tritium release from SiC after 2 hours for various diffusivities and solubilities

	Factor						
Parameter	*10	*5	*2	*1	÷2	÷5	÷10
Diffusivity	1.00	1.00	0.78	0.48	0.26	0.11	0.05
Solubility	1.00	1.00	0.77	0.48	0.26	0.11	0.06

Again, the release from each of these calculations is identical as plotted in Figures 39, 40, and 41 and given numerically in Table 5. Therefore, only the changes in the product of the two parameters can be determined from the fractional tritium release data.

The tritium release rate, on the other hand, is not identical for the diffusivity and solubility studies as shown in Figures 42 and 43, respectively. A change in the diffusion coefficient affects the time to reach steady state release, t_b, whereas a change in the solubility does not. This behavior is also illustrated in Figure 44 which compares the release rate of the data presented in Figures 39, 40, and 41. Thus, the solubility cannot be directly determined from the experimental results but the SiC diffusion coefficient can be calculated from the experimental value of t_b using Equation (26).

5.3 Pressure Results

The nominal pressure of T_2 at 1800°C and 45 atom% burnup in an ATR-3 particle, 1.41×10^7 Pa, was varied to determine the effect on release as shown in Figure 45. From a similar examination of Equation (28) as in Section 5.2, it might be expected that increasing the pressure four times would produce the same tritium release

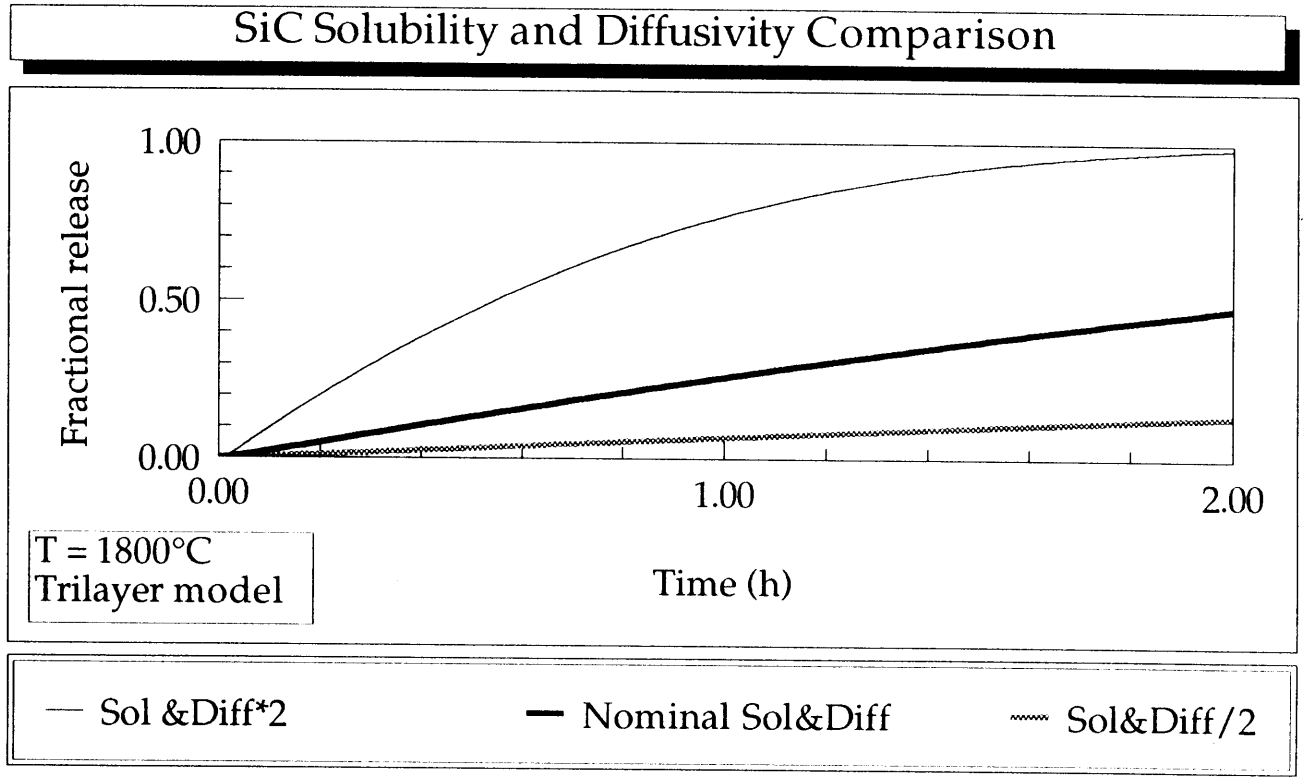

Figure 39. Effect of the SiC solubility and diffusivity on tritium release.

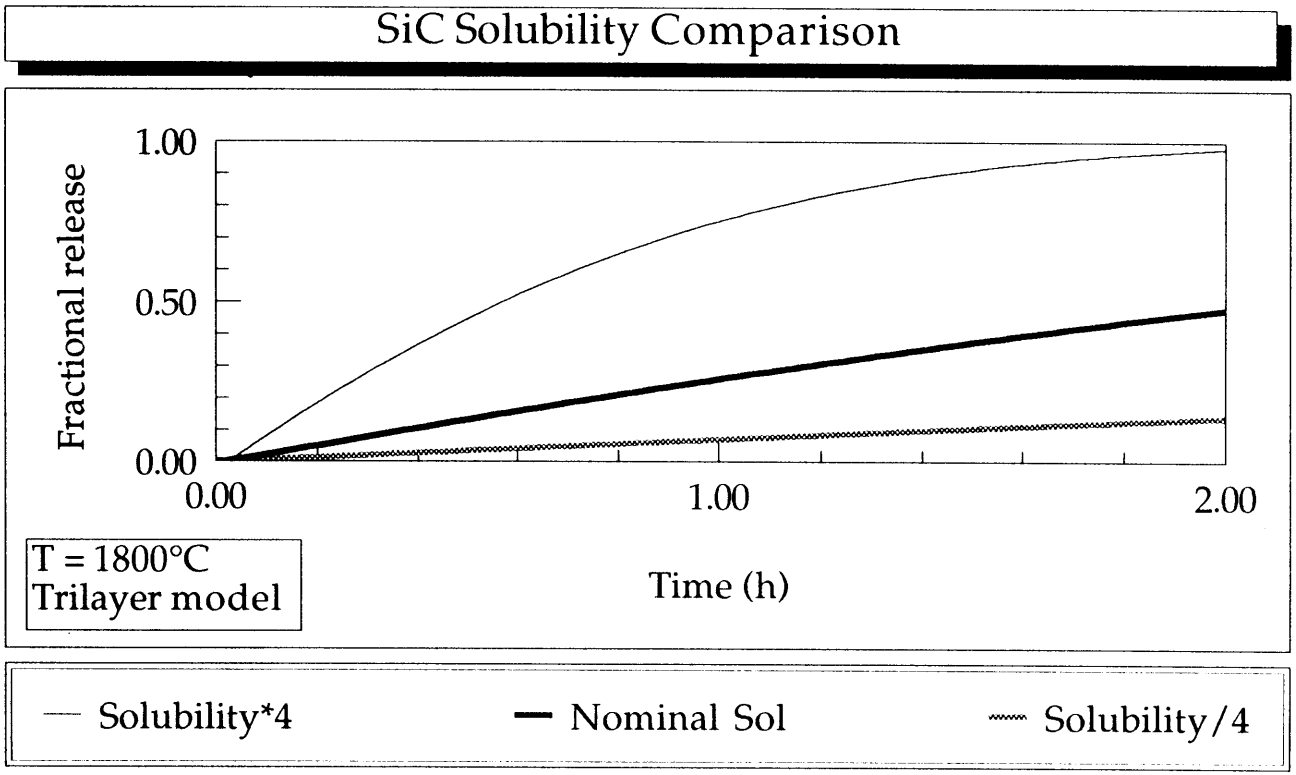

Figure 40. Effect of the SiC solubility on tritium release.

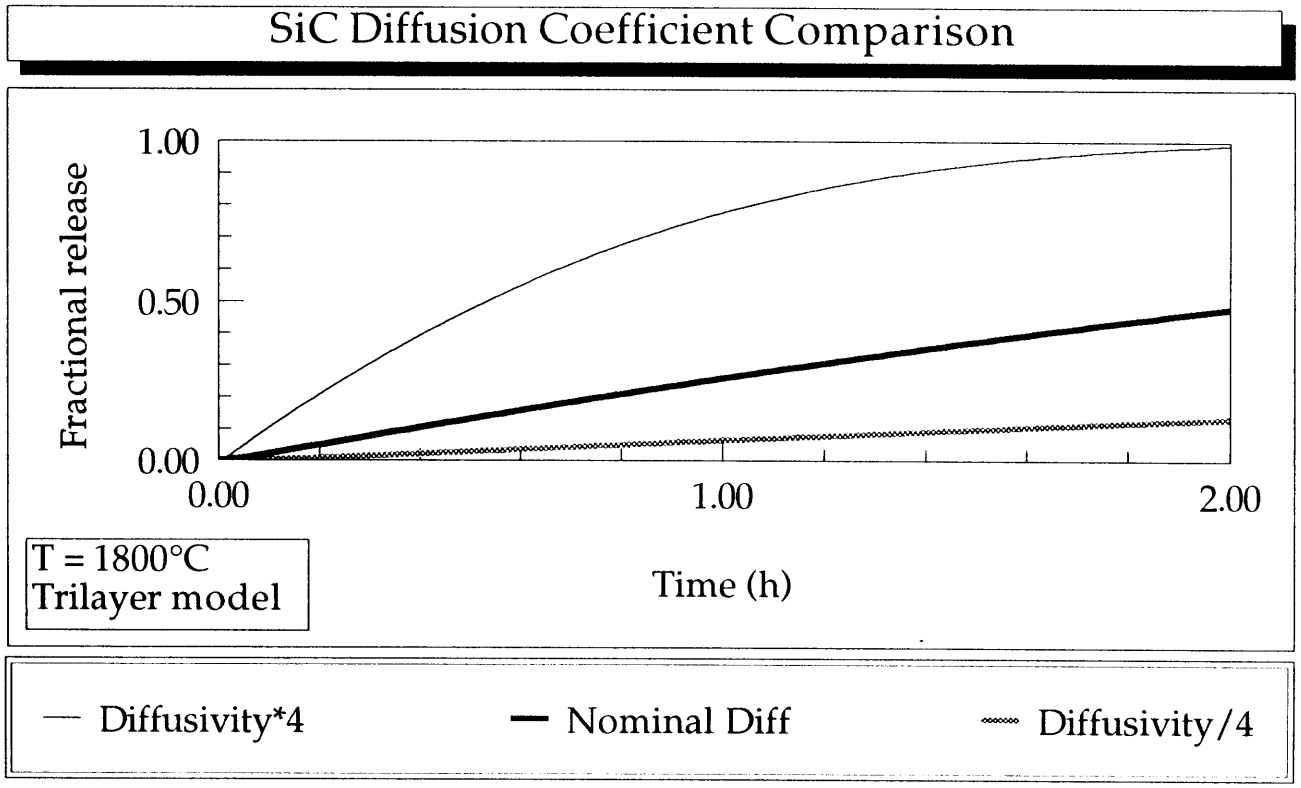

Figure 41. Effect of the SiC diffusion coefficient on tritium release.

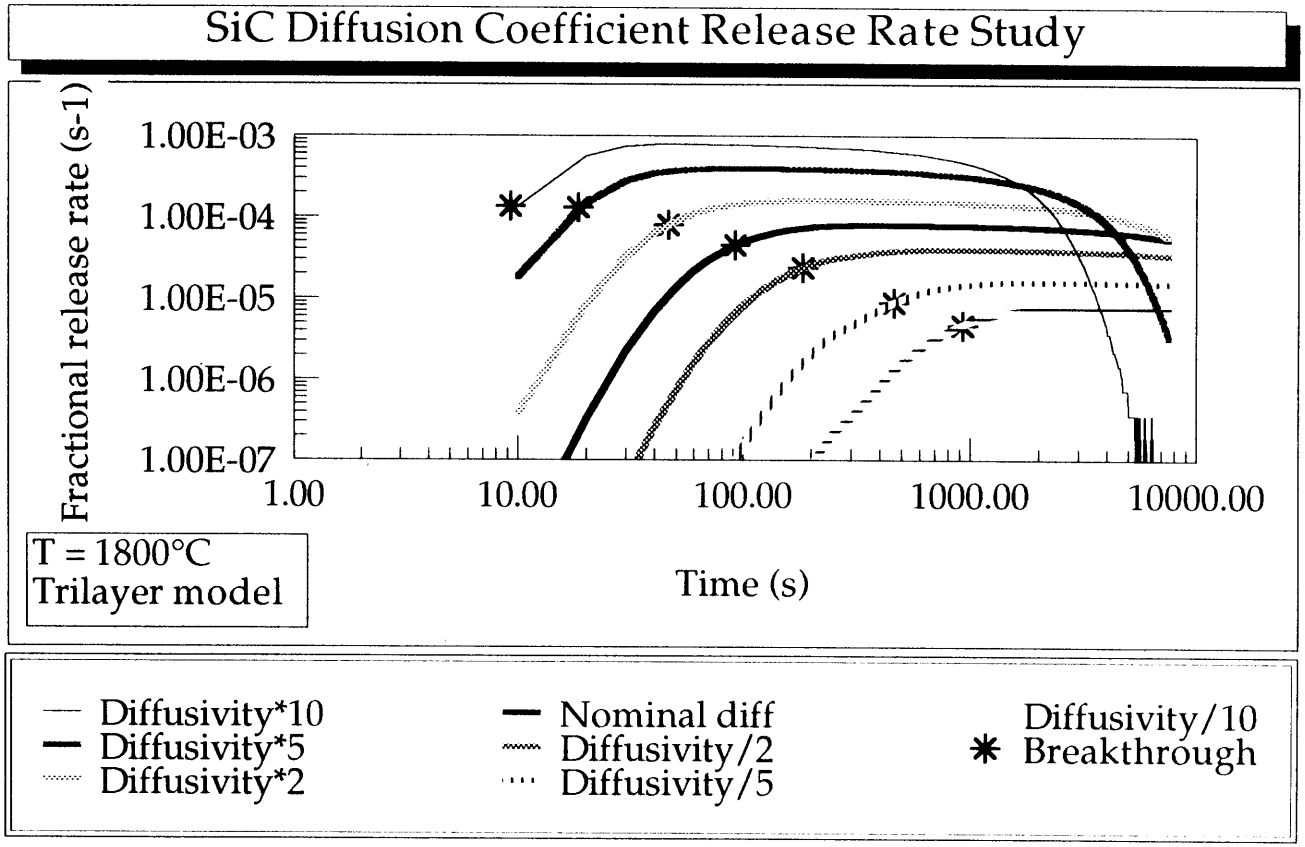

Figure 42. Effect of the SiC diffusion coefficient on the tritium release rate.

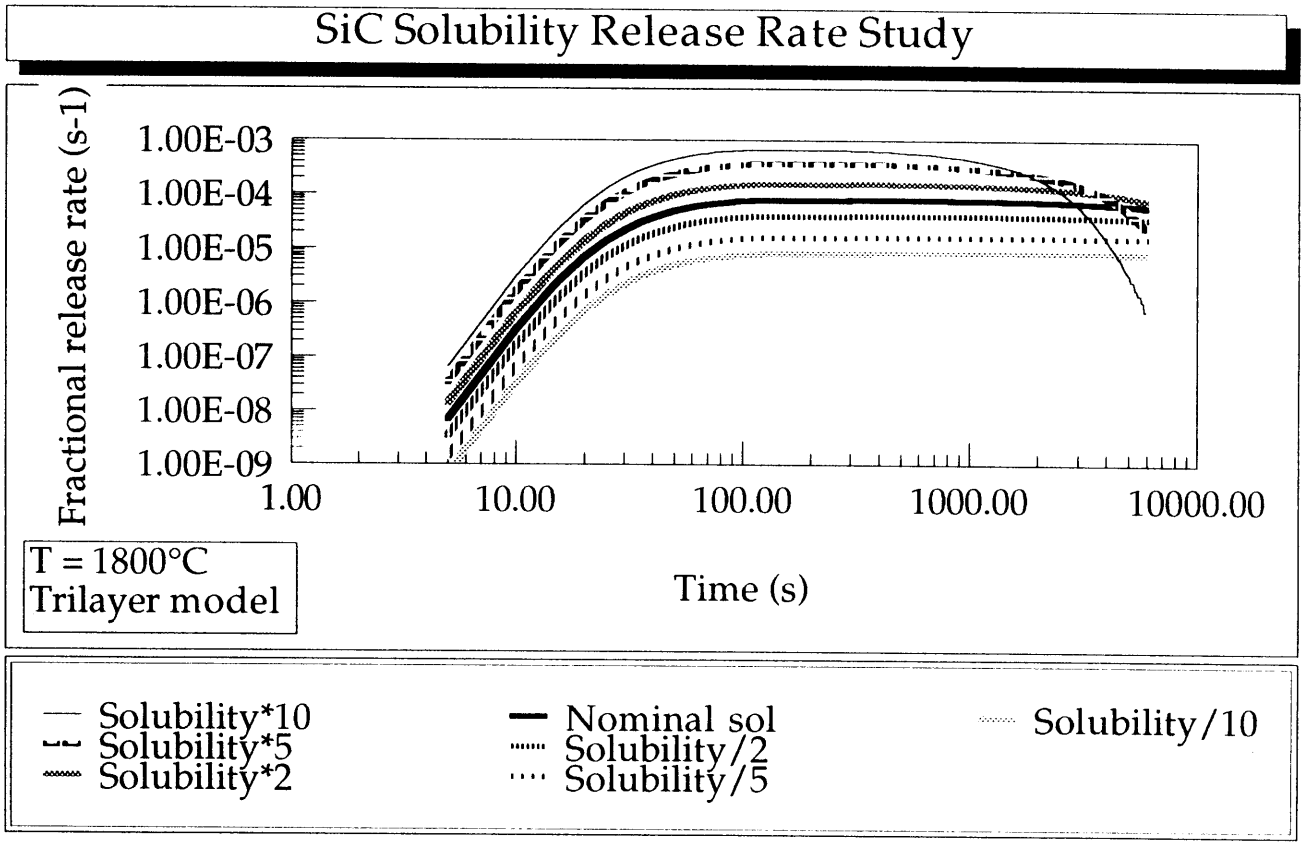

Figure 43. Effect of the SiC solubility on the tritium release rate.

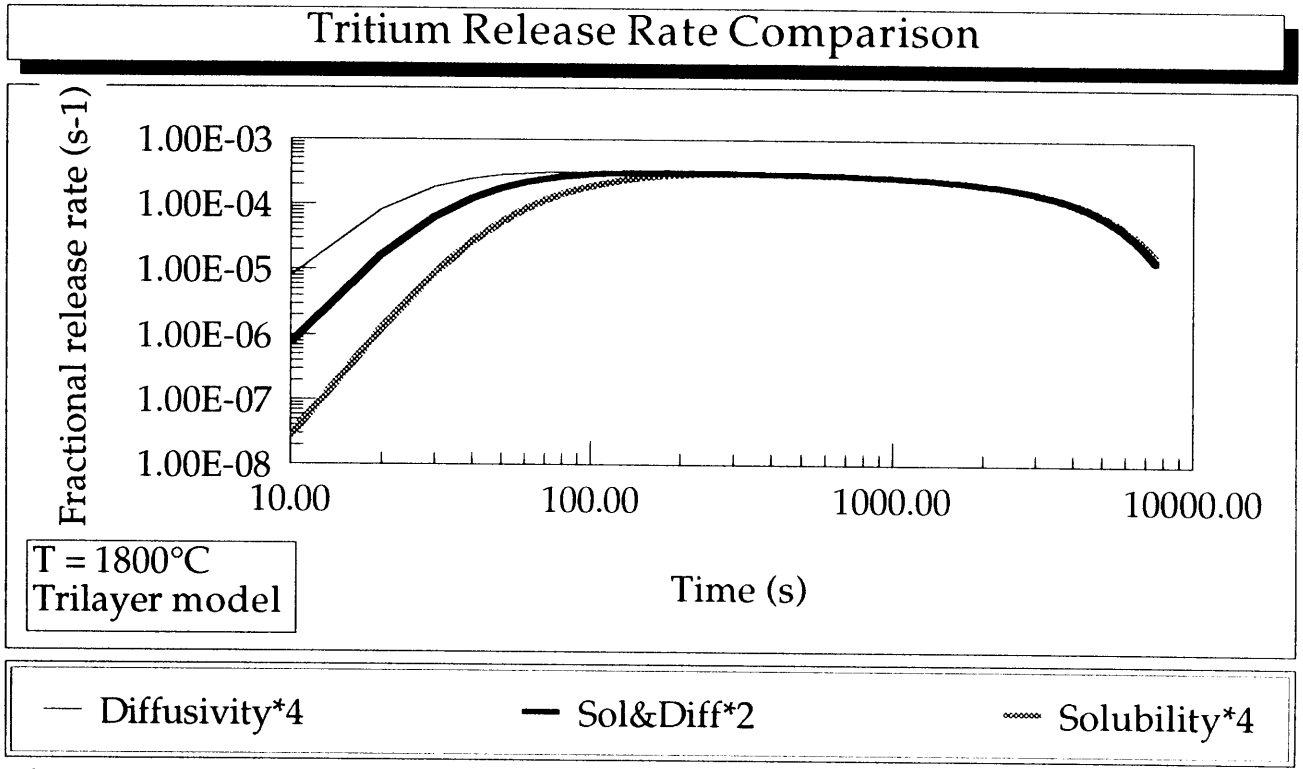

Figure 44. Effect of the SiC solubility and diffusivity on the tritium release rate.

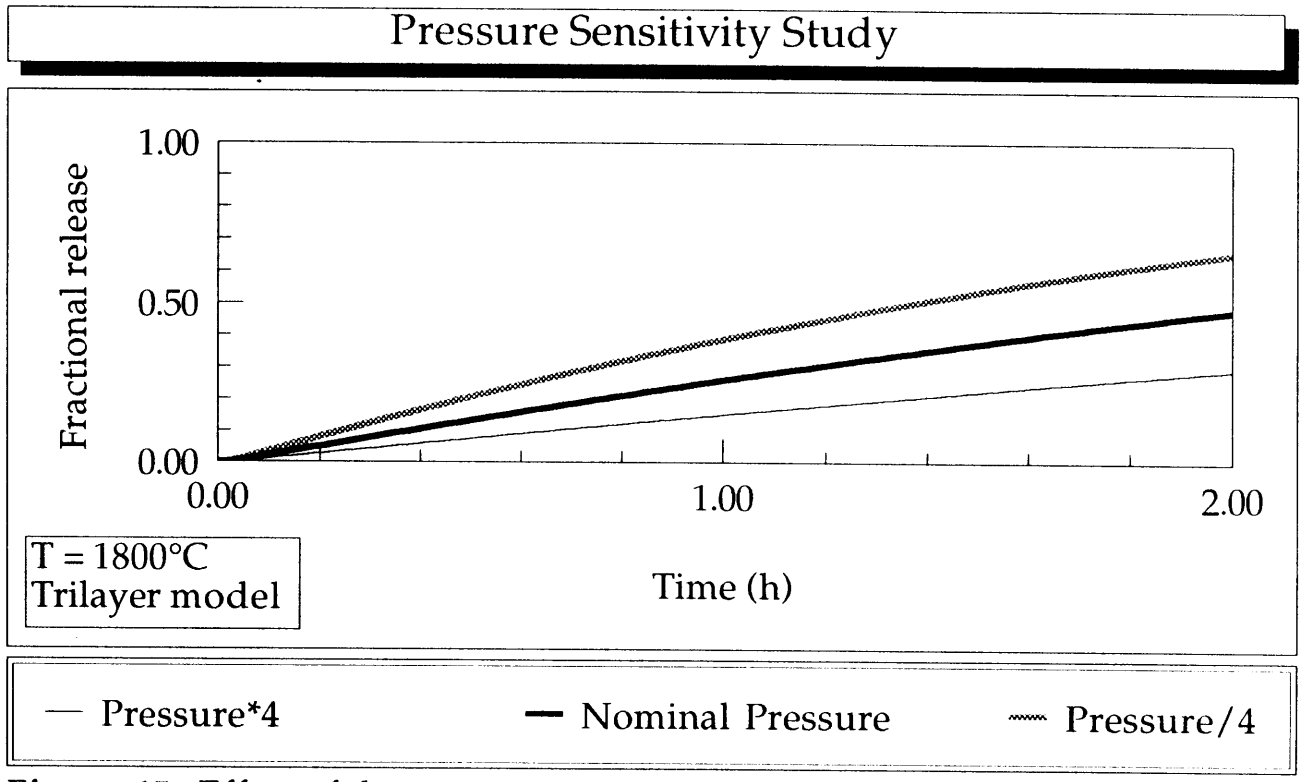

Figure 45. Effect of the tritium partial pressure on fractional tritium release.

Table 5. Fractional tritium release after 2 Hours for SiC solubility and diffusivity comparison

	Factor			
Parameter	Factor	Release	Factor	Release
Diffusivity	*4	0.99	÷4	0.13
Solubility & Diffusivity	*2	0.99	÷2	0.14
Solubility	*4	0.98	÷4	0.14

curve as increasing the solubility to twice the nominal value. However, from studying this comparison in Figure 46, it is obvious that this is not the case. In fact, an increase in the pressure results in a lower fractional release after 2 hours. This observation reiterates the conclusion of Section 4.4; namely, the decrease of the fractional release with increasing pressure (or burnup) indicates that the increased inventory has a greater effect on the release than the larger concentration gradient. Figures 47 and 48 compare the fractional release and the fractional release rate, respectively, for pressures in the range of 18 to 45% burnup, as expected in the LANL experiments. Some variation occurs in the fractional release; however, less of a change is seen in the release rate curves. Thus, a change in pressure within the expected burnup range does not significantly affect the release.

5.4 Trapping Studies

As discussed previously, TMAP also models trapping in materials. Studies by Causey[3] found a trap concentration of approximately 20 parts per million (ppm) traps for tritium in

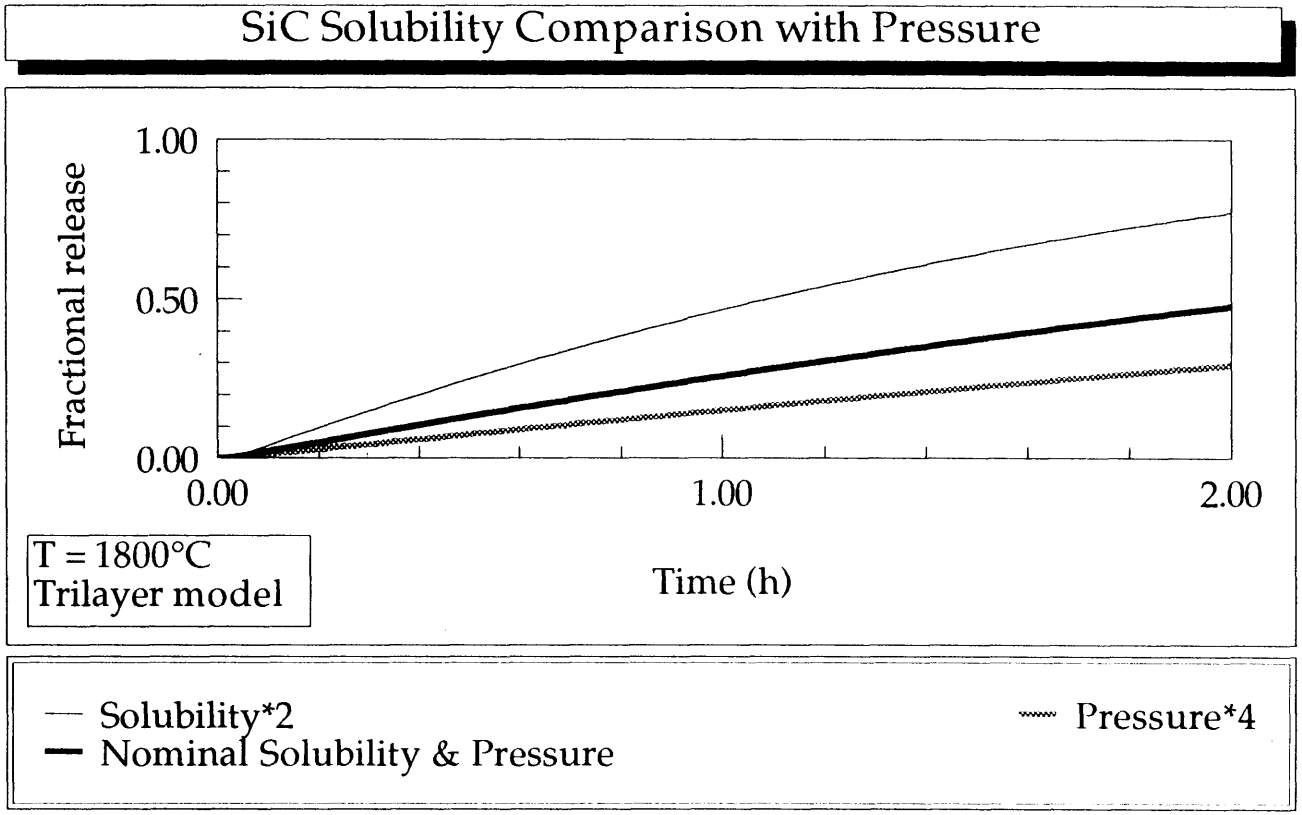

Figure 46. Comparison of the effect of solubility vs pressure on fractional tritium release.

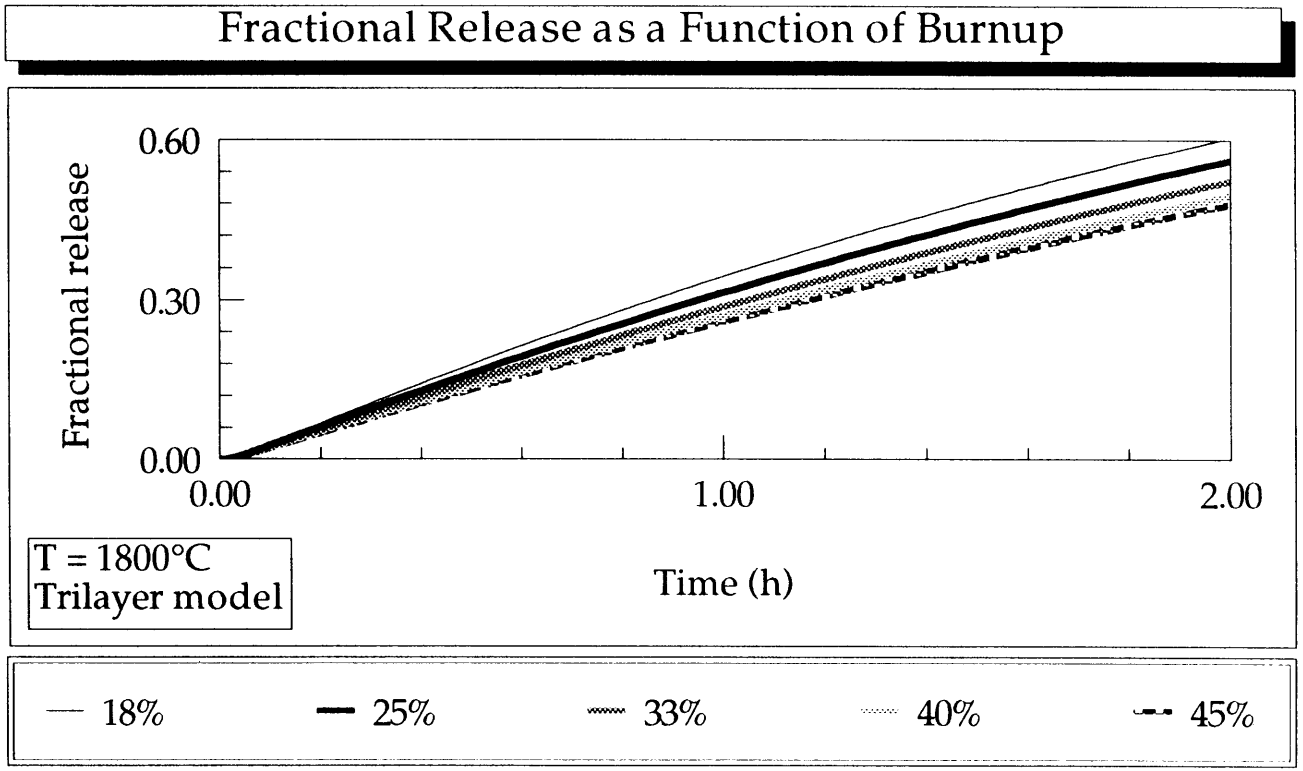

Figure 47. Effect of burnup on fractional tritium release.

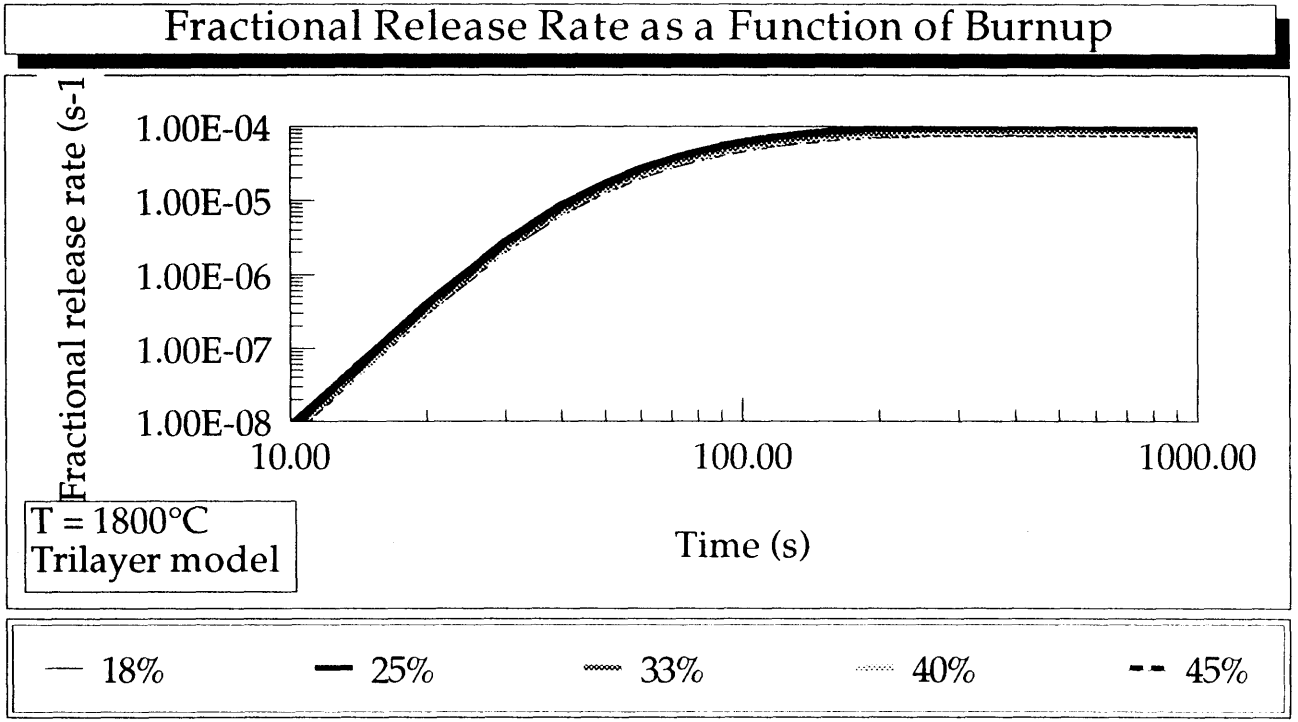

Figure 48. Effect of burnup on the fractional tritium release rate.

unirradiated graphite with a trap binding energy of 4.3 eV. However, the trap concentration was also found to increase rapidly to 1000 ppm at relatively low levels of radiation damage. The trap concentration and energy in SiC have been assumed to be comparable to those in graphite until further studies are completed to determine these parameters. Thus, in the absence of actual trapping data, parametric calculations were performed to determine the separate effects of trap concentration, trapping rate, and resolution rate on tritium release as discussed in the following sections. The SiC model with a constant source was used to simplify the problem and decrease the computational time needed to perform each calculation. The equations and results have been cast in dimensionless form to broaden the applicability of these parametric results. Details of the dimensionless transformation are found in Appendix A.

5.4.1 Effect of Trap Concentration

Figure 49 shows the effect of varying the trap concentration from 0 to 5000 ppm on the fractional tritium release. Time is plotted dimensionlessly as Dt/a^2. Thus for the case of no traps, the dimensionless breakthrough time is 0.166, which corresponds to the value given in Equation (5). The resolution rate was set to zero in these calculations to model irreversible trapping.

All of the results in Figure 49 exhibit a similar time dependence. However, an increase in trap concentration results in an increase in breakthrough time. These results are reasonable because it takes a finite time to fill all of the traps. As the number of traps in the material increases, the time to fill the traps and, thus, the breakthrough time increase. Despite this time shift, the rate of release after breakthrough is not affected, as indicated by the identical slope of the release curves. This constant slope shows that steady state has been reached, all of the traps are saturated, and the rate of tritium permeation is constant for all cases.

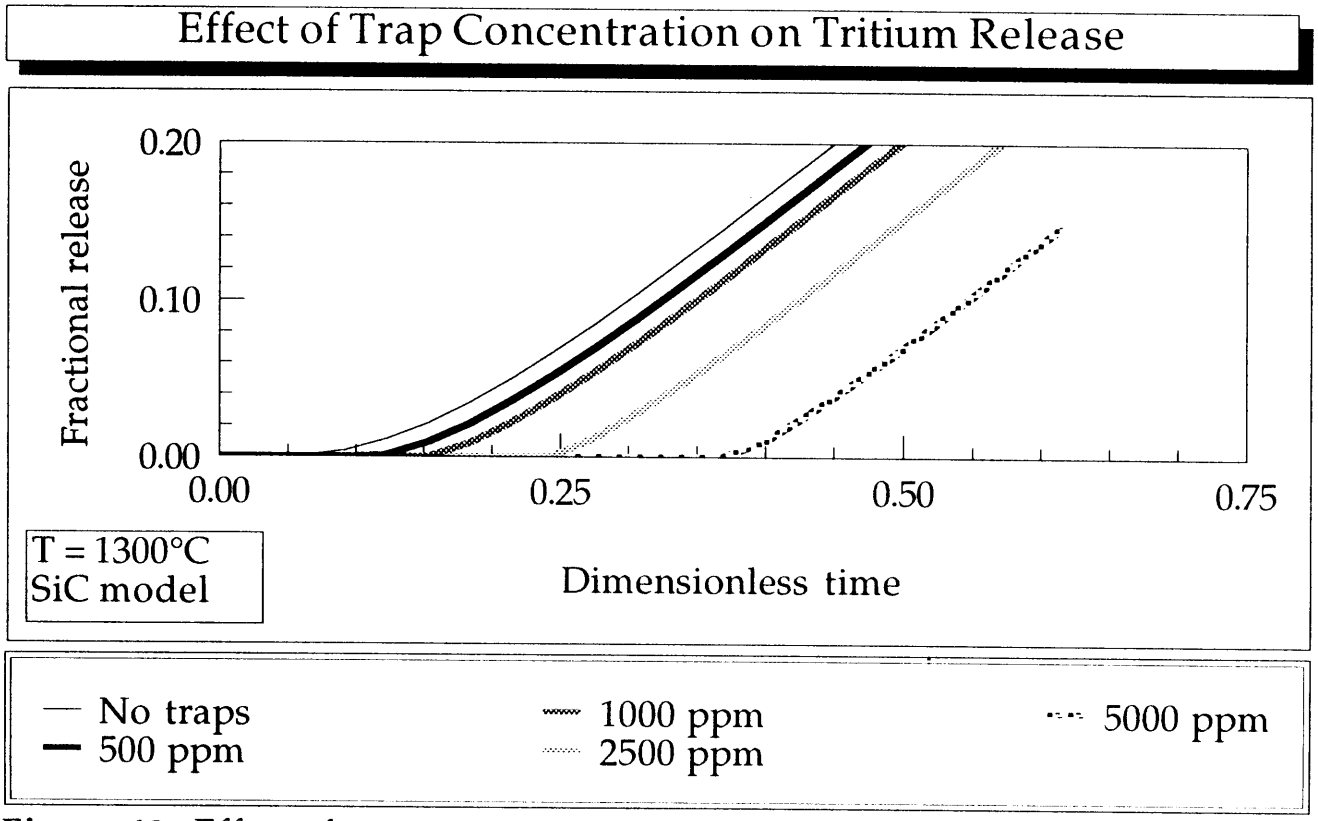

Figure 49. Effect of trap concentration on tritium release from the SiC model at 1300°C.

It is also apparent from Figure 49 that a trap concentration of approximately 1000 ppm or greater is needed to significantly affect the timing of tritium release. This observation results from the fact that the Causey correlation used in the model creates a fairly high tritium solubility in the SiC at the high tritium partial pressures in the void volume. So many atoms are in the matrix that a large trap density is required to affect tritium release. In an ATR-3 particle using Causey's value for solubility,[13] the ratio of tritium atoms in the SiC to trap sites at a trap concentration of 20 ppm is 623:1. At a concentration of 1000 ppm, this ratio drops to 12.5:1. Therefore, based on these calculations, an as-fabricated trap concentration of 20 ppm should not have a significant effect on release. Only after the material undergoes irradiation should the trapping process become important.

5.4.2 Effect of Trapping Rate

In the second set of trapping sensitivity calculations, the effect of the trapping rate on tritium release was studied. The trapping rate was varied as a percentage of the base case value used in the first set of calculations (dimensionless rate = 1.52×10^9). An irreversible trap concentration of 2500 ppm was used in the calculation. As shown in Figure 50, the breakthrough time is not affected by the trapping rate for a fixed trap concentration. However, the trapping rate does affect the transient behavior (i.e., the timing and magnitude) of the release prior to the establishment of steady state. The amount of tritium released during this transient phase depends on the magnitude of the trapping rate relative to the diffusion rate of tritium in the material. At low trapping rates, there is a low probability of tritium being trapped, so more tritium remains mobile; whereas with high trapping rates, a greater amount of tritium resides in the traps and is unavailable for release. Thus, a lower trapping rate results in a higher fractional release. Moreover, the trapping rate also affects the time at which the traps saturate. At high trapping rates, the traps saturate more quickly and a more rapid approach to steady state occurs. At low trapping rates, the

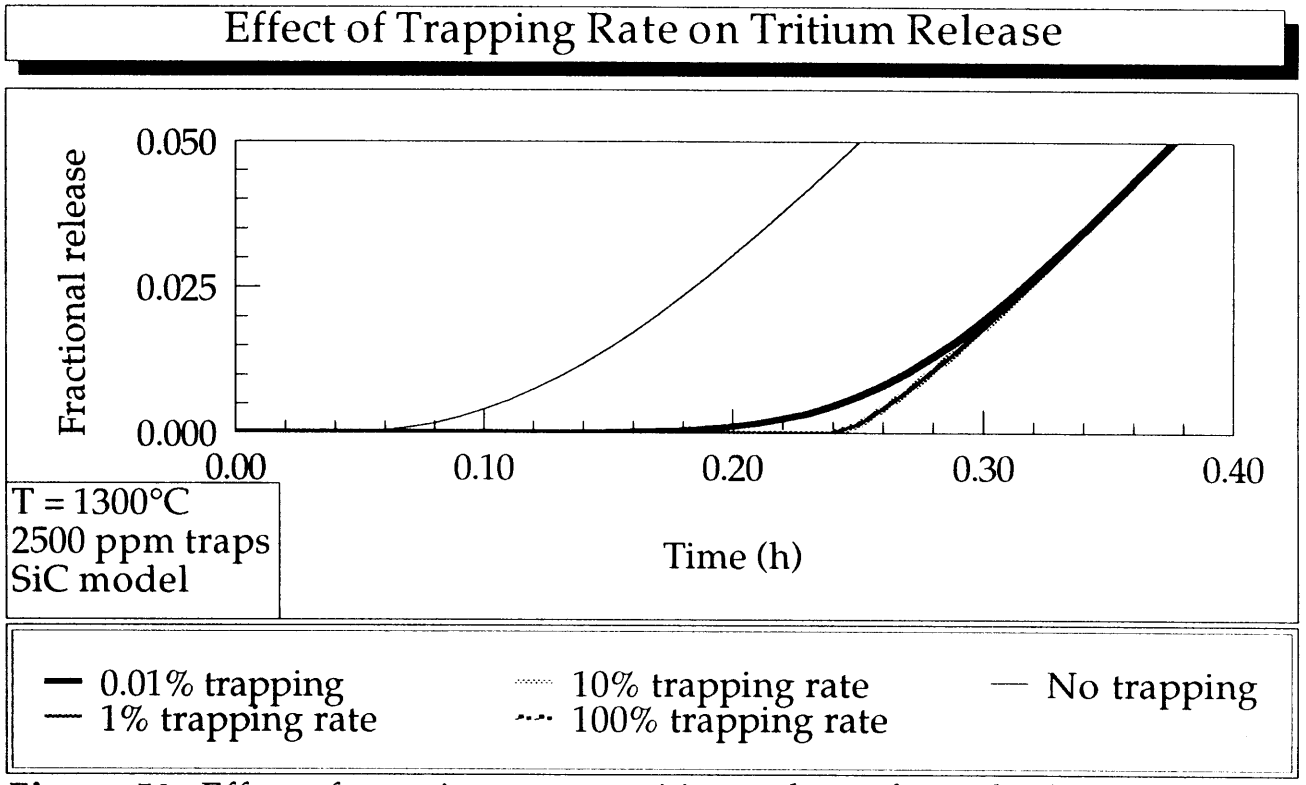

Figure 50. Effect of trapping rate on tritium release from the SiC model at 1300°C with a trap concentration of 2500 ppm. Trap rate given as percentage of 1.52e9, the value derived in Appendix A.

traps saturate more slowly resulting in a more gradual approach to steady state. The transient behavior of tritium release before steady state release is established may be useful to infer information about the trapping rate.

5.4.3 Effect of Resolution Rate

The trap release coefficient could not be determined from Equation (13) because the vibrational frequency of tritium in SiC is not known. Instead, parametric calculations were performed where the resolution rate was chosen as a percentage of the base case trapping rate (1.52×10^9). The dimensionless tritium release for these calculations is shown in Figure 51 for 0.1% resolution, no resolution, and no trapping. At resolution rates greater than or equal to 1% of the trapping rate, the results are very similar to the case of no trapping, indicating that these rates of resolution negate the effects of the traps. Resolution rates below 0.1% are so small that the traps effectively become irreversible. Hence, these two extremes were not plotted. Note that the resolution rate is temperature dependent because it is related to the vibrational frequency. Thus, the resolution rate will increase with the temperature.

A slight change in breakthrough time is evident for the case of 0.1% resolution, as compared to the cases of no traps and no resolution (irreversible trapping). The change in breakthrough time can be explained by considering the physical situation. For irreversible trapping, many of the atoms become bound in the traps as they begin to diffuse into the material. When the traps become saturated locally, the atoms are able to diffuse further into the material. Finally, when all of the traps are filled, breakthrough has been reached and tritium is released at a steady rate from the material. As discussed above, breakthrough time in the case of no trapping is reached earlier than when traps are present because the atoms do not encounter the resistance created by the traps as they diffuse through the material. The case of reversible trapping

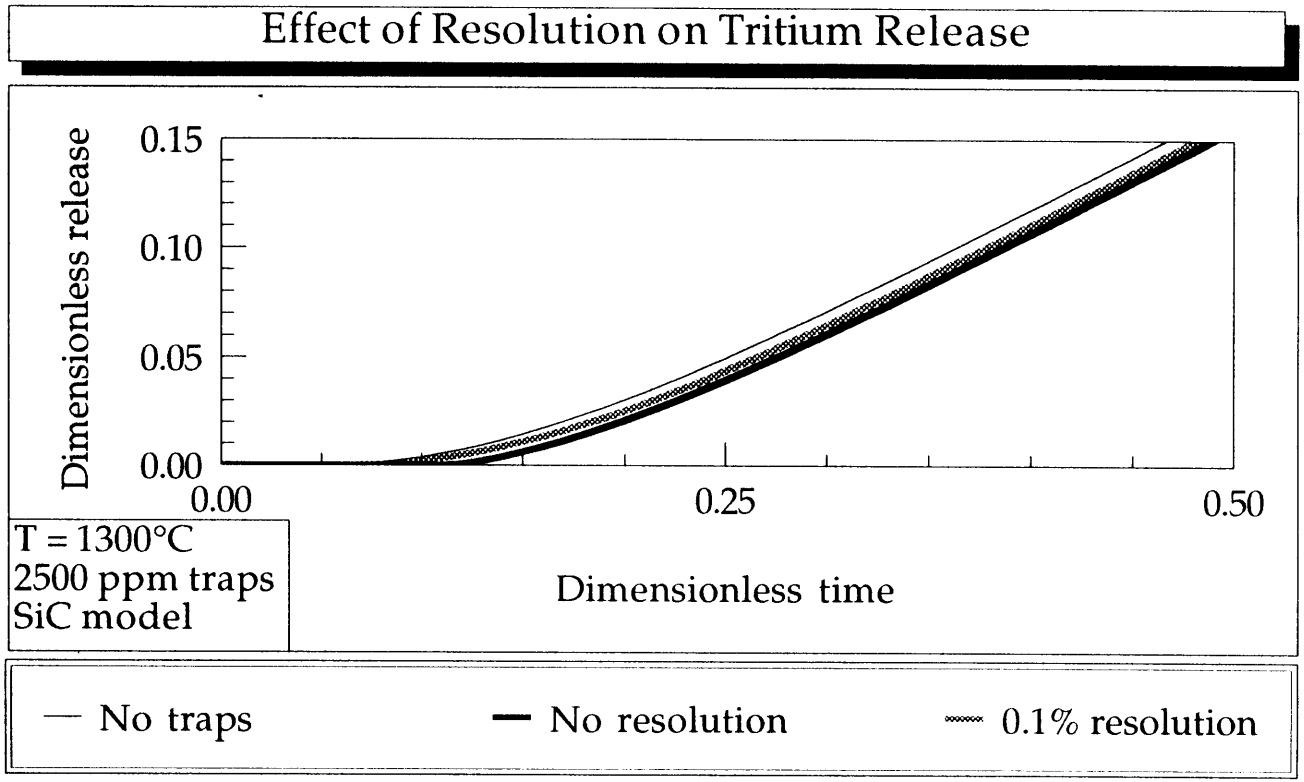

Figure 51. Effect of resolution rate on tritium release from the SiC model at 1300°C with a trap concentration of 2500 ppm. Resolution rate given as percentage of trap rate, 1.52e9, as derived in Appendix A.

(trapping with resolution) is more complex. Although the atoms can be bound in the traps during the diffusion process, there is a finite probability that they can escape from the traps and contribute to the mobile inventory in the material. A larger mobile inventory requires less time to reach steady-state release. Thus, breakthrough time for the case of reversible traps always lies between the breakthrough times for no trapping and no resolution.

5.5 Sensitivity Study Conclusions

This sensitivity study has provided many insights into the roles of the PyC and SiC layers and the effects of their transport parameters. The PyC diffusion coefficient is not an important parameter affecting release and high accuracy in the exact value is not needed. The capacitance or solubility of the PyC is very important because it affects the number of T_2 molecules remaining in the void volume and thus the tritium partial pressure which drives the diffusion process. A high PyC solubility means less molecules remain in the void reducing the pressure resulting in a lowered release rate. The SiC diffusion coefficient and solubility affect the release from the particle in a similar manner to such an extent that only the value of the product of the two parameters can be discerned from the release profile. However, the diffusivity in SiC can be determined from the experimental breakthrough time and then the solubility can be found by matching the release rate assuming trapping effects are negligable. The SiC diffusion coefficient has a significantly greater effect on the breakthrough time than the PyC value such that the PyC term can be neglected. The tritium partial pressure in the void volume does affect the fractional release. However, the effect is small over the anticipated burnup range of 18 to 45%. A trap concentration of 1000 ppm or greater is needed in the SiC layer to affect tritium release. At these high concentrations, the breakthrough time is longer but the release rate after breakthrough is not affected. The amount of change in breakthrough time is determined by the trapping rate or how fast the traps saturate. Resolution rates greater than 1% of the trapping rate negate the

effects of trapping as the atoms are released from the traps at a rate comparable to the rate at which they are being trapped. At low temperatures, trapping may be important because the resolution rate is lower but the higher solubility which results in more tritium atoms in the particle may still negate the trapping effects. The SiC and PyC trapping parameters need to be measured and added to the model before strong conclusions about the effects of trapping can be made.

6. TREL

An analytic solution for the change in pressure in a target particle as a function of time caused by tritium diffusion has been developed and programmed in TREL as explained in the following sections. The new code is simpler than TMAP because it is more specific to the target particle which requires less computing time. Section 6.1 formulates the analytic solution while Section 6.2 explains the coding of the TREL program including the input requirements and the output format of the code. TREL is compared with the TMAP in Section 6.3.

6.1 The Analytic Solution

The time to reach steady state release from the particle is characterized by the breakthrough time. For a particle at a constant temperature, recall that the breakthrough time, t_b, is given analytically by

$$t_b = \frac{\delta^2}{6D} \tag{5}$$

In this case, the diffusion coefficient, D (m^2/s), and the thickness of the layer, δ (m), correspond to the SiC layer. The PyC layers are not included in the calculation because the SiC is the dominant layer in determining the breakthrough time as shown previously in Section 5. Graphically, the breakthrough time is the back extrapolation of the steady state portion of the release curve to time zero. The breakthrough time for a transient heating cycle is more complex and can not be found from a simple equation. The tritium in the SiC is modeled as a diffusion front of atoms traveling through the layer until the front reaches the outer surface, meaning breakthrough has been achieved. Thus, the diffusion process is assumed to be at steady state when the diffusion front reaches the outer surface and the release of atoms begins. Before breakthrough, the tritium front travels a finite distant, x, at each temperature in the transient.

Recall that temperature changes are used to be instantaneous in the particle because of its small size. Thus, the following equations are solved for a constant temperature. The distance as a function of time at temperature is found by rearranging Equation (5) to yield

$$x = \sqrt{6Dt} \tag{29}$$

This equation is plotted in Figure 52 for a constant temperature of 1400°C. Because of the square root dependency, the distances do not add linearly. However, the square of the distance is linear in time. Thus, the following relationship can be used to determine the total distance traveled by the diffusion front even during a temperature ramp:

$$x = \sqrt{\sum_i x_i^2} = \sqrt{\sum_i 6D_i t_i} \tag{30}$$

where

T_i = temperature (K)
x_i = incremental distance at T_i (m)
t_i = time at temperature T_i (s)
D_i = diffusion coefficient at T_i (m^2/s).

The breakthrough time is reached during that time step when the cumulative distance traveled, x, exceeds the thickness of the material, δ. The time the particle was at the temperature when breakthrough occurred, t_n, is found from rearranging Equation (30),

$$t_n = \frac{\delta^2 - x_{n-1}^2}{6D_n} \tag{31}$$

where n is the time step in which x exceeds δ. Thus, the breakthrough time is given by

$$t_b = \sum_i^n t_i \tag{32}$$

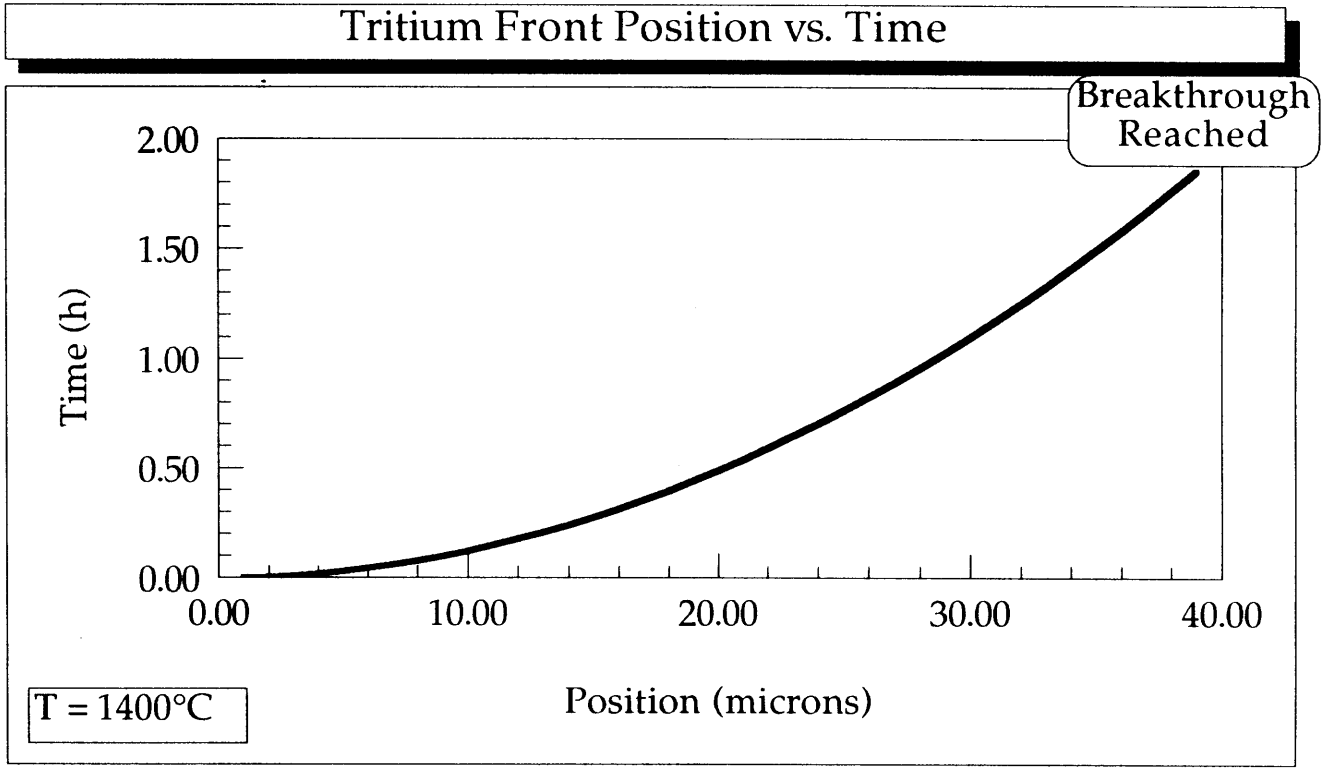

Figure 52. Tritium front position as a function of time before breakthrough.

After breakthrough has been reached, Equation (28) can be used to predict the release rate from the particles, but because the equation is only applicable to steady state, the initial pressure of tritium in the void volume can not be used for P. As discussed previously, the high solubility in the PyC results in a large initial uptake of tritium into the layer that reduces the void volume pressure significantly in the first seconds as illustrated in the plot of the pressure drop in Figure 53. The pressure after this rapid drop can be determined by a simple balance of tritium atoms after the system equilibrates. Because sufficient time has not yet passed for the atoms to have reached the SiC layer, all of the atoms are in either the enclosure or the PyC layer. Thus,

$$N_T(0) = N_{encl} + N_{PyC} \tag{33}$$

where $N_T(0)$ is the number of initial tritium atoms and N is the number of atoms in the enclosure and PyC as indicated. Recall from Section 1 that the concentration in the PyC is given by the following solubility relation

$$C = NS_c P^n \tag{7}$$

Experimental results indicate that Sievert's law (n = 0.5) more correctly expresses the pressure dependency than Henry's law (n = 1.0) but the experimentally determined value of n is not necessarily exactly equal to 0.5. Thus, the following equations for the pressure are solved with a variable n for generality. Expanding the terms of Equation (33) yields

$$\frac{2P_oV}{kT} = \frac{2VP_{eq}}{kT} + (SA\delta)_p P_{eq}^n p \tag{34}$$

where P_o is the initial tritium gas (T_2) pressure (Pa) determined by the particle burnup and ideal gas law (see Table 1), the factor of 2 converts molecules of T_2 to atoms of T, V is the void volume (m^3), k is

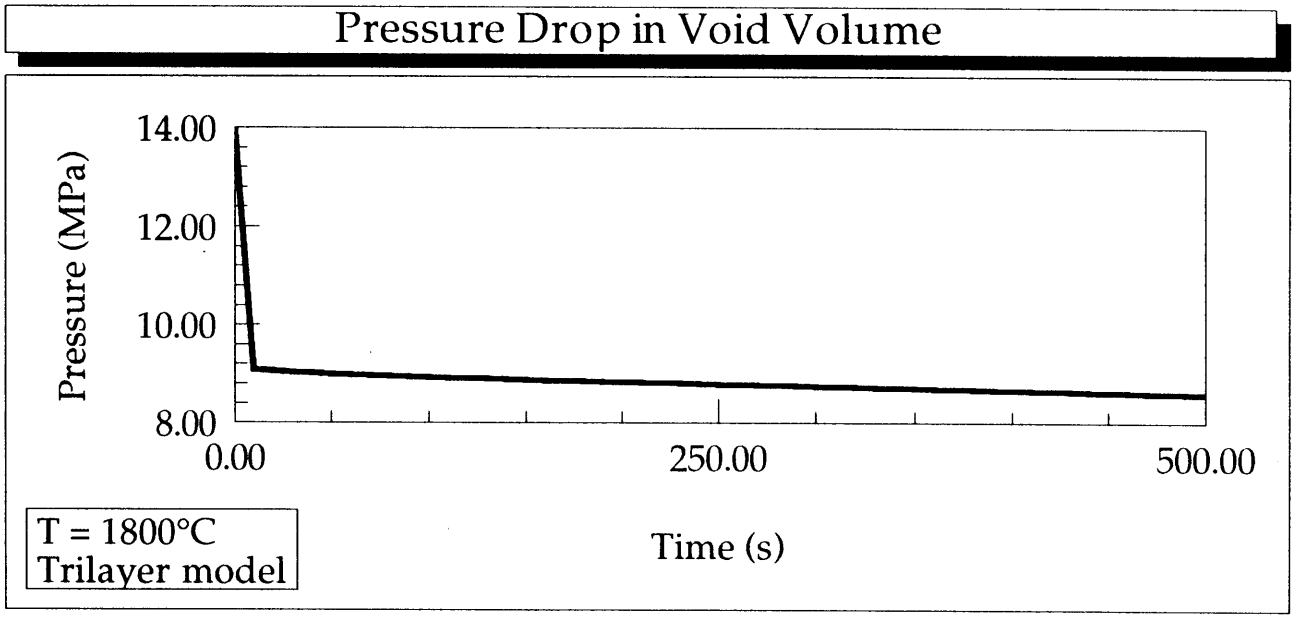

Figure 53. Tritium partial pressure in the void volume over time as calculated by TMAP.

Boltzmann's constant (J/K), T is the temperature (K), S is the solubility (atoms/m^3Pa^n), A is the surface area (m^2), δ is the layer thickness (m), the subscripts p and s denote PyC and SiC terms respectively, and P_{eq} is the equilibrium pressure (Pa) in the enclosure after the initial loading of the PyC. This equation is solved iteratively to determine P_{eq}.

A similar analysis yields the pressure as a function of time once the tritium begins to permeate through the SiC.[18] (The holdup of atoms in the OPyC layer is negligible; thus the OPyC is not included in this analysis and atoms are assumed to be released from the particle after diffusing through the SiC.) The addition of a permeation term to the atom balance to account for atoms that have been released from the particle expands Equation (34) to

$$\frac{2P_oV}{kT} = \frac{2VP(t)}{kT} + (SA\delta)_p P(t)^{n_p} + \int_0^t \left(\frac{DSA}{\delta}\right)_s P(\tau)^{n_s} d\tau \qquad (35)$$

Differentiating this equation with respect to time, t, and assuming the temperature is constant generates

$$\frac{2V}{kT}\frac{dP(t)}{dt} + n_p(SA\delta)_p P(t)^{(n_p-1)}\frac{dP(t)}{dt} + \left(\frac{DSA}{\delta}\right)_s P(t)^{n_s} = 0 \qquad (36)$$

Equation (36) can be rearranged to create

$$\int_{P_{eq}}^{P(t)} \left[\frac{2V}{kT}\left(\frac{\delta}{DSA}\right)_s P^{-n_s} + n_p(SA\delta)_p\left(\frac{\delta}{DSA}\right)_s P^{(n_p-n_s-1)}\right] dP = \int_0^t -d\tau \qquad (37)$$

which is integrated to produce

$$\frac{2V}{kT(1-n_s)}\left(\frac{\delta}{DSA}\right)_s\left(P_{(t)}^{1-n_s}-P_{eq}^{1-n_s}\right)+\frac{n_p(SA\delta)_p}{n_p-n_s}\left(\frac{\delta}{DSA}\right)_s\left(P_{(t)}^{(n_p-n_s)}-P_{eq}^{(n_p-n_s)}\right)=-t \quad (38)$$

Equation (38) can then be solved iteratively to determine P(t). However, if n_p and n_s are both equal to 0.5, L'Hospital's Rule must be used to solve the second term in the equation resulting in the following solution:

$$\frac{4V}{kT}\left(\frac{\delta}{DSA}\right)_s\left(P_{(t)}^{1-n_s}-P_{eq}^{1-n_s}\right)+n_p(SA\delta)_p\left(\frac{\delta}{DSA}\right)_s\ln\left(\frac{P(t)}{P_{eq}}\right)=-t \quad (39)$$

When a temperature change occurs, the direct temperature dependency of P_o and P_{eq} requires the recalculation of these values. In addition, to take into account the tritium atoms that have already been released from the particle, P_o is multiplied by the fraction of atoms remaining in the enclosure and the PyC layer. P(t) is then calculated as a function of the time the particle has been at the new temperature. The temperature across the particle is assumed to be uniform and changes occur instantaneously. This assumption is supported by the good heat transfer properties of the materials and the small size of the particle.

Once the pressure is determined as a function of time, the fractional release, FR, from the particle can be calculated from

$$FR(t+dt)=FR(t)+\int_t^{t+dt}\frac{\left(\frac{DSA}{\delta}\right)_s P(\tau)^{n_s}\,d\tau}{2N_o} \quad (40)$$

An extremely small time step must be used to make this integral result accurate. To avoid this step size dependency in TREL, the fractional amount of tritium in the PyC and the enclosure is subtracted from one to obtain FR. Thus, the equation

$$FR(t) = 1 - \frac{P(t)V}{kTN_o} - \frac{(SA\delta)_p}{2N_o} P(t)^{n_p} \qquad (41)$$

is used in TREL without time step limitations.

6.2 The TREL Code

TREL was programmed in Language Systems Fortran, an ANSI standard F77 system, on a Macintosh SE/30. A flow chart of the operations is shown in Figure 54. A listing of the code, the input, and the output are given in Appendix C.

The iterative solutions are found using a Newton-Raphson Bisecting method.[19] This method is based on the conventional Newton-Raphson method but converges significantly faster. It bisects the step if Newton's method is not decreasing the step size fast enough or if the use of Newton-Raphson would produce a solution outside of the upper and lower limits. In those cases where Newton-Raphson is acceptable, it is used.

TREL uses a namelist to read the input in the format shown in Appendix C. The input variables are as follows with the units given in parentheses:

AREA - layer surface area (m^3)
BUP - ^{6}Li burnup (atom%)
DPYC - PyC thickness (m)
DSIC - SiC thickness (m)
MAXIT - maximum number of iterations to be performed
MLI6 - mass of ^{6}Li (g)
NSTEP - number of time steps
PEXPP - pressure exponent for PyC (n_p)
PEXPS - pressure exponent for SiC (n_s)
SPYCFAC - multiplicative factor for PyC solubility

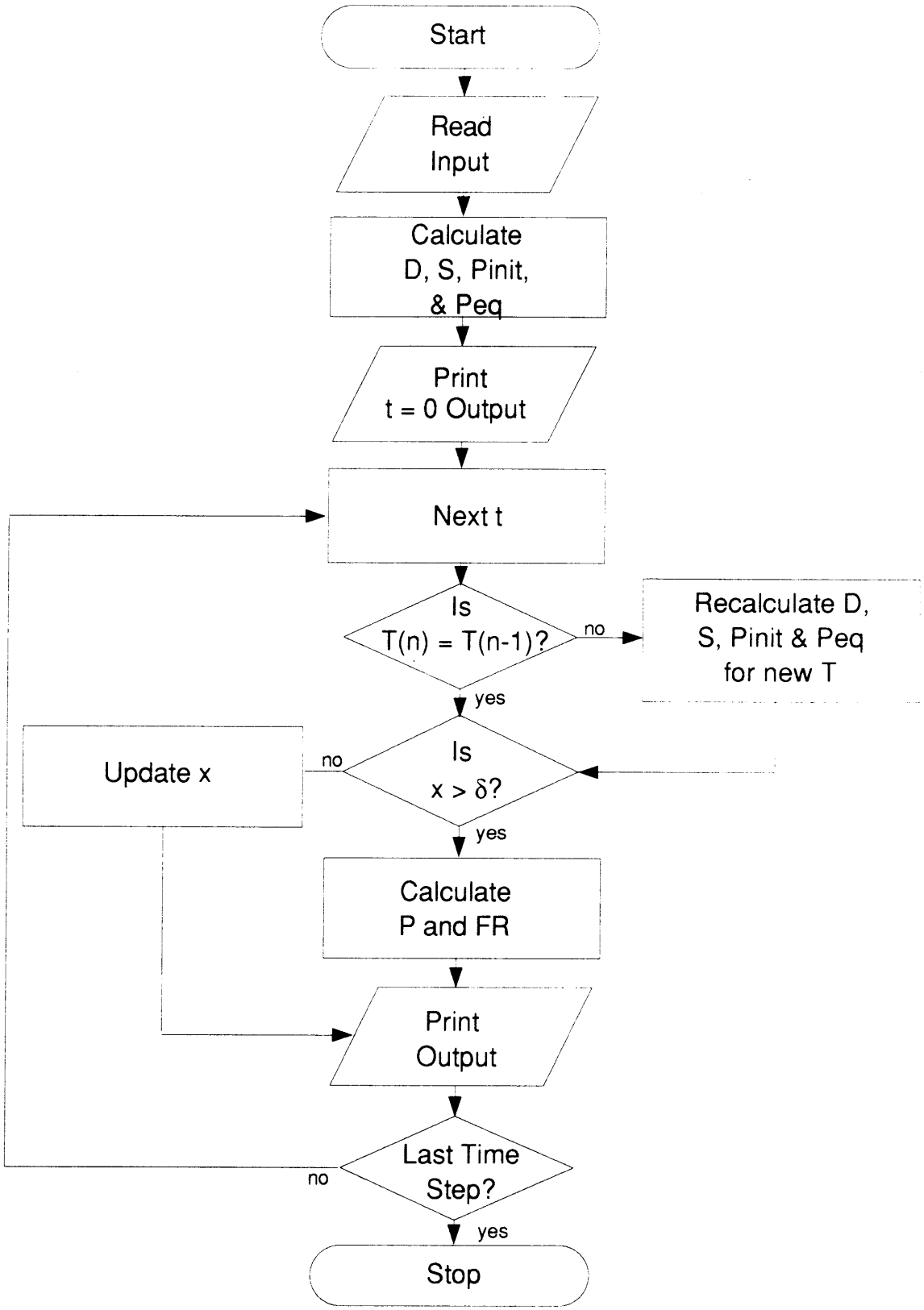

Figure 54. TREL Flow Chart

SSICFAC - multiplicative factor for SiC solubility
DSICFAC - multiplicative factor for SiC diffusivity
TFLAG - time unit flag (0=sec, 1=hrs)
TOL - tolerance for iterative solutions
VVOID - void volume (m^3)
TIME(NSTEP) - time (s)
TEMP(NSTEP) - temperature (K).

The PyC and SiC solubility and diffusivity correlations encoded in TREL are taken from Causey[6,13] but these relations can be scaled with the input parameters SPYCFAC, SSICFAC, and DSICFAC. The first time value inputted must be zero or an error message will be given and program execution terminated. TFLAG gives the user the option of inputting the time in the seconds (TFLAG=0) or in hours (TFLAG=1).

When a temperature change occurs, TREL calculates new initial and equilibrium pressures at this temperature. Then, P(t) is calculated using the length of time the particle has been at the new temperature. In calculating the time at temperature, it assumes the temperature change occurred instantaneously after the last time step computation. Thus, from the following input,

time(4) = 1000
temp(4) = 1773
time(5) = 1500
temp(5) = 1873

TREL would first compute the release at 1773 K after 1000 s. Then P_o would be recalculated for 1873 K and multiplied by the fraction of atoms remaining in the PyC and the enclosure to account for atoms released up to 1000 s that, of course, no longer contribute to the pressure. When computing P(t) for 1500 s, the code uses a time of 500 s in the equation. This convention was chosen because it replicates the format of the data from the LANL experiments where a reading was taken immediately before each temperature change.

Appendix C contains a sample output and plot file for TREL. The plot file contains the time in seconds, time in hours, temperature (K), pressure (Pa), and release from the particle for each time step as well as for the breakthrough time. The release is zero until breakthrough is reached; the actual breakthrough time is the last time in the file with a release of zero. The initial time step lists P_o for the pressure, then P_{eq} is given until breakthrough time is reached, after which P(t) is listed in the remaining time steps. In the output file, the input parameters are listed followed by the time (s), temperature (K), time at temperature (s), pressure (Pa), equilibrium pressure at temperature (Pa), initial number of atoms, fraction of atoms remaining in the enclosure and the PyC, and the fraction of atoms released from the particle. The breakthrough time is also indicated by a line of output appearing between the regular outputs in time sequence.

6.3 TREL vs. TMAP

TREL release predictions compare remarkably well with TMAP predictions. As shown in Figure 55, the fractional release calculated by the two codes varies by less than 1%. Because the TMAP calculation includes the OPyC layer, this result indicates that the OPyC layer can be neglected in the TREL calculation. Figure 56 compares the pressure calculated by each code indicating the pressures vary by less than 3%. Note the pressure and the release do not vary by the same percent even though they are directly related to one another. This disparity is explained by the fact that TMAP calculates the release in the time dependent manner of Equation (40) whereas TREL uses Equation (41).

Although TMAP is more versatile than TREL, TREL does have some advantages. In TMAP, the temperature of the layers can be changed but not the temperature of an enclosure, or in this case, the void volume. Because the pressure in the volume is determined by the temperature dependent ideal gas law, TMAP is not accurate for analyzing release during temperature ramps as occur in the LANL

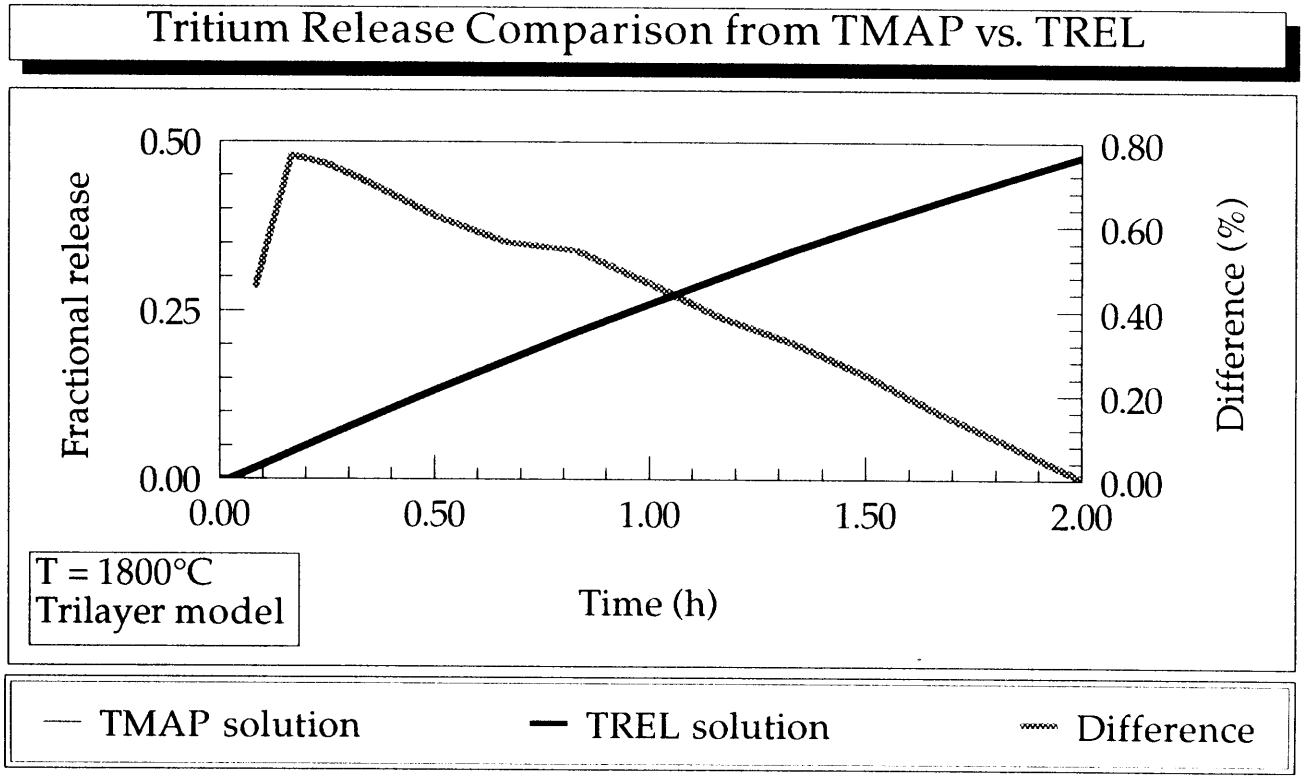

Figure 55. Comparison of the fractional release as predicted by TMAP vs. TREL.

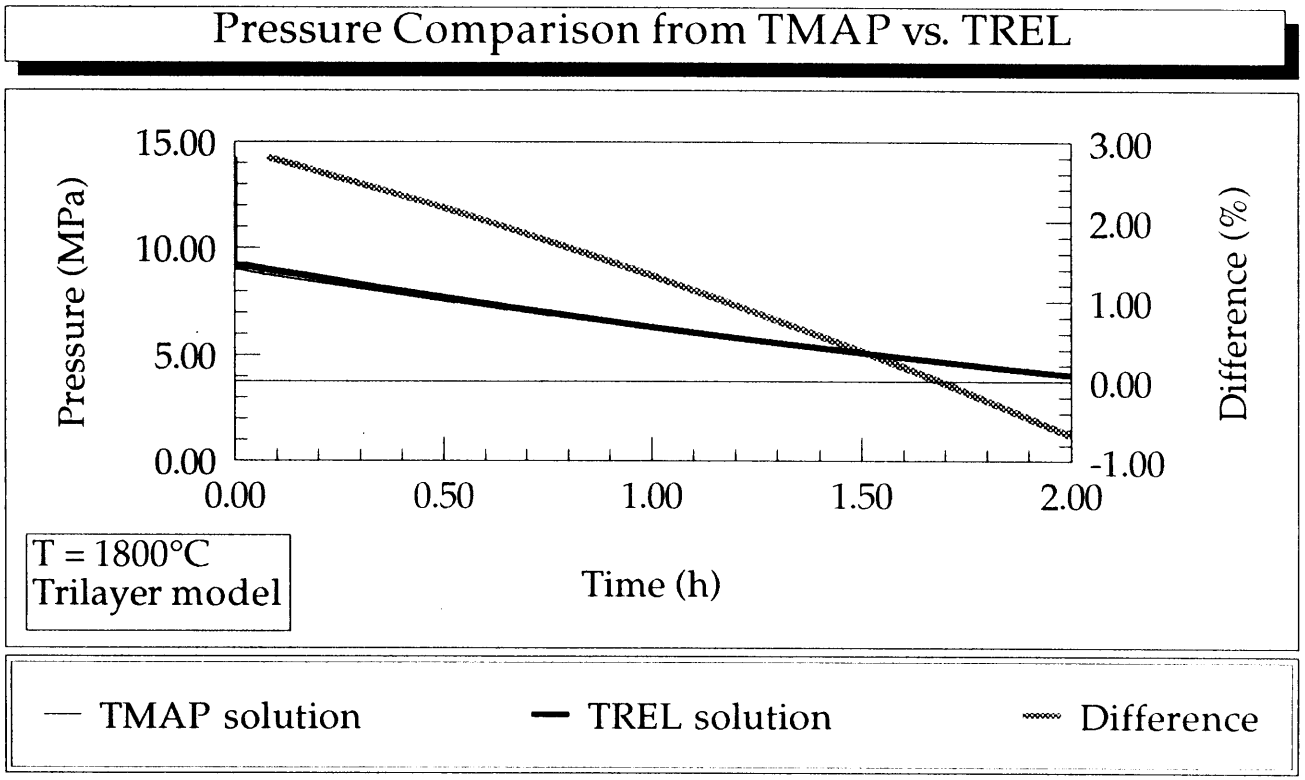

Figure 56. Comparison of the pressure as predicted by TMAP vs. TREL.

tests whereas TREL is capable of modeling this situation. TMAP is only capable of modeling Sievert's or Henry's laws whereas any value of n can be inputted in TREL for the PyC or the SiC. Although calculations were not performed using this option, experimental results may indicate a value other than 0.5 or 1.0 for this parameter and TREL will be capable of modeling it. The computer time required to run a problem is significantly reduced with TREL compared to TMAP. In TMAP, the fractional release is computed with a time step dependent formula that requires a time step of 0.1 s for accuracy. Thus, TMAP calculations at 1200°C require from 24 to 48 hours to reach 90% release whereas the problem can be solved with TREL in less than one minute using a time step as great as 48 hours if desired. On the other hand, TREL does not model trapping or thermal gradients. However, these effects have not yet proven to be important in modeling NP-MHTGR target particles.

Thus, TREL can be used to predict tritium release from the NP-MHTGR target particles at the current state of the model. Its accuracy rivals that of TMAP with the added benefits of significantly reduced computing time and transient modeling capabilities. However, if trapping or thermal driven diffusion is found to be important, TREL will have to be updated or abandoned.

7. COMPARISON OF MODEL PREDICTIONS WITH EXPERIMENTAL RESULTS

In this section, TREL calculations were compared with experimental results to determine the tritium transport parameters (diffusivity and solubility) in the TRISO-coated particle to best describe the LPI experiments. These results were then compared with tritium release data from target compacts.

7.1 Solubility Determination using the LPI-1 Experimental Data

The Loose Particle Irradiation test, LPI-1, was conducted to demonstrate the stability of target particles under design operating conditions and to determine the threshold for particle failure at various ^{6}Li burnups. The particles were irradiated in three phases termed A, B, and C. The position of each of the capsules during irradiation is shown in Table 6. Characteristics of the particles studied are given in Table 7. In the first phase (LPI-1A), 36 capsules each containing 500 target particles were irradiated in the Advanced Test Reactor (ATR) at the INEL to burnups between 20 to 24%. Some of the particles (capsules 7A and 7C) were electrically heated to 1200°C[20] and subsequently, the 7C particles were reheated to 1685°C.[21] The amount of tritium released from the particle was measured to determine tritium release characteristics and to check for signs of particle failure during each test. The remaining particle capsules were irradiated for another cycle in ATR to attain a maximum burnup of 38% in the second phase of the test (LPI-1B).[22] Again two capsules of particles (5B and 9B) were heated to 1200°C[23] and one capsule (12C) was heated to 1685°C.[24] In the 12C high temperature test, the particles were split into two batches, 12C-1 and 12C-2. Test 12C-1 used a sweep gas mixture of helium with 1% hydrogen while test 12C-2 used pure helium to determine the effect of hydrogen in the sweep gas. Peak burnups of 55% were expected in the phase three irradiation (LPI-1C) where the remaining particles were irradiated for a third ATR cycle. LPI-1C particles were not studied because the large internal pressures resulting from the high

Table 6. LPI-1 capsule irradiation configuration

LPI-1A			LPI-1B			LPI-1C
1A	1B	1C	1A	1B	1C	2B
2A	2B	2C	2A	2B	2C	2A
3A	3B	3C	3A	3B	3C	3A
4A	4B	4C	4A	spacer	4C	4C
5A	5B	5C	5A	5B	5C	6C
6A	6B	6C	6A	6B	6C	6B
7A	7B	7C	spacer	spacer	spacer	1A
8A	8B	8C	spacer	8B	8C	8B
9A	9B	9C	9A	9B	9C	8C
10A	10B	10C	10A	10B	10C	10C
11A	11B	11C	11A	11B	11C	11A
12A	12B	12C	12A	spacer	12C	12A

Table 7. Characteristics of LPI tests

	LPI-1A 7C	LPI-1A 7C	LPI-1B 12C-1	LPI-1B 12C-2	LPI-1B 5B/9B
No. of particles	747	747	236	239	951
Burnup (%)	22.0	22.0	25.4	25.4	36.9
Tritium inventory (Ci)	1.179	1.179	0.640	0.648	4.083
Fast fluence ($x10^{19}n/cm^2$)	1.35-1.85	1.35-1.85	~6.0	~6.0	6.76-7.01
Maximum Temp (°C)	1200	1600	1685	1685	1200
Time (h)	87	87	168	168	72
Particle type	ATR-1	ATR-1	ATR-1	ATR-1	ATR-1
S_c ($x10^{-9}$ $Pa^{0.5}$)	a	3.084	5.782	4.681	a
Q_S (kJ/mole)	57.17	57.17	57.17	57.17	57.17

a. Particles only used to determine Q_S.

burnups caused particle failure and the tritium release due to diffusion could not be separated from that resulting from particle failure.

The LPI postirradiation heating tests can be modeled as permeation experiments. Recall that the diffusivity and solubility both have an Arrhenius temperature dependence, such that

$$D = D_c \exp(-Q_D/RT) \tag{42}$$

$$S = S_c N \exp(-Q_S/RT) P^{0.5} \tag{43}$$

where Q_D is the activation energy for diffusion (kJ/mole), Q_S is the heat of formation for the solubility (kJ/mole), N is the host material number density (m^{-3}), and D_c and S_c are the diffusivity (m^2/s) and solubility constants (Pa^{-n}). At equilibrium, the flow rate of atoms, m, is given by Equation (8) which can be expanded using Equations (42) and (43), such that

$$m = \frac{D_c S_c N \exp\left(-\frac{Q_D+Q_S}{RT}\right) P^{0.5} A}{\delta} \tag{44}$$

The equilibrium concentration of tritium, C, in the sweep gas is related to m as given by

$$C = \frac{m}{Q_{flow}} = \frac{D_c S_c N \exp\left(-\frac{Q_D+Q_S}{RT}\right) P^{0.5} A}{Q_{flow}\delta} \tag{45}$$

where Q_{flow} is the volumetric flow rate of the sweep gas in the experiment. Equation (45) can be simplified to

$$C = C_o \exp\left(\frac{-Q}{RT}\right) \tag{46}$$

where

$$Q = Q_D + Q_S \tag{47}$$

and

$$C_o = \frac{D_c S_c N P^{0.5} A}{\delta Q_{flow}}. \tag{48}$$

The equilibrium concentration was measured in the LPI experiments over the temperature range of 1000 to 1400°C using capsule 7C, 5B and 9B particles. The data were fit with a correlation in the form of Equation (46) as shown in Figure 57. The breakthrough times predicted with Causey's diffusion coefficient[13] agree with the experimental values to within the published uncertainty. Thus, the diffusivity relation was assumed to be correct and the LPI data were used to determine a new solubility relation. Q_S was calculated by fitting the equilibrium concentration to an Arrhenius relation given by Equation (46). Then the value of Q_D (308 kJ/mole) was subtracted from Q to obtain the value of 57.17 kJ/mole for Q_S.

The value of S_c, the preexponential factor, was determined empirically by varying the solubility scaling factor in TREL until the prediction matched the data from the 7C and the 12C high temperature tests. Figures 58 and 59 compare the fractional release and the fractional release rate, respectively, of the 7C tritium release data with the TREL prediction using an S_c of 3.084×10^{-9} $Pa^{-0.5}$ and the previously determined value of 57.17 kJ/mole for Q_S. TREL slightly overpredicts the 1200°C release rate but matches the data at 1300 and 1400°C very well. Particle failure occured at 1500 and 1600°C as indicated by the peaks in the data. As expected, the TREL prediction is below the peak tritium release rate when failure occurs and then is higher than the data at later times because the failed particles no longer contribute to the release rate. The 12C-1 test required a value of 5.782×10^{-9} $Pa^{-0.5}$ for S_c in TREL to accurately match the data as shown in Figures 60 and 61 and a value of 4.681×10^{-9} $Pa^{-0.5}$ for S_c was used in the 12C-2 test as shown in Figures 62 and 63. These plots are quite similar with the model in

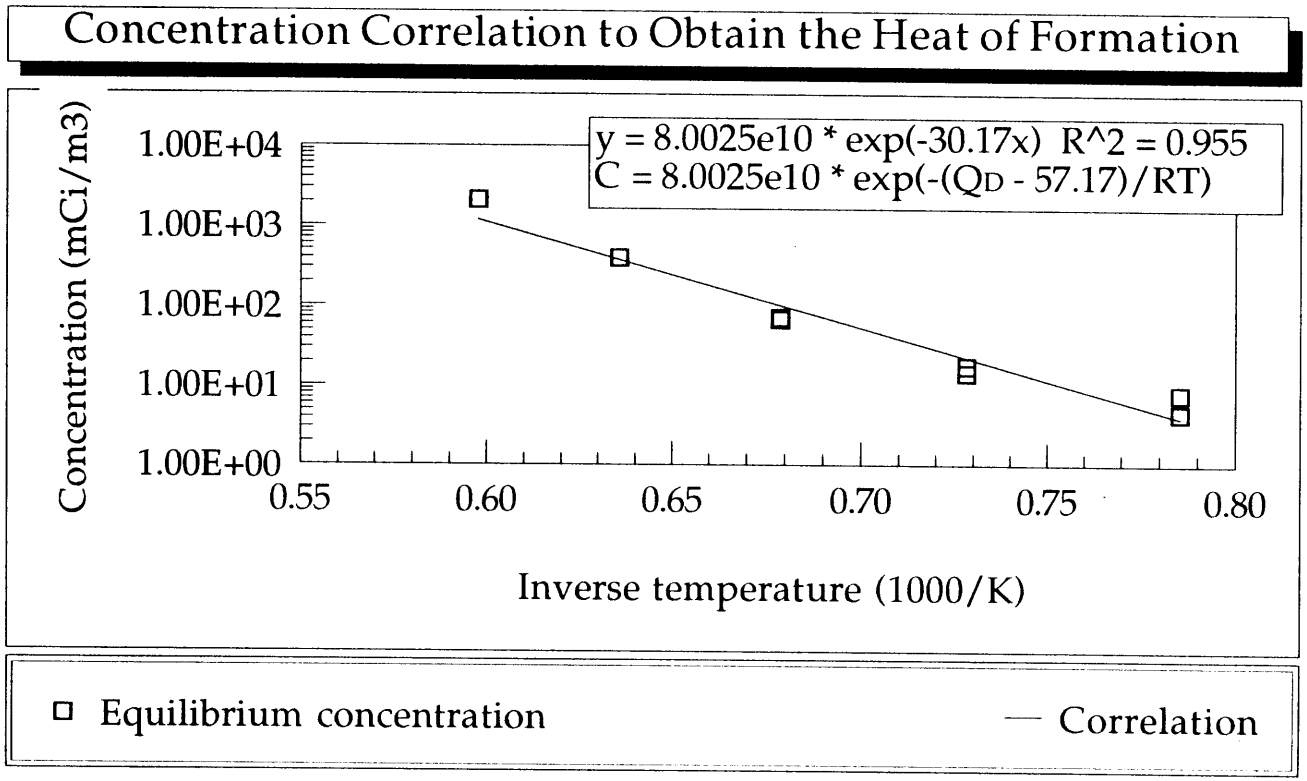

Figure 57. Fit of the equilibrium concentration from the LPI experiments versus inverse temperature. The solubility heat of formation, Qs, is calculated to be 57.17 kJ/mole from the correlation.

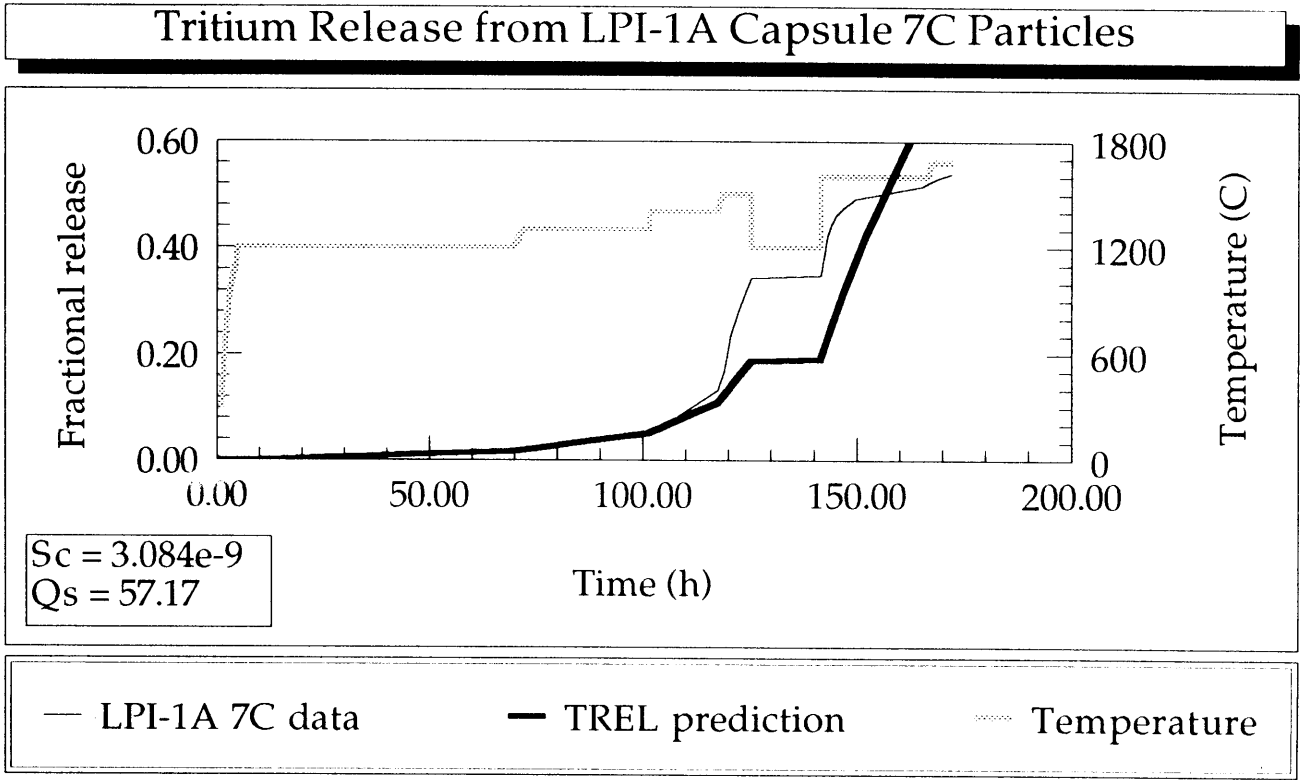

Figure 58. Tritium release from LPI-1A capsule 7C particles compared with the TREL prediction using Sc = 3.084e-9 Pa-0.5 and Qs = 57.17 kJ/mole.

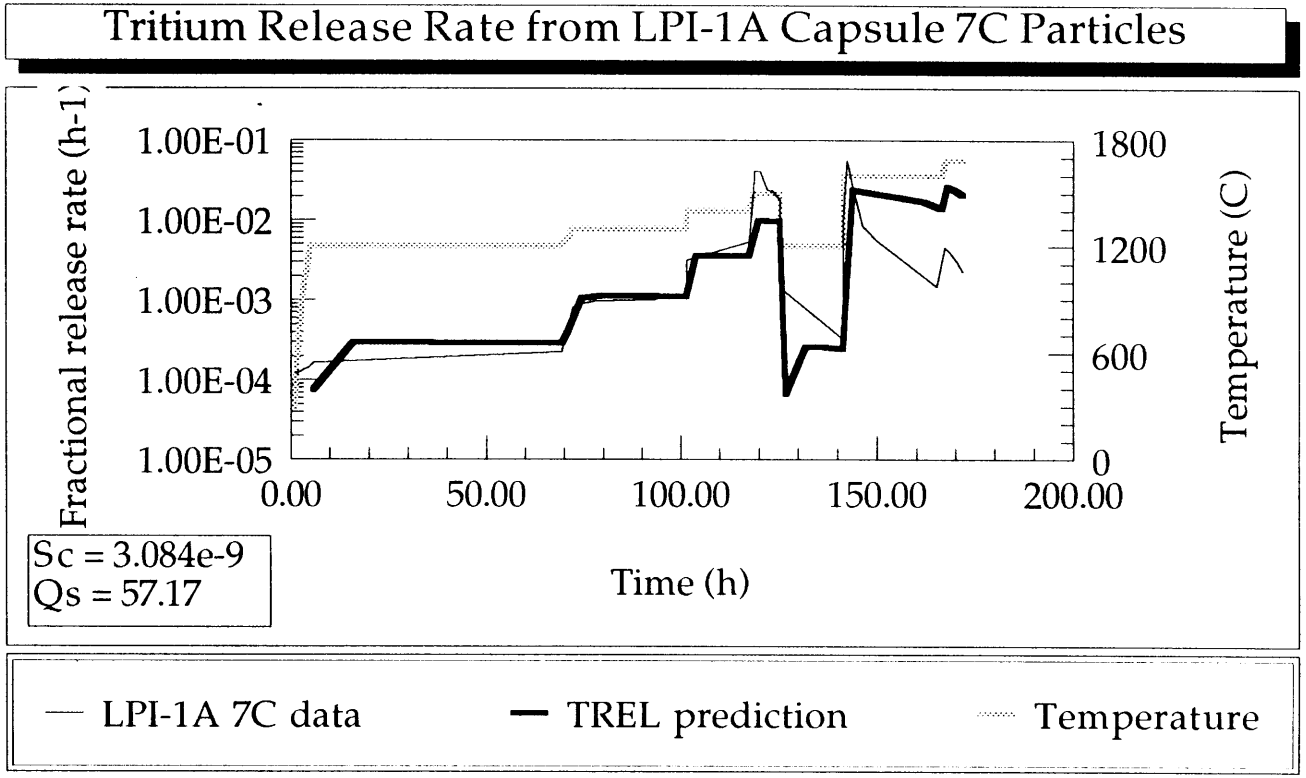

Figure 59. Tritium release rate from LPI-1A capsule 7C particles compared with the TREL prediction using Sc = 3.084e-9 Pa-0.5 and Qs = 57.17 kJ/mole.

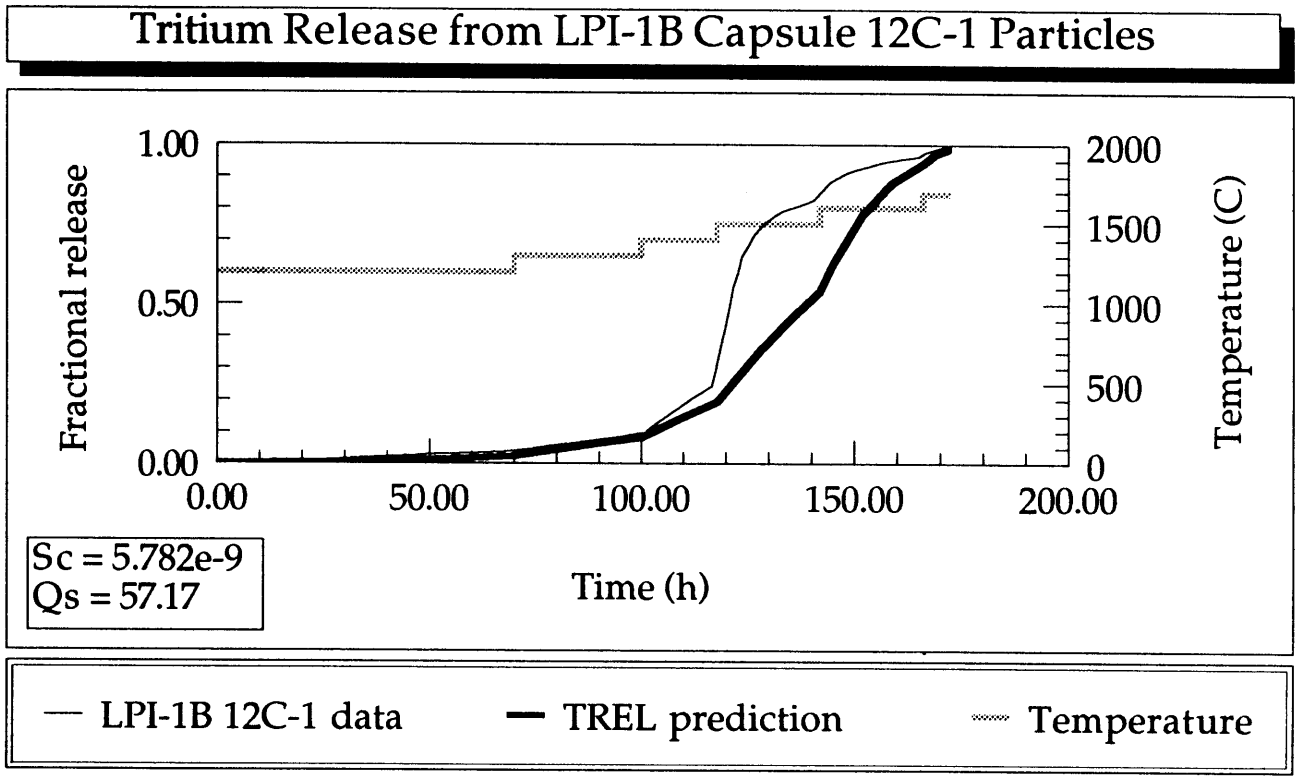

Figure 60. Tritium release from LPI-1B capsule 12C-1 particles compared with the TREL prediction using Sc = 5.782e-9 Pa-0.5 and Qs = 57.17 kJ/mole.

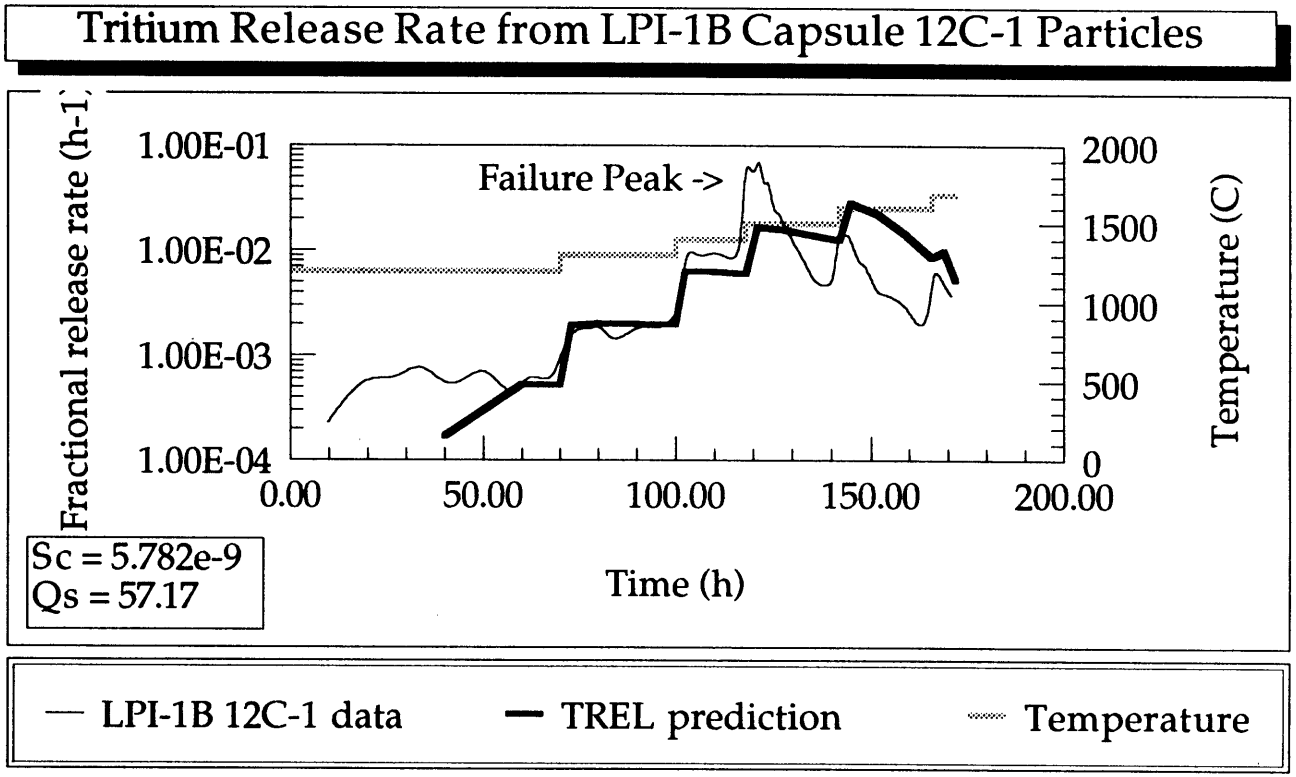

Figure 61. Tritium release rate from LPI-1B capsule 12C-1 particles compared with the TREL prediction using Sc = 5.782e-9 Pa-0.5 and Qs = 57.17 kJ/mole.

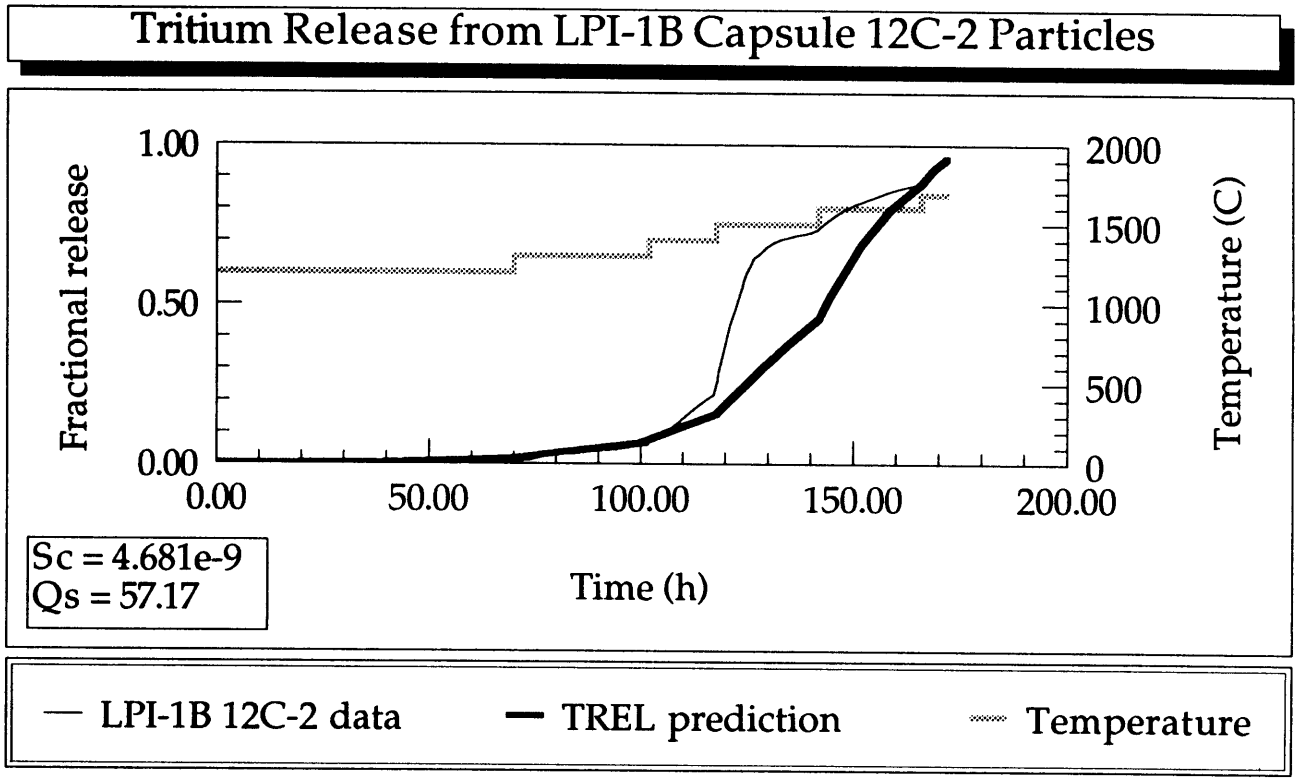

Figure 62. Tritium release from LPI-1B capsule 12C-2 particles compared with the TREL prediction using Sc = 4.681e-9 Pa-0.5 and Qs = 57.17 kJ/mole.

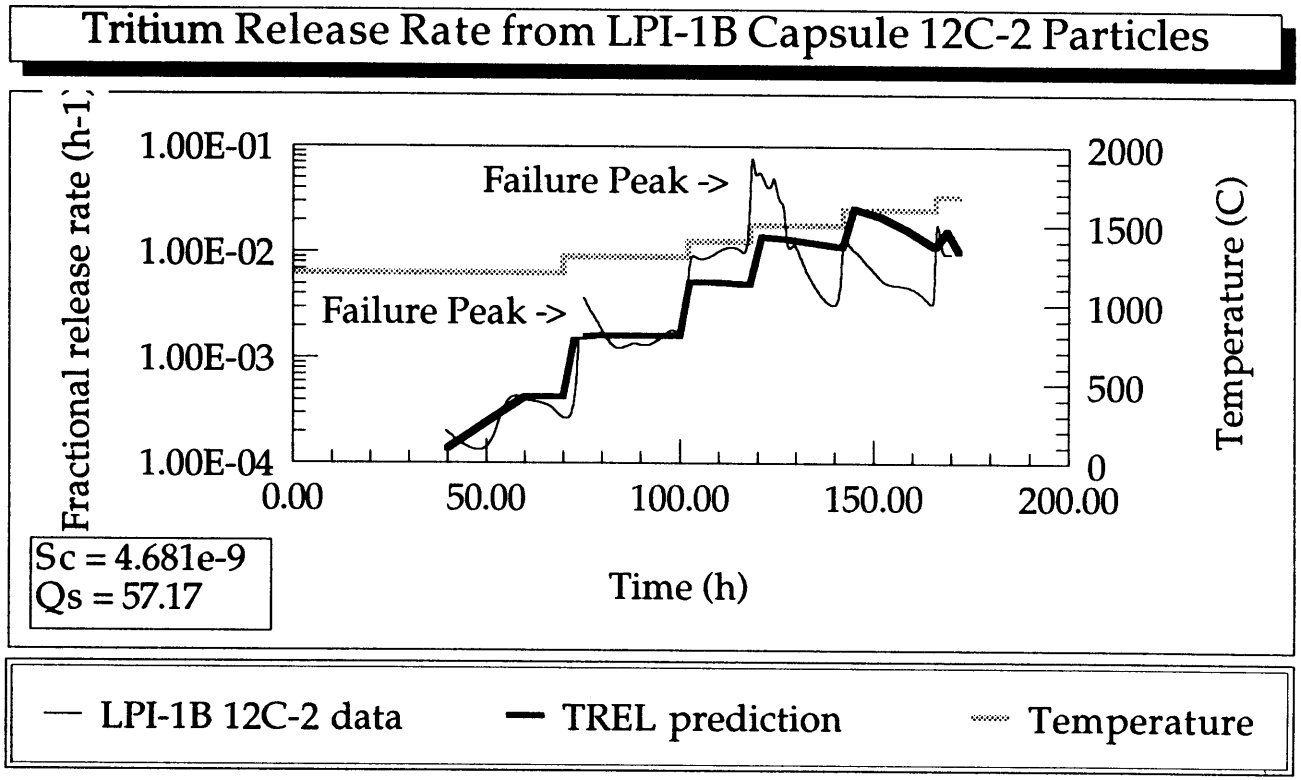

Figure 63. Tritium release rate from LPI-1B capsule 12C-2 particles compared with the TREL prediction using Sc = 4.681e-9 Pa-0.5 and Qs = 57.17 kJ/mole.

predicting the 1200 and 1300°C release rate, underpredicting the 1400°C data and the 1500°C data where particle failure occurred, and thus overpredicting the 1600 and 1685°C data. In general the fitted TREL release agreed very well with the data. Thus, a best estimate value of S_C was calculated to be 4.516×10^{-9} $Pa^{-0.5}$, the average value from the three tests, with an uncertainty of 1.357×10^{-9}. Therefore, after multiplying S_C by the number density of atoms in the SiC, the solubility correlation determined from the LPI data is

$$S = 2.149 \times 10^{20} \exp\left(\frac{57170}{8.314T}\right) P^{0.5} \quad (49)$$

The release rate from each of the three tests is compared with the rate from TREL using the best estimate solubility correlation in Figure 64. As mentioned in Chapter 1, experiments to measure the SiC diffusivity and solubility where performed in 1992/ by Causey at Sandia National Laboratory-Livermore. The results, which became available after the above solubility was determined empirically, indicate the diffusion coefficient is reduced by approximately an order of magnitude and the solubility preexponential is increased by an order of magnitude with a new value of Q_S equal to 66.2 kJ/mole compared to Causey's previous measurements. Because of the change in diffusivity, the new solubility can not be compared directly to the empirical relation. Therefore, the permeability, the product of the diffusivity and the solubility, is compared as shown in Figure 65. The empirical permeability is significantly reduced compared to the original relation found by Causey but it is very close his new result measured at Sandia.

7.2 Data Comparisons to Model Predictions using the New Solubility Relation

Predictions of the TREL code using the solubility relation determined in Section 7.1 were compared with the tritium release

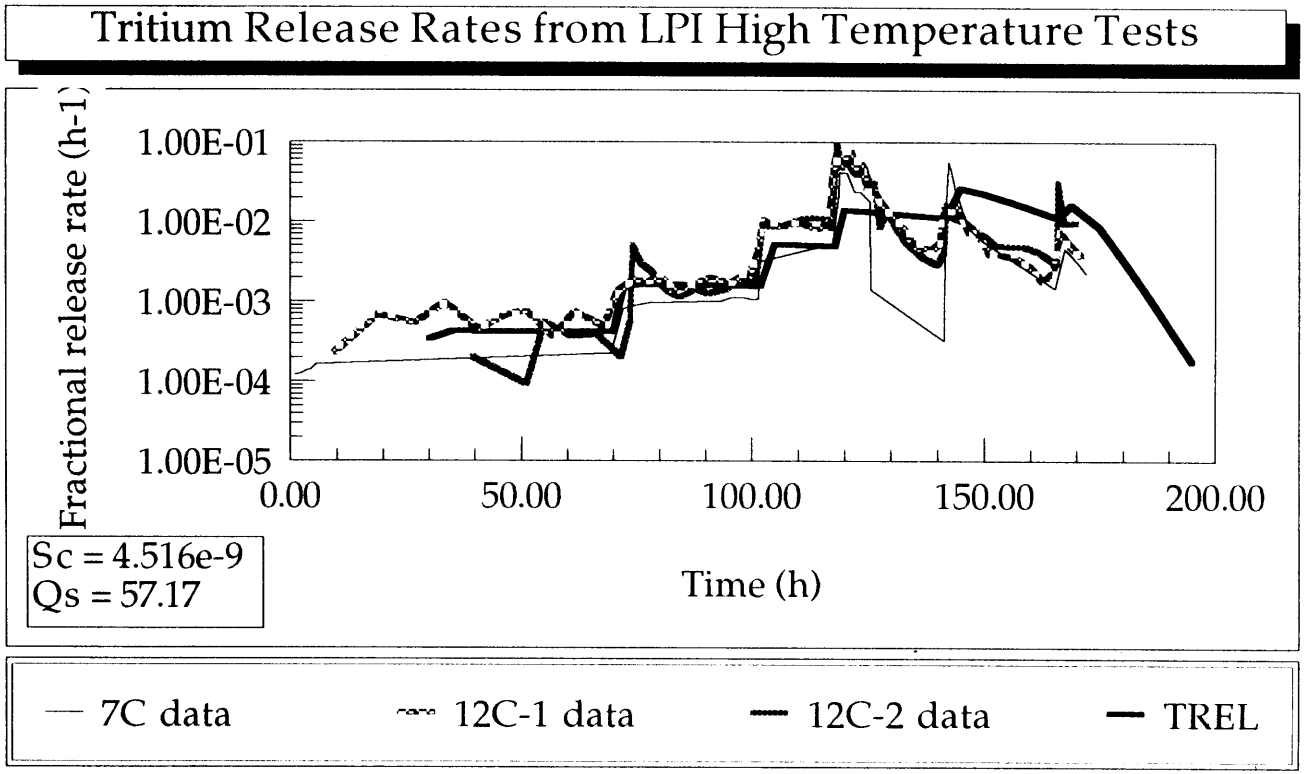

Figure 64. Tritium release rates from the LPI particles in capsules 7C and 12C compared with the TREL prediction using Sc =4.516e-9 Pa-0.5 and Qs = 57.17 kJ/mole.

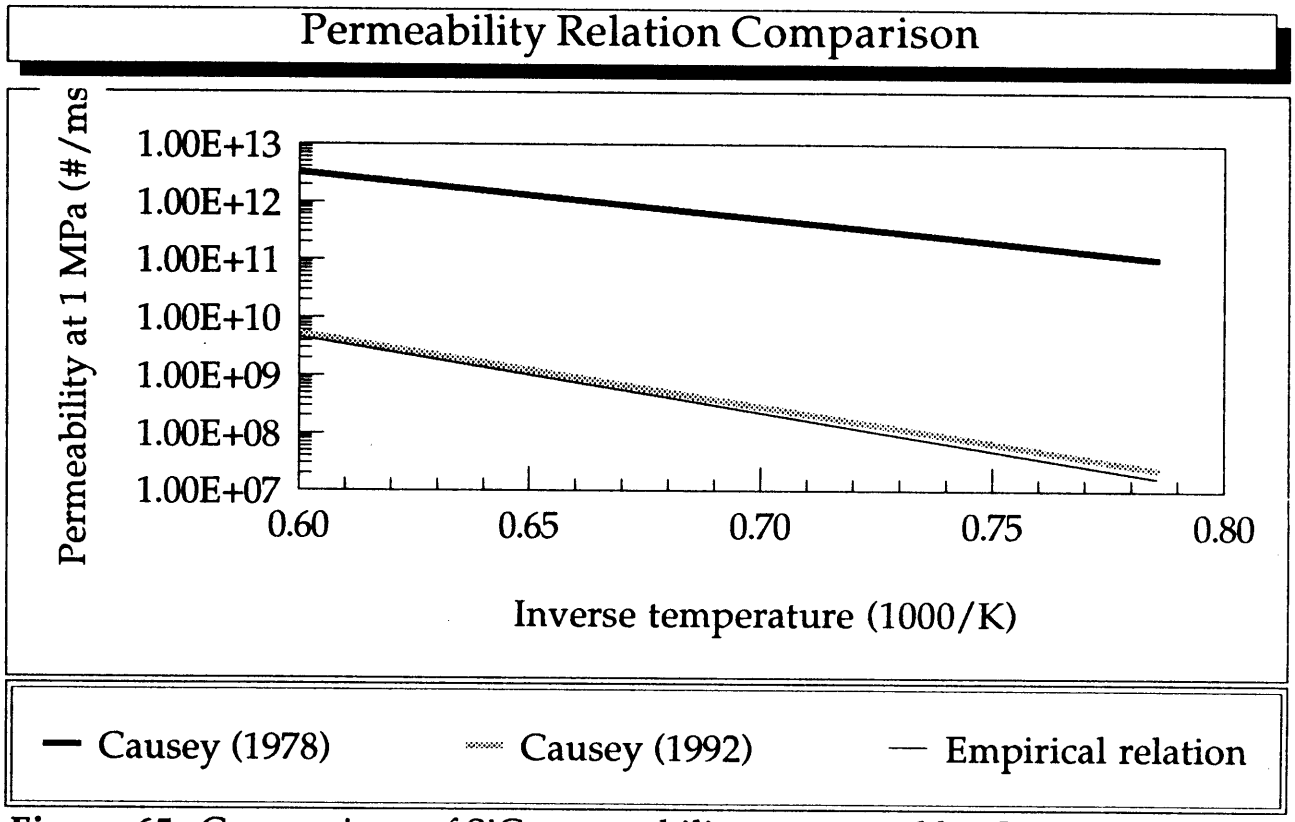

Figure 65. Comparison of SiC permeability measured by Causey in 1978, Causey in 1992, and the empirical relation found in this study.

Table 8. Characteristics of compact tests

	Omega West	LANL Test 6
No. of particles	3610	3610
Burnup (%)	4.17	19.0
Tritium inventory (Ci)	0.747	3.358
Fast fluence (n/cm^2)	low[a]	$2.0\text{-}6.5 \times 10^{20}$
Maximum Temp (°C)	1626	1900
Time (h)	125.4	51.98
Particle type	ATR-3	ATR-3
S_c ($Pa^{-0.5}$)	4.516×10^{-9}	4.516×10^{-9}
Q_S (kJ/mole)	57.17	57.17

a. not measured

The Omega West compact was irradiated to a burnup of 4.17%. Figure 66 indicates that the the integral release predicted by TREL matches very well with the data while Figure 67 shows the release rate from TREL is within a factor of two of the data. The LANL Test 6 compact was irradiated under NP-MHTGR operating conditions (~780°C) and reached a burnup of 19.7%. TREL with the new solubility relation does not match this data as well as shown in Figure 68 and 69. The integral release comparison is poor because the release rate is only within a factor of five of the data.

The LPI particles were fabricated using the ATR-1 geometry parameters while the particles in the two compact tests met ATR-3 specifications. The ATR-1 particles were fabricated first and studies show that the lithium contamination in the layers was greater than in the ATR-3 particles that were fabricated using a refined process. However, the differences in particle types do not appear to significantly affect the release at these temperatures as indicated by the fact that the solubility relation reasonably predicts release from both particle types.

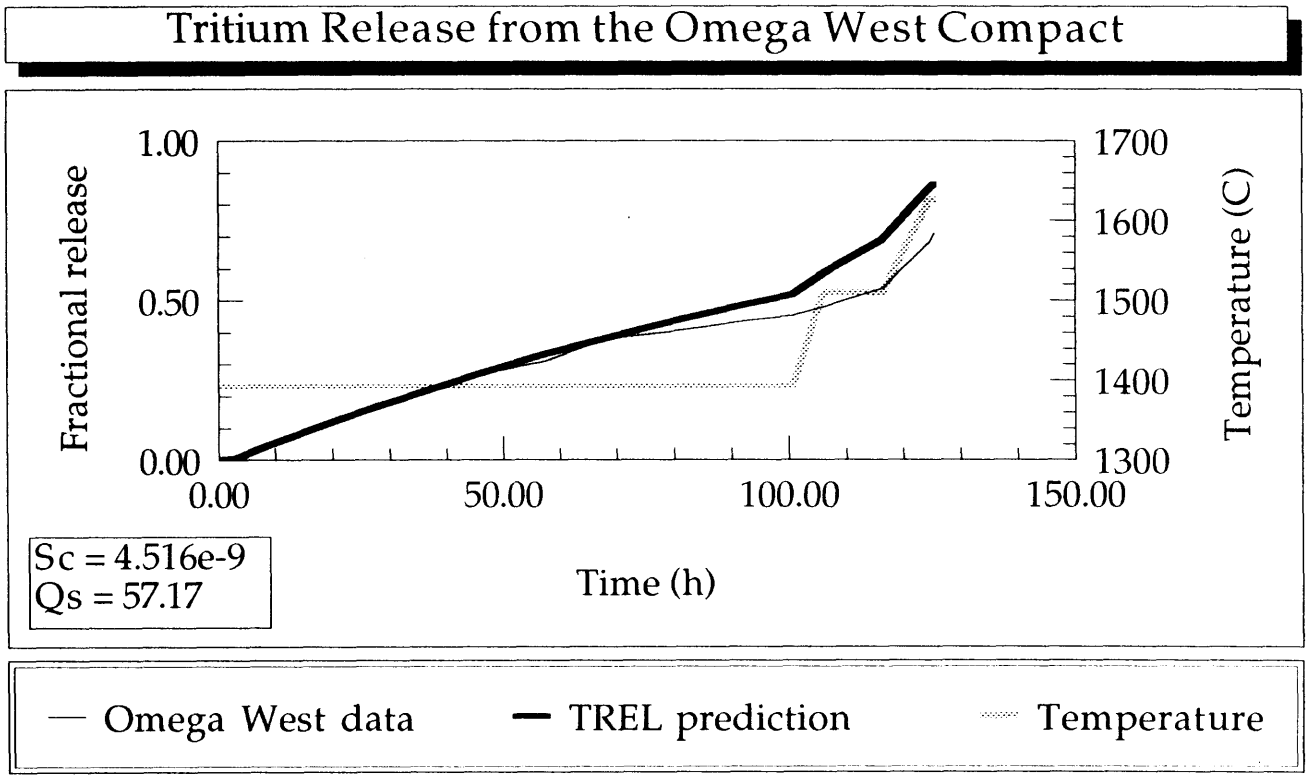

Figure 66. Tritium release from the Omega West compact compared with the TREL prediction using Sc = 4.516e-9 Pa-0.5 and Qs = 57.17 kJ/mole.

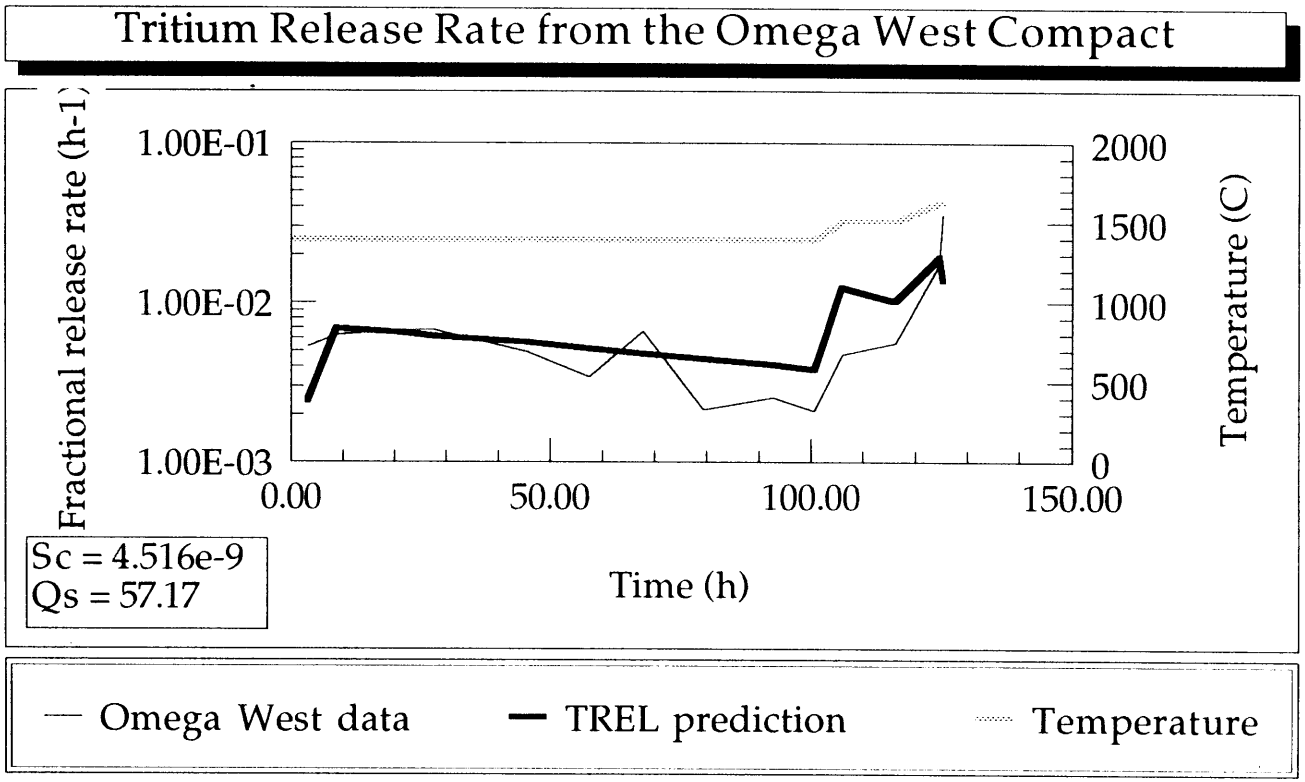

Figure 67. Tritium release rate from the Omega West compact compared with the TREL prediction using Sc = 4.516e-9 Pa-0.5 and Qs = 57.17 kJ/mole.

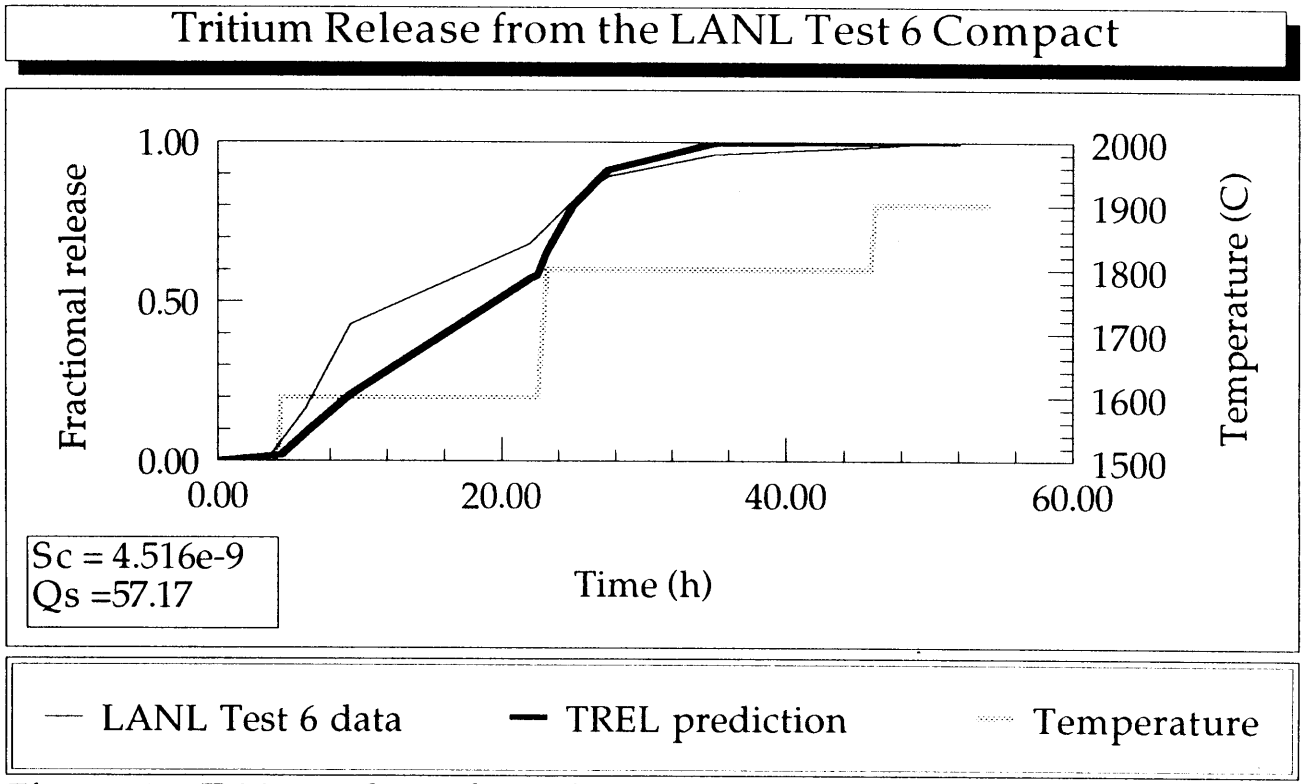

Figure 68. Tritium release from the LANL Test 6 compact compared with the TREL prediction using Sc = 4.516e-9 Pa-0.5 and Qs = 57.17 kJ/mole.

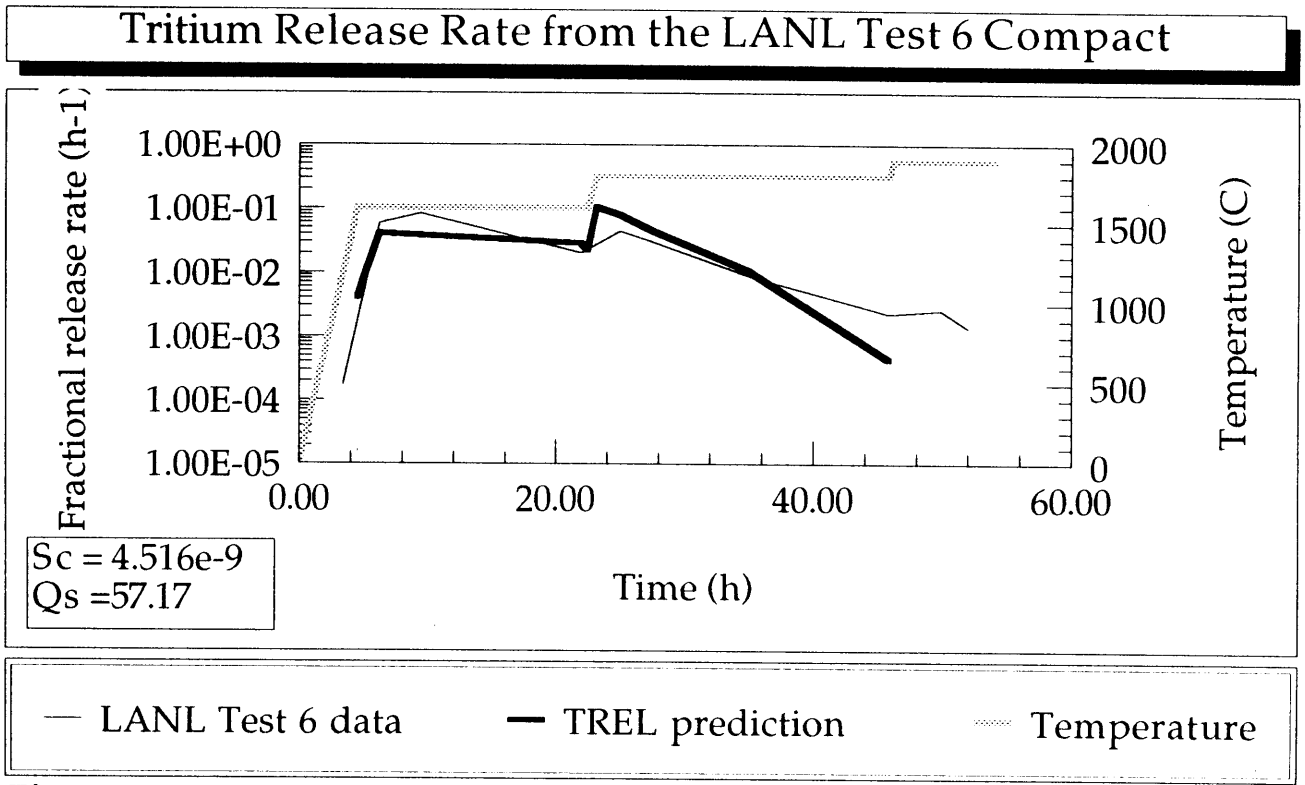

Figure 69. Tritium release rate from the LANL Test 6 compact compared with the TREL prediction using Sc = 4.516e-9 Pa-0.5 and Qs = 57.17 kJ/mole.

in the ATR-3 particles that were fabricated using a refined process. However, the differences in particle types do not appear to significantly affect the release at these temperatures as indicated by the fact that the solubility relation reasonably predicts release from both particle types.

Although particle geometry differences appear to be accounted for in the model, other effects may not be. The fact that the LANL Test 6 results compared least favorably with the TREL prediction using the new solubility correlation suggest that fast fluence may influence tritium release from these particles or that the solubility correlation does not extrapolate to the higher temperature range of Test 6. The LPI particles and the Omega West compact received an integrated fast fluence on the order of 10^{19} n/cm^2 while the LANL Test 6 compact received a fast fluence of 2.0 to 6.5 x 10^{21} n/cm^2. The postirradiation heating test of the Test 6 compact reached a maximum temperature of 1900°C whereas the LPI particles and the Omega West compact reached temperatures of only 1600 to 1700°C. The new solubility relation was correlated to data for the 1000 to 1400°C range and may not be accurate at higher temperatures. Therefore, to test these theories, data from particles with a high fast fluence should be analyzed and equilibrium release data at temperatures greater than 1400°C should be taken and fit with a new solubility correlation.

8. SUMMARY AND CONCLUSIONS

Tritium permeation through the NP-MHTGR target particles was studied to support the Tritium Target Development Program. The findings were incorporated into a model to predict tritium release from the particles.

8.1 The Final NP-MHTGR Target Particle Model

Calculations using TMAP provided insight in developing a basic model. The importance of modeling the pyrocarbon layers was discovered when comparing the amount of tritium released from the SiC model and the trilayer model. Initially, the SiC layer was suspected to be the dominant barrier to tritium diffusion, but the sensitivity study revealed the role of the PyC as a capacitor for tritium atoms. The high solubility of this material allows it to hold a substantial quantity of tritium. Thus, the tritium partial pressure applied to the SiC layer is reduced when the IPyC layer is modeled explicitly. Because this pressure drives the permeation process, the release rate of tritium is also reduced, and the release from the trilayer model is slower than from the SiC model. This pressure argument also explains why the release from a depleting tritium source model is slower than that from a constant source as shown by the TMAP calculations. Thus, the depleting source is used to model the finite tritium source in the particles. The calculations also indicated that modeling the solubility has a significant effect on the release. The values of the solubility for PyC and SiC vary such that the concentration across the PyC/SiC interface is discontinous when the solubility is included. Therefore, the solubility effects cannot be ignored. However, trapping was found to be relatively unimportant because the number of tritium atoms in the particle is much greater than the number of traps in the TRISO coatings. Moreover, at high temperatures, the traps are generally reversible and the TMAP calculations showed the effect of trapping on release to be minimal when resolution occured. At low temperatures, trapping may be important because the resolution rate is lower but the higher

solubility which results in more tritium atoms in the particle may still negate the trapping effects. The SiC and PyC trapping parameters need to be measured and added to the model before strong conclusions about the effects of trapping can be made.

Sensitivity studies also using TMAP revealed that the particle can be considered in terms of a simple electrical analogy. The IPyC acts as a capacitor for tritium atoms because of its high solubility. The SiC layer provides a resistance to tritium release because of its low diffusivity. Thus, at high temperatures, rapid uptake of tritium occurs in the PyC until equilibrium between the PyC and the void volume is established. Release is determined by permeation through the SiC. Tritium release continues in a quasi-steady process until the PyC capacitor drains, releasing its tritium.

A simple analytic solution was developed to describe this behavior and encoded into TREL. Results from TREL matched within 2% of detailed TMAP trilayer model results indicating that the analytic solution is valid and the OPyC layer can be neglected in the release model. The TREL computing time is significantly reduced from that of TMAP and TREL allows temperature changes in the void volume which is not possible in the current version of TMAP. Therefore, the TREL code is faster and more functional without sacrificing accuracy.

The LPI experiments were used to determine an empirical SiC solubility relation. Because the SiC solubility relation had the highest uncertainty of the input parameters, the internal pressure, the SiC diffusivity, and the PyC transport parameters were assumed to be correct and the data were used to update the solubility. This new correlation was then used in TREL and compared to two other sets of data. The updated model compared well with the Omega West compact data; however, the comparison with the LANL Test 6 compact data was not fully explained by the TREL model.

To summarize, the following parameters and conditions were

included in the final model for the NP-MHTGR target particles.

- Depleting source boundary condition
- Modeling the IPyC and SiC layers of the TRISO coating
- Solubility effects in the IPyC and the SiC using Sievert's Law
- The PyC diffusivity and solubility relations given by Causey[6]
- The SiC diffusivity relation given by Causey[13]
- The SiC solubility relation given by Equation (49)

8.2 Further Work

The tritium release model compared well with data from particles subjected to a low fast fluence The comparison with the higher fluence and temperature compact was poorer. It is possible that a higher fast fluence may affect the microstructure of the layers and cause diffusion mechanisms found to be unimportant in this study to affect the release. For example, the increased radiation damage may make trapping more important. Thus, tritium release data from particles with a high fast fluence should be studied using TREL to possibly find another correlation coupling fast fluence effects with the SiC solubility. Another possible explanation for the greater discrepancy is that the solubility relation may not be accurate over the higher temperature range of the Test 6 heating test. Equilibrium tritium release rates from the particle should be measured at temperatures greater than 1400°C to verify the accuracy of the solubility at high temperatures. A new empirical solubility correlation may be needed if the high temperature values are not predicted by the solubility correlation presented in Section 7.1.

The TREL code should also be coupled with a particle failure model. TARGET is a particle failure code also written to model NP-MHTGR target particles[26] and is a prime candidate for this task. A combination of the two codes could predict tritium release from tests with higher temperatures and particle burnups where particle failure occurs.

9. REFERENCES

1. B. J. Merrill, J. L. Jones, and D. F. Holland, *TMAP/MOD1 Tritium Migration Analysis Program Code Description and User's Manual,* EGG-EP-7404, April 1988.

2. R. W. Thomas et al., *NP-MHTGR Tritium Target Performance Demonstration and Qualification Program Plan,* EGG-NPR-8797, March 1990, (UCNI).

3. R. A. Causey, *Research Plan for Small-Scale Laboratory Experiments on the Behavior of Tritium in the NP-MHTGR Tritium Target Materials,* SAND91-8208, UC-420, April 1991.

4. W. Jost, *Diffusion in Solids, Liquids, and Gases,* New York: Academic Press Inc., 1960.

5. D. R. Olander, *Fundamental Aspects of Nuclear Reactor Fuel Elements,* National Technical Information Service, Springfield, VA, 1976.

6. R. A. Causey et al., "The Interaction of Tritium with Graphite and its Impact on Tokamak Operation," *Journal of Nuclear Materials,* 162-164, 1989, pp. 151-161.

7. G.R. Longhurst, et al., *Radiation Effects on Tritium Permeation and Retention in Fusion Reactor First Walls,* EGG-FT-6194, March 1983.

8. S. Hinotani, et al., "Effects of Fe_3C and Mo_2C Precipitation on Hydrogen Diffusivity and Hydrogen Embrittlement in Iron Alloys," *Materials Science and Engineering,* Vol 76, pp. 57-69, 1985.

9. A. Turnbull and M.W. Carroll, *Effect of Temperature and H_2S Concentration on Hydrogen Diffusion and Trapping in a 13% Chromium Martensitic Stainless Steel in Acidified NaCl,* NPL Report DMA(A)172, December 1988.

10. K. Okuno and H. Kudo, "Diffusion-Controlled Tritium Release from Neutron-Irradiated g-$LiAlO_2$," *Journal of Nuclear Materials*, 138, 1986, pp. 210-214.

11. A. A. Lucas, "Helium in Metals," *Physica*, 127B, 1984, pp. 225-239.

12. R. A. Causey et al., "Hydrogen Diffusion and Solubility in Pyrolytic Carbon," *Carbon*, 17, 1979, pp. 323-328.

13. R. A. Causey et al., "Hydrogen Diffusion and Solubility in Silicon Carbide," *Journal of the American Ceramic Society*, 61, 5-6, May-June 1978.

14. R. B. Evan III and M. T. Morgan, *Mathematical Description of Fission Product Transport in Coated Particles During Postirradiation Anneals*, ORNL-4969, June 1974.

15. M. T. Morgan and A. P. Malinauskas, "Cesium Release and Transport in BISO-coated Fuel Particles," *Nuclear Technology*, Vol. 35, September 1977, p. 457-464.

16. W. M. Rohsenow, and H. Choi, *Heat, Mass, and Momentum Transfer*, New Jersey: Prentice-Hall Inc., 1961.

17. H. S. Carslaw and J. C. Jaeger, *Conduction of Heat in Solids*, Oxford: University Press, 1959.

18. B. McQuillan, personal communication, August 1991.

19. W. H. Press et al., Numerical Recipes, Cambridge University Press, 1986, p. 258.

20. D. H. Meikrantz letter to R. E. Korenke, "Tritium Diffusion Tests on LPI-1 Particles at 1200°C," DHM-20-90, June 8, 1990.

21. D. H. Meikrantz and J. D. Baker letter to R. E. Korenke, "Results of High Temperature Particle Diffusion Tests - Samples 7A, 7C," DHM-20-91/JDB-09-91, July 2, 1991.

22. Z. R. Martinson, et al., *NPR-MHTGR Loose Target Particle Irradiation Phase 2 (LPI-1-B) Test Results*, NPRD-90-049, October 1990.

23. D. H. Meikrantz letter to R. E. Korenke, "Tritium Diffusion Test on LPI-1B Particles at 1200°C," DHM-21-90, July 10, 1990.

24. D. H. Meikrantz and J. D. Baker letter to R. E. Korenke, "LPI High Temperature Test on Particles from Capsule 12C," DHM-29-91/JDB-13-91, October 14, 1991.

25. R. A. Causey, "Materials Research Testing," presented at the NP-MHTGR Tritium Target Development Program Review, Idaho Falls, ID, February 13-14, 1992.

26. R. G. Bennett and G. K. Miller, *Target: A Monte Carlo Code for NP-MHTGR Target Particle Modeling*, NPRD-91-036, October 1991.

APPENDIX A

SUPPORTING CALCULATIONS FOR INPUT MODELS

This appendix contains supporting calculations for the TMAP input models. Table A-1 contains the details of the input model for the ATR-1 particles. This model was used in the calculations presented in Sections 4.1 through 4.4 and 7.1. The ATR-3 model, as shown in Table A-2, was used in calculations in Sections 4.5 and 7.2. The dimensionless equations and input for the SiC model used in Section 5.4 for the parametric trapping study are given in Table A-3. Values for the number densities, diffusivities, and solubilities for PyC and SiC, and the method used to calculate the tritium partial pressure in an ATR-3 particle are given at the end of this appendix.

Table A-1. Geometrical model used for ATR-1 particles

Parameter	Value
Particle void volume (m^3)	5.2×10^{-11}
Kernel diameter (μm)	455
Porous buffer thickness (μm)	96
Tritium partial pressure (Pa)	1.0×10^6 when modeled as T 5.0×10^5 when modeled as T_2
IPyC	
Thickness (μm)	63
Number of nodes	9
Node thickness (μm)	1 node = 3.0 6 nodes = 10.0 2 surface nodes = 0.0 (fixed by code)
Surface area (m^2)	1.83×10^{-6}

Table A-1. (continued)

Parameter	Value
SiC	
Thickness (μm)	33
Number of nodes	9
Node thickness (μm)	1 node = 3.0 6 nodes = 5.0 2 surface nodes = 0.0 (fixed by code)
Surface area (m^2)	2.16×10^{-6}
OPyC	
Thickness (μm)	25
Number of nodes	7
Node thickness (μm)	5 nodes = 5.0 2 surface nodes = 0.0 (fixed by code)
Surface area (m^2)	2.43×10^{-6}

Table A-2. Geometrical model used for ATR-3 particles

Parameter	Value
Particle void volume (m^3)	7.41×10^{-11}
Kernel diameter (μm)	505
Porous buffer thickness (μm)	102
Surface area for all layers (m^2)	2.68×10^{-6}
Tritium pressure	Given in Table 1
IPyC	
Thickness (μm)	68
Number of nodes	11
Node thickness (μm)	1 node = 8.0 4 nodes = 15.0 2 surface nodes = 0.0 (fixed by code)

Table A-2. (continued)

Parameter	Value
SiC	
Thickness (μm)	39
Number of nodes	10
Node thickness (μm)	1 node = 4.0 7 nodes = 5.0 2 surface nodes = 0.0 (fixed by code)
OPyC	
Thickness (μm)	30
Number of nodes	8
Node thickness (μm)	6 nodes = 5.0 2 surface nodes = 0.0 (fixed by code)

The diffusion and trapping equations are listed below:

$$\frac{\partial C}{\partial t} = D\frac{\partial^2 C}{\partial x^2} - \frac{\partial C^T}{\partial t} \qquad \frac{\partial C^T}{\partial t} = w\frac{X_T^e}{N}C - rC^T \qquad X_T^e = X_T^0 - C^T$$

These equations were cast in dimensionless form using the following transformations:

$$\tau = \frac{Dt}{a^2} \qquad u = \frac{C}{C_o} \qquad X = \frac{x}{a}$$

$$v = \frac{C^T}{C_o} \qquad \beta_o = \frac{X_T^e}{N} \qquad y = \frac{N}{C_o}$$

$$\alpha_T = w\frac{a^2}{D} \qquad \alpha_R = r\frac{a^2}{D}$$

Thus, the dimensionless diffusion and trapping equations are:

$$\frac{\partial u}{\partial \tau} = \frac{\partial^2 u}{\partial X^2} - \frac{\partial v}{\partial \tau} \qquad \frac{\partial v}{\partial \tau} = \alpha_T \beta u - \alpha_R v \qquad \beta = \beta_o - \frac{v}{y}$$

The release is given by:

$$\text{Release (atoms)} = A\int -D\frac{\partial C}{\partial x}\partial t$$

$$\text{Dimensionless Release} = C_o Aa\int \frac{\partial u}{\partial X}\partial \tau$$

$$\text{Fractional Release} = \frac{A}{C_o V}\int -D\frac{\partial C}{\partial x}\partial t$$

Table A-3. Dimensionless SiC model used for trapping studies

Parameter	Formula	Value
Particle void volume (m^3)	V	7.41×10^{-11}
Constant surface concentration (atoms/m^3) (used for fractional release calculations)	C_o	4.93×10^{26}
SiC		
Surface area	A	1.0
Thickness	a	1.0
Number of nodes		12
Node thickness		10 nodes = 0.1 2 surface nodes = 0.0
Number density	y	96.51
Diffusion coefficient	D	1.0
Trapping rate	α_T	1.52×10^9
Resolution rate	α_R	1.52×10^9

Diffusivity and Solubility Expressions Used in TMAP Model

SiC

Diffusion coefficient:

$$D = 1.58 \times 10^{-4} \exp \frac{-308000}{8.314 * T(K)} \qquad (m^2/s)$$

Solubility = (Solubility constant * number density * pressure$^{1/2}$)
(Note: Actual data indicate an exponent of 0.44. The value of 1/2 for the exponent is required by TMAP, which is within the experiment uncertainty.)

Solubility constant:

$$S = 2.75 \times 10^{-11} \exp \frac{37000}{1.987*T(K)} \quad (Pa^{-1/2})$$

Number density:

$$N = \frac{\rho N_{avg}}{A} = \frac{3.16\ g/cm^3 * 6.023 \times 10^{23}}{40\ g/gmole}$$

$$= 4.758 \times 10^{22} \quad (cm^{-3})$$

$$= 4.758 \times 10^{28} \quad (m^{-3})$$

Therefore, Solubility $= 1.31 \times 10^{18} \exp \frac{37000}{1.987*T(K)} * P^{1/2}(Pa)$ (m^{-3})

PyC

Diffusion coefficient:

$$D = 1.0 \times 10^{-1} \exp \frac{-64000}{1.987*T(K)} \quad (m^2/s)$$

Solubility = (Solubility constant * number density * pressure$^{1/2}$)
(Note: Actual data indicate an exponent of 0.49.)

Solubility constant (Reference 12):

$$S = 1.60 \times 10^{-10} \exp \frac{33300}{1.987*T(K)} \quad (Pa^{-1/2})$$

Number density:

$$N = \frac{\rho N_{avg}}{A} = \frac{1.78\ g/cm^3 * 6.023 \times 10^{23}}{12\ g/gmole}$$

$$= 8.934 \times 10^{22} \quad (cm^{-3})$$

$$= 8.934 \times 10^{28} \quad (m^{-3})$$

Therefore, Solubility (Reference 12)

$$= 1.43 \times 10^{19} \exp \frac{33300}{1.987*T(K)} P^{1/2}(Pa) \quad (m^{-3})$$

Solubility constant (Reference 6):

$$S = 2.024 \times 10^{-7} \exp \frac{19270}{8.314*T(K)} \quad (Pa^{-1/2})$$

Therefore, Solubility (Reference 6)

$$= 1.808 \times 10^{22} \exp \frac{19270}{8.314*T(K)} P^{1/2}(Pa) \quad (m^{-3})$$

Particle Internal Tritium Pressure Calculation

Assumptions:

(a) Pressure is given by ideal gas law PV = nRT.
(b) Two moles of gas are generated for each ^6Li atom burned in the proportion: 0.5 moles T_2, 1 mole He, 0.5 moles CO.
(c) Gas volume for expansion is the void volume in the buffer plus as-fabricated porosity in the lithium aluminate kernel, which is assumed to be open and connected.

Using ATR-3 geometry, as given in Table A-2:

$$\text{Buffer volume} = \frac{4}{3}\pi(r_o^3 - r_i^3)$$

$$= \frac{4\pi}{3}[(354.5)^3 - (252.5)^3](10^{-6})^3$$
$$= 1.192 \times 10^{-10}\ m^3$$

Buffer density = 0.89 g/cm^3
Theoretical density = 2.25 g/cm^3

Buffer void volume =
[1 - (actual density/theoretical density)]*Buffer volume

$$= (1 - \frac{0.89}{2.25})(1.192 \times 10^{-10})$$
$$= 7.205 \times 10^{-11}\ m^3$$

Kernel density = 3.5 g/cm^3
Theoretical density = 3.61 g/cm^3

$$\text{Kernel void volume} = (1 - \frac{3.5}{3.61}) \frac{4\pi}{3} (252.5 \times 10^{-6})^3$$
$$= 2.05 \times 10^{-12} \text{ m}^3$$

$$\text{Total void volume} = 7.205 \times 10^{-11} + 2.05 \times 10^{-12}$$
$$= 7.41 \times 10^{-11} \text{ m}^3$$

Ideal Gas Law Calculation of Pressure

n = number of moles of tritium = 0.5 (Burnup)* $m_{Li\text{-}6}/A_{Li\text{-}6}$
where,
Burnup = atom% burnup
$m_{Li\text{-}6}$ = mass of ^{6}Li per particle (g) = (1.62×10^{-6} g)
$A_{Li\text{-}6}$ = atomic weight of ^{6}Li = (6.0),
and the constant 0.5 represents the fact that 0.5 moles of tritium gas are generated for every mole of ^{6}Li burned.

Thus, the tritium partial pressure is

$$P(\text{Pa}) = nRT/V_{Void}$$
$$= \frac{0.5\ (1.62 \times 10^{-6})(8.314)(T*\text{Burnup})}{(6)(7.41 \times 10^{-11})}$$
$$= 1.515 \times 10^4\ (T*\text{Burnup})$$

APPENDIX B

SAMPLE TMAP INPUT DECKS

This appendix contains sample input decks for TMAP calculations. The ATR-1 particle geometry is modeled in the first deck, the second deck lists the input for the ATR-3 particle geometry, and the dimensionless input is given in the third deck.

B.1 Input Deck for ATR-1 Particle Geometry

```
title input
   Tritium diffusion through PyC,SiC,PyC layer in NPR particles
   at 1200°C with depleting source and solubility
end of title input
$
$
main input
   dspcnme=t,end                    $ diffusion specie name
   espcnme=t2,end                   $ enclosure specie name
   segnds=9,9,7,end                 $ number of nodes/segment
   nbrencl=2,end                    $ number of enclosures
   linksegs=1,2,3,end               $ segments to be linked
end of main input
$
$
enclosure input
  start func,1 .                          $ enclosure 1
   etemp=1473.0,end                 $ temperature in enclosure
   esppres=t2,5.0e5,end             $ pressure in enclosure
   reaction=nequ,0,end              $ reactions in enclosure
   evol=5.2e-11,end                 $ volume of enclosure
  start bdry,2                            $ enclosure 2
   etemp=1473.0,end                 $ temperature in enclosure
   esppres=t2,0.0,end               $ pressure in enclosure
end of enclosure input
$
$
thermal input
```

```
   start thermseg                                    $ IPyC layer
    delx=0.0,1*3.0e-6,6*1.0e-5,0.0,end    $ spacial noding
    dtemp=9*1473.0,end                    $ initial temperature in layer
   start thermseg                                    $ SiC layer
    delx=0.0,1*3.0e-6,6*5.0e-6,0.0,end    $ spacial noding
    dtemp=9*1473.0,end                    $ initial temperature in layer
   start thermseg                                    $ OPyC layer
    delx=0.0,5*5.0e-5,0.0,end             $ spacial noding
    dtemp=7*1473.0,end                    $ initial temperature in layer
 end of thermal input
 $
 $
 diffusion input
   start diffseg                                     $ IPyC layer
    dconc=t,9*0.0,end                     $ initial layer concentration
    dcoef=t,equ,1,end                     $ diffusion coefficient
    qstrdr=t,equ,5,end                    $ heat of transport/R
    spcsrc=t,equ,5,srcpf,9*0.0,end        $ specie source flux
    difbcl=lawdep,encl,1,t,t2,pexp,0.5,solcon,equ,4,end   $ left b. c.
    difbcr=link,t,solcon,equ,4,end        $ right boundary condition
    surfa=1.83e-6,end                     $ surface area
   start diffseg                                     $ SiC layer
    dconc=t,9*0.0,end                     $ initial layer concentration
    dcoef=t,equ,2,end                     $ diffusion coefficient
    qstrdr=t,equ,5,end                    $ heat of transport/R
    spcsrc=t,equ,5,srcpf,9*0.0,end        $ specie source flux
    difbcl=link,t,solcon,equ,3,end        $ left boundary condition
    difbcr=link,t,solcon,equ,3,end        $ right boundary condition
    surfa=2.16e-6,end                     $ surface area
   start diffseg                                     $ OPyC layer
    dconc=t,7*0.0,end                     $ initial layer concentration
    dcoef=t,equ,1,end                     $ diffusion coefficient
    qstrdr=t,equ,5,end                    $ heat of transport/R
    spcsrc=t,equ,5,srcpf,7*0.0,end        $ specie source flux
    difbcl=link,t,solcon,equ,4,end        $ left boundary condition
    difbcr=sconc,encl,2,t,t2,nsurfs,2,conc,const,0.0,end   $ right b. c.
    surfa=2.43e-6,end                     $ surface area
 end of diffusion input
 $
 $
```

```
equation input
    y = 1.0e-1*exp(-64000./(1.987*temp)),end     $ 1 PyC diffusion coef
    y = 1.58e-4*exp(-308000./(8.314*temp)),end   $ 2 SiC diffusion coef
    y = 1.31e18*exp(37000./(1.987*temp)),end     $ 3 SiC solubility
    y = 1.43e19*exp(33300./(1.987*temp)),end     $ 4 PyC solubility
    y = 0.0,end                                  $ 5 misc
end of equation input
$
$
table input
end of table input
$
$
control input
    time=0.0,end                    $ beginning time
    tstep=0.1,end                   $ time step
    timend=2.592e5,end              $ time end
    nprint=7200,end                 $ print data for every n steps
    itermx=20000,end                $ max number of iterations
    delcmx=1.0e-5,end               $ tolerance
end of control input
$
$
plot input                          $ data included in plot file
    nplot=3600,end                  $ plot after nth time step
    plotseg=1,2,3,end               $ plot for these segments
    plotencl=1,2,end                $ plot for these enclosures
    dname=t,end                     $ plot for this diff species
    ename=t2,end                    $ plot for this encl species
    dplot=moblinv,end               $ plot parameters for diff
    eplot=conc,diff,end             $ plot parameters for encl
end of plot input
$
$
end of data
```

B.2 Input Deck for ATR-3 Particle Geometry

```
title input
```

```
    Tritium diffusion through TRISO coating for ATR-3 geometry
    1800°C, 45 atom% burnup, with depleting source and solubility
end of title input
$
$
main input
    dspcnme=t,end                          $ diffusion specie name
    espcnme=t2,end                         $ enclosure specie name
    segnds=11,10,6,end                     $ number of nodes/segment
    nbrencl=2,end                          $ number of enclosures
    linksegs=1,2,3,end                     $ segments to be linked
end of main input
$
$
enclosure input
  start func,1                                  $ enclosure 1
    etemp=2073.0,end                       $ temperature in enclosure
    esppres=t2,1.41e+07,end                $ pressure in enclosure
    reaction=nequ,0,end                    $ reactions in enclosure
    evol=7.41e-11,end                      $ volume of enclosure
  start bdry,2                                  $ enclosure 2
    etemp=2073.0,end                       $ temperature in enclosure
    esppres=t2,0.0,end                     $ pressure in enclosure
end of enclosure input
$
$
thermal input
  start thermseg                                $ IPyC layer
    delx=0.0,12.0e-6,8*7.0e-6,0.0,end      $ spacial noding
    dtemp=11*2073.0,end                    $ initial temperature in layer
  start thermseg                                $ SiC layer
    delx=0.0,4.0e-6,7*5.0e-6,0.0,end       $ spacial noding
    dtemp=10*2073.0,end                    $ initial temperature in layer
  start thermseg                                $ OPyC layer
    delx=0.0,2*5.0e-6,2*10.0e-6,0.0,end    $ spacial noding
    dtemp=6*2073.0,end                     $ initial temperature in layer
end of thermal input
$
$
diffusion input
```

```
   start diffseg                                          $ IPyC layer
    dconc=t,11*0.0,end                                  $ initial layer concentration
    dcoef=t,equ,1,end                                   $ diffusion coefficient
    qstrdr=t,equ,5,end                                  $ heat of transport/R
    spcsrc=t,equ,5,srcpf,11*0.0,end                     $ specie source flux
    difbcl=lawdep,encl,1,t,t2,pexp,0.5,solcon,equ,4,end  $ left b. c.
    difbcr=link,t,solcon,equ,4,end                      $ right boundary condition
    surfa=2.68e-6,end                                   $ surface area
   start diffseg                                              $ SiC layer
    dconc=t,10*0.0,end                                  $ initial layer concentration
    dcoef=t,equ,2,end                                   $ diffusion coefficient
    qstrdr=t,equ,5,end                                  $ heat of transport/R
    spcsrc=t,equ,5,srcpf,10*0.0,end                     $ specie source flux
    difbcl=link,t,solcon,equ,3,end                      $ left boundary condition
    difbcr=link,t,solcon,equ,3,end                      $ right boundary condition
    surfa=2.68e-6,end                                   $ surface area
   start diffseg                                              $ OPyC layer
    dconc=t,6*0.0,end                                   $ initial layer concentration
    dcoef=t,equ,1,end                                   $ diffusion coefficient
    qstrdr=t,equ,5,end                                  $ heat of transport/R
    spcsrc=t,equ,5,srcpf,6*0.0,end                      $ specie source flux
    difbcl=link,t,solcon,equ,4,end                      $ left boundary condition
    difbcr=sconc,encl,2,t,t2,nsurfs,2,conc,const,0.0,end  $ right b. c.
    surfa=2.68e-6,end                                   $ surface area
end of diffusion input
$
$
equation input
    y = 1.0e-1*exp(-64000./(1.987*temp)),end     $ 1 PyC diffusion coef
    y = 1.58e-4*exp(-308000./(8.314*temp)),end   $ 2 SiC diffusion coef
    y = 1.31e18*exp(37000./(1.987*temp)),end     $ 3 SiC solubility
    y = 1.43e19*exp(33300./(1.987*temp)),end     $ 4 PyC solubility
    y = 0.0,end                                  $ 5 misc
end of equation input
$
table input
end of table input
$
$
control input
```

```
    time=0.0,end                    $ beginning time
    tstep=1.0,end                   $ time step
    timend=100.0,end                $ time end
    nprint=50,end                   $ print data for every n steps
    itermx=10000,end                $ max number of iterations
    delcmx=1.0e-7,end               $ tolerance
end of control input
$
$
plot input                          $ data included in plot file
    nplot=5,end                     $ plot after nth time step
    plotseg=1,2,3,end               $ plot for these segments
    plotencl=1,2,end                $ plot for these enclosures
    dname=t,end                     $ plot for this diff species
    ename=t2,end                    $ plot for this encl species
    dplot=moblinv,end               $ plot parameters for diff
    eplot=conc,diff,end             $ plot parameters for encl
end of plot input
$
$
end of data
```

B.3 Input Deck for Dimensionless Geometry

```
title input
    Tritium diffusion in SiC layer w/constant source & no solubility
    1300°C  45 at% Bu  2500 ppm traps 0.1% Resolution Dimensionless
end of title input
$
$
main input
    dspcnme=t,end                   $ diffusion specie name
    espcnme=t2,end                  $ enclosure specie name
    segnds=12,end                   $ number of nodes/segment
    nbrencl=2,end                   $ number of enclosures
end of main input
$
$
enclosure input
```

```
   start bdry,1                                    $ enclosure 1
    etemp=1573.0,end                              $ temperature in enclosure
    esppres=t2,1.07e+07,end                       $ pressure in enclosure
   start bdry,2                                    $ enclosure 2
    etemp=1573.0,end                              $ temperature in enclosure
    esppres=t2,0.0,end                            $ pressure in enclosure
end of enclosure input
$
$
thermal input
  start thermseg
   delx=0.0,10*.1,0.0,end                         $ spacial noding
   dtemp=12*1573.0,end                            $ initial temperature in layer
end of thermal input
$
$
diffusion input
  start diffseg
   dconc=t,12*0.0,end                             $ initial layer concentration
   ctrap=t,12*0.0,end                             $ initial trapped conc
   dcoef=t,equ,1,end                              $ diffusion coefficient
   qstrdr=t,const,0.0,end                         $ heat of transport/R
   trapping=cetrpi,5.e-4,nbrden,96.31,t,alpht,equ,2,alphr,equ,3,end
                                                  $ trap info
   spcsrc=t,const,0.0,srcpf,12*0.0,end            $ specie source flux
   difbcl=sconc,encl,1,t,t2,nsurfs,2,conc,const,1.0,end   $ left b. c.
   difbcr=sconc,encl,2,t,t2,nsurfs,2,conc,const,0.0,end   $ right b. c.
   surfa=1.0,end                                  $ surface area
end of diffusion input
$
$
equation input
   y = 1.0,end                                    $ 1 diffusion coefficient
   y = 1.52e9,end                                 $ 2 trapping rate
   y = 1.52e6,end                                 $ 3 resolution rate
end of equation input
$
$
table input
end of table input
```

```
$
$
control input
    time=0.0,end                        $ beginning time (s)
    tstep=0.001,end                     $ time step (s)
    timend=1.0,end                      $ end time (s)
    nprint=100,end                      $ print data for every n steps
    itermx=10000,end                    $ max number of iterations
    delcmx=1.0e-7,end                   $ tolerance
end of control input
$
$
plot input                              $ data included in plot file
    nplot=10,end                        $ plot data every nth step
    plotseg=1,end                       $ plot for these segments
    plotencl=1,2,end                    $ plot for these enclosures
    dname=t,end                         $ plot for this diff species
    ename=t2,end                        $ plot for this encl species
    dplot=moblinv,trapinv,end           $ plot parameters for diff
    eplot=diff,end                      $ plot parameters for encl
end of plot input
$
$
end of data
```

APPENDIX C

TREL CODE DESCRIPTION

C.1 TREL Code Listing

```
      PROGRAM TRELTB
C
C     THIS PROGRAM CALCULATES TRITIUM RELEASE FROM
C     TRISO-COATED PARTICLES USING AN ANALYTIC
C     SOLUTION DOCUMENTED IN EDF-NPR-MHTGR-0347
C
C     CODING BY S.L. HARMS   AUGUST/SEPTEMBER/1991
C     REVIEWED BY D.A. PETTI
C
C     INPUT VARIABLES - IN NAMELISTS INPUT AND TT
C
C          AREA - SURFACE AREA (M3)
C          BUP - LI6 BURNUP (ATOM%)
C          DPYC - PYC THICKNESS (M)
C          DSIC - SIC THICKNESS (M)
C          MAXIT - MAXIMUM NUMBER OF ITERATIONS
C          MLI6 - MASS OF LI6 (Kg)
C          NSTEP - NUMBER OF TIME STEPS
C          PEXPP - PRESSURE EXPONENT FOR PYC
C          PEXPS - PRESSURE EXPONENT FOR SIC
C          SPYCFAC - FACTOR OF PYC SOLUBILITY
C          SSICFAC - FACTOR OF SIC SOLUBILITY
C          DSICFAC - FACTOR OF SIC DIFFUSIVITY
C          TFLAG - TIME FLAG  0=SEC, 1=HRS
C          TOL - TOLERANCE
C          VVOID - VOLUME OF VOID (M3)
C          TIME(NSTEP) - TIME (S)
C          TEMP(NSTEP) - TEMP (K)
C
C     OTHER VARIABLES
C          CON - CONSTANT USED IN EQUATIONS
C          DF - DERIVATIVE OF F(P) W/RESPECT TO P
C          DT - TIME STEP
C          DX - CHANGE IN P IN ROOT FINDER
```

```
C       DXOLD - STORAGE VARIABLE FOR DX
C       EXP - EXPONENT USED IN EQUATIONS
C       FH - HIGH ESTIMATE OF F(P) IN ROOT FINDER ROUTINE
C       FL - LOW ESTIMATE OF F(P) IN ROOT FINDER ROUTINE
C       FR - FRACTIONAL RELEASE OVER TIME
C       FRAC - FRACTION OF ATOMS IN ENCLOSURE AND PYC
C       J - COUNTER
C       K - BOLTZMANN'S CONSTANT
C       N - COUNTER
C       NENCL - NUMBER OF ATOMS IN ENCLOSURE
C       NO - INITIAL NUMBER OF ATOMS OF T2 IN VOID
C            VOLUME
C       NPYC - NUMBER OF ATOMS IN PYC
C       P - PRESSURE (PA)
C       PCON - CONSTANT OF PYC TERMS USED OFTEN -
C            PYCS*AREA*DPYC
C       PEQ - EQUILIBRIUM PRESSURE (PA)
C       PH - HIGH P ESTIMATE IN ROOT FINDER ROUTINE
C       PL - LOW P ESTIMATE IN ROOT FINDER ROUTINE
C       PO - INITIAL PRESSURE (PA)
C       PYCS - PYC SOLUBILITY
C       R - GAS CONSTANT
C       SCON - CONSTANT OF SIC TERMS USED OFTEN-
C            SICD*SICS*AREA/DSIC
C       SICD - SIC DIFFUSIVITY
C       SICS - SIC SOLUBILITY
C       T - TEMPERATURE VARIABLE IN SUBROUTINES
C       TB - BREAKTHROUGH TIME FOR PROBLEM
C       TCHANGE - TIME OF TEMPERATURE CHANGE IF ANY
C       TFRAC - FRAC OF TIME STEP IN BREAKTHROUGH TIME
C       TM - TIME VARIABLE IN SUBROUTINES
C       TTEMP - TIME AT TEMPERATURE
C       X - POSITION IN LAYER BEFORE BREAKTHROUGH
C       XOLD - TEMPORARY STORAGE VARIABLE FOR X
C       XSQRD - X*X
C
      REAL*8 AREA,BUP,DPYC,DSIC,MLI6,PEXPP,PEXPS,SPYCFAC
      REAL*8 SSICFAC,DSICFAC,TOL,VVOID,TIME(200),TEMP(200)
      REAL*8 DT,FR,FRAC,NO,NENCL,NPYC,P,PEQ,PO,PCON,R,
      REAL*8 SCON,SICD,TFRAC,TB,TCHANGE,TTEMP
```

```
      REAL*8  X,XOLD,XSQRD
      INTEGER*4  J,MAXIT,N,NSTEP,TFLAG
      CHARACTER*40 TITLE
      NAMELIST/INPUT/ TITLE,AREA,BUP,DPYC,DSIC,MAXIT,
      &MLI6,NSTEP,PEXPP,PEXPS,SPYCFAC,SSICFAC,DSICFAC,
     &TFLAG,TOL,VVOID
      NAMELIST/TT/TIME,TEMP
C
       OPEN  (UNIT=7,FILE='HD:MPW:TREL:TREL.INP',
     &            STATUS='OLD')
      OPEN  (UNIT=8,FILE='HD:MPW:TREL:TREL.OUT',
     &           STATUS='NEW')
      OPEN  (UNIT=9,FILE='HD:MPW:TREL:TREL.PLT',
     &           STATUS='NEW')
C
      READ(7,NML=INPUT)
      WRITE(8,NML=INPUT)
      READ(7,NML=TT)
      WRITE(9,5) TITLE
 5    FORMAT(2X,A40)
      WRITE(9,10)' ',' ',' ','Pressure','Fractional'
      WRITE(9,10)' Time(s) ',' Time(h) ',' Temp (K) ','(Pa)',' Release '
 10   FORMAT(2X,5(2X,A10))
C
C     CHECK TFLAG - IF TIME IN HRS, CONVERT TO SEC
C
      IF (TFLAG .EQ. 1) THEN
            DO 15 N = 1,NSTEP
               .    TIME(N) = TIME(N)*3600.0
 15         CONTINUE
      ENDIF
C
C    INITIALIZE VARIABLES
C
      DT = 0.0
      FR = 0.0
      FRAC=1.0
      J = 1
      NPYC = 0.0
      R = 8.314
```

```
      TB = 0.0
      TCHANGE = 0.0
      TFRAC = 0.0
      TTEMP = 0.0
      X = 0.0
      XOLD = 0.0
      XSQRD = 0.0
      IF (TIME(J) .NE. 0.0) THEN
        WRITE(8,*)'ERROR: THE FIRST TIME STEP MUST EQUAL 0.0'
        STOP
      ENDIF
C
C     CALCULATE DIFFUSIVITY, SOLUBILITY AND
C     BREAKTHROUGH TIME AT INITIAL TEMP
C
        CALL  DIFFSOL(AREA,DPYC,DSIC,DSICFAC,SSICFAC,
     &              SPYCFAC,PCON,SCON,SICD,TEMP(J))
C
C     CALCULATE INITIAL PRESSURE, EQUILIBRIUM PRESSURE &
C     # OF ATOMS OF T2 IN VOID VOLUME
C
      CALL PINIT(BUP,FRAC,MAXIT,MLI6,PCON,PEQ,PEXPP,
     &           PO,TEMP(J),TOL,VVOID)
      NO = PO*6.023E23*VVOID/(R*TEMP(J))
      NENCL=NO
      P = PO
C
C     CALCULATE BREAKTHROUGH TIME
C
 20   IF ((J-1) .EQ. NSTEP) GO TO 100
      IF (X .LT. DSIC) THEN
        CALL PLOT(TIME(J),FR,P,TEMP(J))
        CALL TBOUT(TIME(J),TTEMP,TEMP(J))
        P = PEQ
        J = J + 1
C
C     RECALCULATE PO AND PEQ IF TEMPERATURE CHANGES
C
      IF (TEMP(J) .NE. TEMP(J-1)) THEN
        CALL  DIFFSOL(AREA,DPYC,DSIC,DSICFAC,SSICFAC,
```

```
     &          SPYCFAC,PCON,SCON,SICD,TEMP(J))
           CALL PINIT(BUP,FRAC,MAXIT,MLI6,PCON,PEQ,PEXPP,
     &          PO,TEMP(J),TOL,VVOID)
           P = PEQ
         ENDIF
C
C    UPDATE X TO TIME STEP
C
           DT = TIME(J) - TIME(J-1)
           XSQRD = XSQRD + 6*SICD*DT
           XOLD = X
           X = SQRT(XSQRD)
           GO TO 20
         ELSE
C
C    X>DSIC - CALCULATE FRACTION OF LAST TIME STEP
C    CONTRIBUTINGTO BREAKTHROUGH AND FIND P AND FR
C    FOR OTHER FRACTION
C
           TFRAC = (DSIC*DSIC-XOLD*XOLD)/(6*SICD)
           TB = TIME(J-1) + TFRAC
           TCHANGE = TB
           TTEMP = TIME(J) - TB
           CALL PLOT(TB,FR,P,TEMP(J))
           WRITE(8,22)'Breakthrough time of ',TB,' s has been reached.'
22         FORMAT(/2X,A21,F7.1,A20)
           CALL ROOTS(MAXIT,P,PEQ,PCON,PEXPP,PEXPS,SCON,
     &          TOL,TTEMP,TEMP(J),VVOID)
           CALL FREL(FR,FRAC,NO,NENCL,NPYC,P,PCON,PEXPP,
     &         TEMP(J),VVOID)
           CALL PLOT(TIME(J),FR,P,TEMP(J))
           CALL OUTPUT(FR,FRAC,NO,NENCL,NPYC,P,PEQ,TIME(J),
     &          TTEMP,TEMP(J))
         ENDIF
         IF (J .EQ. NSTEP) GO TO 100
C
C    UPDATE PRESSURE, FR, AND THE OUTPUT FILES FOR
C    REMAINDER OF PROBLEM CHECK FOR A TEMPERATURE
C    CHANGE AT EACH STEP
C
```

```
      DO 25 N = J+1,NSTEP
       IF (TEMP(N) .NE. TEMP(N-1)) THEN
        TCHANGE = TIME(N-1)
        CALL  DIFFSOL(AREA,DPYC,DSIC,DSICFAC,SSICFAC,
     &              SPYCFAC,PCON,SCON,SICD,TEMP(N))
        CALL PINIT(BUP,FRAC,MAXIT,MLI6,PCON,PEQ,PEXPP,
     &            PO,TEMP(N),TOL,VVOID)
        P = PEQ
       ENDIF
       TTEMP = TIME(N) - TCHANGE
       CALL  ROOTS(MAXIT,P,PEQ,PCON,PEXPP,PEXPS,SCON,
     &           TOL,TTEMP,TEMP(N),VVOID)
       CALL FREL(FR,FRAC,NO,NENCL,NPYC,P,PCON,PEXPP,
     &          TEMP(N),VVOID)
       CALL PLOT(TIME(N),FR,P,TEMP(N))
       CALL OUTPUT(FR,FRAC,NO,NENCL,NPYC,P,PEQ,TIME(N),
     &           TTEMP,TEMP(N))
 25  CONTINUE
 100  END
C
C
      SUBROUTINE  DIFFSOL(A,DPYC,DSIC,DSICFAC,SSICFAC,
     &                              SPYCFAC,PCON,SCON,SICD,T)
C
C   THIS SUBROUTINE CALCS THE DIFFUSIVITY AND THE
C   SOLUBILITY FOR PYC AND SIC (ALL CAUSEY RELATIONS
C   EXCEPT SIC SOL FROM EQUATION (49) OF THESIS
C   PCON AND SCON ARE CONSTANTS USED OFTEN IN THE
C   PRESSURE EQUATIONS
C
      REAL*8  A,DPYC,DSIC,DSICFAC,SSICFAC,SPYCFAC,SICD,T
      REAL*8  PCON,SCON,R,PYCS,SICS
       R = 8.314
       PYCS = 1.808E22*SPYCFAC*EXP(19270.0/(R*T))
       SICS = 2.148E20*SSICFAC*EXP(57170.0/(R*T))
       SICD = 1.58E-4*DSICFAC*EXP(-308000.0/(R*T))
       PCON = PYCS*A*DPYC
       SCON = SICD*SICS*A/DSIC
      RETURN
      END
```

```
C
      SUBROUTINE PINIT(BUP,FRAC,MAXIT,MLI6,PCON,PEQ,
     &                 PEXPP,PO,T,TOL,VVOID)
C
C     THIS SUBROUTINE CALCS THE INITIAL PRESSURE, PO, AND
C     THE EQUILIBRIUM PRESSURE, PEQ, W/USE OF NEWTON-
C     RAPHSON BISECTING METHOD
C
      REAL*8 BUP,FRAC,MLI6,PEQ,PEXPP,PO,PCON,T,TOL,VVOID
      REAL*8 CON,DF,DX,DXOLD,F,FH,FL,K,PH,PL,R,SWP
      INTEGER*4 L,MAXIT
        R = 8.314
        K = 1.38E-23
        CON = 2*VVOID/(K*T)
        PO = 0.5*MLI6*R*T*BUP*FRAC/(100*6*VVOID)
        PH = PO
        FH = FPEQ(PH,CON,PEXPP,PO,PCON)
        PL = 0.99*PO
30      PL = 0.95*PL
        FL = FPEQ(PL,CON,PEXPP,PO,PCON)
        IF (FL*FH .GE. 0.0) GO TO 30
        IF (FL .GT. 0.0) THEN
        SWP = PL
        PL = PH
        PH = SWP
        SWP = FL
        FL = FH
        FH = SWP
        ENDIF
        PEQ = 0.5*(PL + PH)
        DXOLD = ABS(PH - PL)
        DX = DXOLD
        F = FPEQ(PEQ,CON,PEXPP,PO,PCON)
        DF = DFDPEQ(PEQ,CON,PEXPP,PCON)
        DO 35 L = 1,MAXIT
          IF ((((PEQ-PH)*DF-F) * ((PEQ-PL)*DF-F) .GE. 0.0)
     &    .OR. (ABS(2.0*F) .GT. ABS(DXOLD*DF))) THEN
            DXOLD = DX
            DX = 0.5*(PH - PL)
            PEQ = PL + DX
```

```
        ELSE
          DXOLD = DX
          DX = F/DF
          PEQ = PEQ - DX
        ENDIF
        IF (ABS(DX) .LT. TOL) RETURN
        F = FPEQ(PEQ,CON,PEXPP,PO,PCON)
        DF = DFDPEQ(PEQ,CON,PEXPP,PCON)
        IF (F .LT. 0.0) THEN
          PL = PEQ
          FL = F
        ELSE
          PH = PEQ
          FH = F
        ENDIF
 35   CONTINUE
      WRITE(8,*) 'EXCEEDING MAXIMUM ITERATIONS'
      STOP
      RETURN
      END
C
      FUNCTION FPEQ(P,CON,PEXPP,PO,PCON)
C
C     THIS FUNCTION COMPUTES F(PEQ) TO DETERMINE PEQ
C      IN ROOT FINDER
C
      REAL*8 FPEQ,CON,P,PEXPP,PO,PCON
       FPEQ = CON*P + PCON*P**PEXPP - CON*PO
      RETURN
      END
C
      FUNCTION DFDPEQ(P,CON,PEXPP,PCON)
C
C     THIS FUNCTION COMPUTES DF/DPEQ FOR ROOT FINDER
C
      REAL*8 DFDPEQ,P,CON,PEXPP,PCON,EXP
       EXP = PEXPP - 1
       DFDPEQ = CON + PEXPP*PCON*P**EXP
      RETURN
      END
```

```
C
      SUBROUTINE ROOTS(MAXIT,P,PEQ,PCON,PEXPP,PEXPS,
     &                          SCON,TOL,TM,T,VVOID)
C
C     THIS SUBROUTINE CALCS THE PRESSURE USING A
C     NEWTON RAPHSON - BISECTION METHOD
C
      REAL*8 P,PEQ,PCON,PEXPP,PEXPS,SCON,TOL,TM,T,VVOID
      REAL*8 DF,DX,DXOLD,F,FH,FL,PH,PL,SWP
      INTEGER*4 L,MAXIT
       PH = P
       FH = FP(PH,PCON,PEQ,PEXPP,PEXPS,SCON,TM,T,VVOID)
       PL = 0.8*P
40     PL = 0.95*PL
       FL = FP(PL,PCON,PEQ,PEXPP,PEXPS,SCON,TM,T,VVOID)
       IF (FL*FH .GE. 0.0) GO TO 40
       IF(FL .GT. 0.0) THEN
        SWP = PL
        PL = PH
        PH = SWP
        SWP = FL
        FL = FH
        FH = SWP
       ENDIF
       P = 0.5*(PL + PH)
       DXOLD = ABS(PH - PL)
       DX = DXOLD
       F = FP(P,PCON,PEQ,PEXPP,PEXPS,SCON,TM,T,VVOID)
       DF = DFDP(P,PCON,PEXPP,PEXPS,SCON,T,VVOID)
       DO 45 L = 1,MAXIT
        IF((((P-PH)*DF-F) * ((P-PL)*DF-F) .GE. 0.0)
     &   .OR. (ABS(2.0*F) .GT. ABS(DXOLD*DF))) THEN
          DXOLD = DX
          DX = 0.5*(PH - PL)
          P = PL + DX
        ELSE
          DXOLD = DX
          DX = F/DF
          P = P - DX
        ENDIF
```

```
      IF (ABS(DX) .LT. TOL) RETURN
      F = FP(P,PCON,PEQ,PEXPP,PEXPS,SCON,TM,T,VVOID)
      DF = DFDP(P,PCON,PEXPP,PEXPS,SCON,T,VVOID)
      IF(F .LT. 0.0)THEN
        PL = P
        FL = F
      ELSE
        PH = P
        FH = F
      ENDIF
 45   CONTINUE
      WRITE(8,*) 'EXCEEDING MAXIMUM ITERATIONS'
      STOP
    RETURN
    END
C
    FUNCTION
    FP(P,PCON,PEQ,PEXPP,PEXPS,SCON,TM,T,VVOID)
C
C   THIS FUNCTION COMPUTES THE PRESSURE AS A
C   FUNCTION OF TIME
C
    REAL*8 FP,P,PEQ,PEXPP,PEXPS,PCON,SCON,TM,T,VVOID
    REAL*8 CON1,CON2,EXP1,EXP2,K,PTERM2
     K = 1.38D-23
     EXP1 = 1 - PEXPS
     CON1 = 2*VVOID/(EXP1*SCON*K*T)
     EXP2 = PEXPP-PEXPS
     CON2 = PEXPP*PCON/SCON
C
C   CHECK IF PEXPP=PEXPS AND SOLVE SECOND TERM
C   ACCORDINGLY
C
     IF (EXP2 .EQ. 0) THEN
       PTERM2 = LOG(P) - LOG(PEQ)
     ELSE
       PTERM2 = 1/EXP2*(P**EXP2 - PEQ**EXP2)
     ENDIF
     FP = TM + CON1*(P**EXP1 - PEQ**EXP1) + CON2*PTERM2
    RETURN
```

```
      END
C
      FUNCTION DFDP(P,PCON,PEXPP,PEXPS,SCON,T,VVOID)
C
C     THIS FUNCTION CALCS DF/DP FOR NEWTON'S METHOD
C
      REAL*8 DFDP,P,PEXPP,PEXPS,PCON,SCON,T,VVOID
      REAL*8 CON1,CON2,EXP1,EXP2,K,PTERM2
        K = 1.38D-23
        EXP1 = -PEXPS
        CON1 = 2*VVOID/(K*T*SCON)
        EXP2 = PEXPP-PEXPS-1
        CON2 = PEXPP*PCON/SCON
C
C     CHECK IF PEXPP=PEXPS AND SOLVE SECOND TERM
      ACCORDINGLY
C
        IF (EXP2 .EQ. -1) THEN
          PTERM2 = 1/P
        ELSE
          PTERM2 = P**EXP2
        ENDIF
        DFDP = CON1*P**EXP1 + CON2*PTERM2
      RETURN
      END
C
      SUBROUTINE FREL(FR,FRAC,NO,NENCL,NPYC,P,PCON,
     &                        PEXPP,T,VVOID)
C
C     THIS SUBROUTINE CALCULATES THE FRACTIONAL
C     RELEASE, FR, ANDTHE FRACTION OF ATOMS REMAINING
C     IN THE ENCL AND PYC, FRAC
C
      REAL*8 FR,FRAC,NO,P,PCON,PEXPP,T,VVOID
      REAL*8 K,NENCL,NPYC
        K = 1.38E-23
        NENCL = VVOID*P/(K*T)
        NPYC = PCON*P**PEXPP/2
        FRAC = (NENCL+NPYC)/NO
        FR = 1 - FRAC
```

```
      RETURN
      END
C
      SUBROUTINE PLOT(TIMESEC,FR,P,T)
C
C     THIS SUBROUTINE PRINTS TO THE PLOT FILE
C
      REAL*8 TIMESEC,FR,P,T,TIMEHR
        TIMEHR = TIMESEC/3600.0
        WRITE(9,70) TIMESEC,TIMEHR,T,P,FR
 70     FORMAT(2X,5(2X,1PE10.3))
      RETURN
      END
C
      SUBROUTINE TBOUT(TM,TTEMP,T)
C
C     THIS SUBROUTINE PRINTS THE OUTPUT BEFORE
C     BREAKTHROUGH IS REACHED
C
      REAL*8 TM,TTEMP,T
        WRITE(8,80)'Time(s) = ',TM
        WRITE(8,82)'After ',TTEMP,' sec at ',T,' K'
        WRITE(8,84)'Breakthrough time has not been reached so'
        WRITE(8,84)'tritium has not been released from the particle.'
 80     FORMAT(//2X,A10,1X,F10.1,A1)
 82     FORMAT(2X,A6,F10.1,A8,F6.1,A1/)
 84     FORMAT(2X,A)
      RETURN
      END
C
      SUBROUTINE OUTPUT(FR,FRAC,NO,NENCL,NPYC,P,PEQ,
     &                  TM,TTEMP,T)
C
C     THIS SUBROUTINE PRINTS TO THE OUTPUT FILE
C
      REAL*8 FR,FRAC,NO,NENCL,NPYC,P,PEQ,TM,TTEMP,T
      REAL*8 ENCCENT,FRCENT,PYCCENT
        FRCENT = FR*100
        ENCCENT = NENCL/NO*100
        PYCCENT = NPYC/NO*100
```

```
      WRITE(8,90)'Time(s) = ',TM
      WRITE(8,92)'After ',TTEMP,' sec at ',T,' K'
      WRITE(8,94)'The pressure now is ',P,' Pa.'
      WRITE(8,94)'Equ. pressure when raised to this temperature was
     &   ',PEQ,' Pa.'
      WRITE(8,94)'Of the ',NO,' initial atoms,'
      WRITE(8,96) ENCCENT,'% of the atoms remain in enclosure 1.'
      WRITE(8,96) PYCCENT,'% of the atoms remain in the PyC.'
      WRITE(8,96) FRCENT,'% of the atoms have been released from
     &   the particle.'
90    FORMAT(//2X,A10,1X,F10.1,A1)
92    FORMAT(2X,A6,F10.1,A8,F6.1,A1/)
94    FORMAT(2X,A,1PE11.4,A)
96    FORMAT(2X,F8.3,A)
      RETURN
      END
```

C.2 TREL Input

```
$INPUT
TITLE = 'COMPARISON OF TREL W/TMAP AT 1800C'
AREA = 2.68E-6
BUP = 45.0
DPYC = 68E-6
DSIC = 39E-6
MAXIT = 25
MLI6 = 1.62E-6
NSTEP = 15
PEXPP = 0.5
PEXPS = 0.5
SPYCFAC = 0.839
SSICFAC = 1.0
DSICFAC = 1.0
TFLAG = 0
TOL = 1.0E-6
VVOID = 7.41E-11
$END
$TT
TIME(1) = 0.0
TEMP(1) = 2073.0
TIME(2) = 300.0
TEMP(2) = 2073.0
TIME(3) = 600.0
TEMP(3) = 2073.0
TIME(4) = 900.0
TEMP(4) = 2073.0
TIME(5) = 1200.0
TEMP(5) = 2073.0
TIME(6) = 1800.0
TEMP(6) = 2073.0
TIME(7) = 2400.0
TEMP(7) = 2073.0
TIME(8) = 3000.0
TEMP(8) = 2073.0
TIME(9) = 3600.0
TEMP(9) = 2073.0
TIME(10) = 4200.0
```

TEMP(10) = 2073.0
TIME(11) = 4800.0
TEMP(11) = 2073.0
TIME(12) = 5400.0
TEMP(12) = 2073.0
TIME(13) = 6000.0
TEMP(13) = 2073.0
TIME(14) = 6600.0
TEMP(14) = 2073.0
TIME(15) = 7200.0
TEMP(15) = 2073.0
$END

C.3 TREL Plot File

COMPARISON OF TREL W/TMAP AT 1800C

Time (s)	Time (h)	Temp (K)	Pressure (Pa)	Fractional Release
0.000E+00	0.000E+00	2.073E+03	1.413E+07	0.000E+00
9.257E+01	2.571E-02	2.073E+03	9.183E+06	0.000E+00
3.000E+02	8.333E-02	2.073E+03	8.997E+06	1.651E-02
6.000E+02	1.667E-01	2.073E+03	8.731E+06	4.047E-02
9.000E+02	2.500E-01	2.073E+03	8.470E+06	6.407E-02
1.200E+03	3.333E-01	2.073E+03	8.214E+06	8.731E-02
1.800E+03	5.000E-01	2.073E+03	7.717E+06	1.327E-01
2.400E+03	6.667E-01	2.073E+03	7.238E+06	1.767E-01
3.000E+03	8.333E-01	2.073E+03	6.778E+06	2.194E-01
3.600E+03	1.000E+00	2.073E+03	6.336E+06	2.606E-01
4.200E+03	1.167E+00	2.073E+03	5.913E+06	3.004E-01
4.800E+03	1.333E+00	2.073E+03	5.508E+06	3.389E-01
5.400E+03	1.500E+00	2.073E+03	5.121E+06	3.760E-01
6.000E+03	1.667E+00	2.073E+03	4.752E+06	4.117E-01
6.600E+03	1.833E+00	2.073E+03	4.400E+06	4.461E-01
7.200E+03	2.000E+00	2.073E+03	4.065E+06	4.792E-01

C.4 TREL Output File

```
$INPUT
TITLE='COMPARISON OF TREL W/TMAP AT 1800C      ',
AREA=2.680000000000000E-06,
BUP=45.0000000000000,
DPYC=6.800000000000000E-05,
DSIC=3.900000000000000E-05,
MAXIT=25,
MLI6=1.620000000000000E-06,
NSTEP=15,
PEXPP=0.500000000000000,
PEXPS=0.500000000000000,
SPYCFAC=0.839000000000000,
SSICFAC=1.00000000000000,
DSICFAC=1.00000000000000,
TFLAG = 0,
TOL=1.000000000000000E-06,
VVOID=7.409999999999999E-11
$END


Time(s) =       0.0
After      0.0 sec at 2073.0

Breakthrough time has not been reached so
tritium has not been released from the particle.

Breakthrough time of    92.6 s has been reached.


Time(s) =     300.0
After     207.4 sec at 2073.0

The pressure now is  8.9967E+06 Pa.
Equ. pressure when raised to this temperature was  9.1832E+06 Pa.
Of the  3.6590E+16 initial atoms,
 63.689% of the atoms remain in enclosure 1.
 34.660% of the atoms remain in the PyC.
  1.651% of the atoms have been released from the particle.
```

Time(s) = 600.0
After 507.4 sec at 2073.0

The pressure now is 8.7311E+06 Pa.
Equ. pressure when raised to this temperature was 9.1832E+06 Pa.
Of the 3.6590E+16 initial atoms,
61.809% of the atoms remain in enclosure 1.
34.145% of the atoms remain in the PyC.
4.047% of the atoms have been released from the particle.

Time(s) = 900.0
After 807.4 sec at 2073.0

The pressure now is 8.4703E+06 Pa.
Equ. pressure when raised to this temperature was 9.1832E+06 Pa.
Of the 3.6590E+16 initial atoms,
59.962% of the atoms remain in enclosure 1.
33.631% of the atoms remain in the PyC.
6.407% of the atoms have been released from the particle.

Time(s) = 1200.0
After 1107.4 sec at 2073.0

The pressure now is 8.2142E+06 Pa.
Equ. pressure when raised to this temperature was 9.1832E+06 Pa.
Of the 3.6590E+16 initial atoms,
58.150% of the atoms remain in enclosure 1.
33.119% of the atoms remain in the PyC.
8.731% of the atoms have been released from the particle.

Time(s) = 1800.0
After 1707.4 sec at 2073.0

The pressure now is 7.7165E+06 Pa.
Equ. pressure when raised to this temperature was 9.1832E+06 Pa.

Of the 3.6590E+16 initial atoms,
54.627% of the atoms remain in enclosure 1.
32.100% of the atoms remain in the PyC.
13.274% of the atoms have been released from the particle.

Time(s) = 2400.0
After 2307.4 sec at 2073.0

The pressure now is 7.2378E+06 Pa.
Equ. pressure when raised to this temperature was 9.1832E+06 Pa.
Of the 3.6590E+16 initial atoms,
51.237% of the atoms remain in enclosure 1.
31.088% of the atoms remain in the PyC.
17.675% of the atoms have been released from the particle.

Time(s) = 3000.0
After 2907.4 sec at 2073.0

The pressure now is 6.7778E+06 Pa.
Equ. pressure when raised to this temperature was 9.1832E+06 Pa.
Of the 3.6590E+16 initial atoms,
47.981% of the atoms remain in enclosure 1.
30.084% of the atoms remain in the PyC.
21.935% of the atoms have been released from the particle.

Time(s) = 3600.0
After 3507.4 sec at 2073.0

The pressure now is 6.3364E+06 Pa.
Equ. pressure when raised to this temperature was 9.1832E+06 Pa.
Of the 3.6590E+16 initial atoms,
44.856% of the atoms remain in enclosure 1.
29.088% of the atoms remain in the PyC.
26.056% of the atoms have been released from the particle.

Time(s) = 4200.0
After 4107.4 sec at 2073.0

The pressure now is 5.9133E+06 Pa.
Equ. pressure when raised to this temperature was 9.1832E+06 Pa.
Of the 3.6590E+16 initial atoms,
41.861% of the atoms remain in enclosure 1.
28.100% of the atoms remain in the PyC.
30.039% of the atoms have been released from the particle.

Time(s) = 4800.0
After 4707.4 sec at 2073.0

The pressure now is 5.5083E+06 Pa.
Equ. pressure when raised to this temperature was 9.1832E+06 Pa.
Of the 3.6590E+16 initial atoms,
38.994% of the atoms remain in enclosure 1.
27.121% of the atoms remain in the PyC.
33.885% of the atoms have been released from the particle.

Time(s) = 5400.0
After 5307.4 sec at 2073.0

The pressure now is 5.1213E+06 Pa.
Equ. pressure when raised to this temperature was 9.1832E+06 Pa.
Of the 3.6590E+16 initial atoms,
36.254% of the atoms remain in enclosure 1.
26.150% of the atoms remain in the PyC.
37.595% of the atoms have been released from the particle.

Time(s) = 6000.0
After 5907.4 sec at 2073.0

The pressure now is 4.7519E+06 Pa.
Equ. pressure when raised to this temperature was 9.1832E+06 Pa.
Of the 3.6590E+16 initial atoms,
33.639% of the atoms remain in enclosure 1.

25.190% of the atoms remain in the PyC.
41.171% of the atoms have been released from the particle.

Time(s) = 6600.0
After 6507.4 sec at 2073.0

The pressure now is 4.3999E+06 Pa.
Equ. pressure when raised to this temperature was 9.1832E+06 Pa.
Of the 3.6590E+16 initial atoms,
31.148% of the atoms remain in enclosure 1.
24.239% of the atoms remain in the PyC.
44.613% of the atoms have been released from the particle.

Time(s) = 7200.0
After 7107.4 sec at 2073.0

The pressure now is 4.0651E+06 Pa.
Equ. pressure when raised to this temperature was 9.1832E+06 Pa.
Of the 3.6590E+16 initial atoms,
28.777% of the atoms remain in enclosure 1.
23.298% of the atoms remain in the PyC.
47.924% of the atoms have been released from the particle.